**Distribution Agreement**

In presenting this thesis or dissertation as a partial fulfillment of the requirements for an advanced degree from Emory University, I hereby grant to Emory University and its agents the non-exclusive license to archive, make accessible, and display my thesis or dissertation in whole or in part in all forms of media, now or hereafter known, including display on the world wide web. I understand that I may select some access restrictions as part of the online submission of this thesis or dissertation. I retain all ownership rights to the copyright of the thesis or dissertation. I also retain the right to use in future works (such as articles or books) all or part of this thesis or dissertation.

Signature:

_____ _____

Alexandra A. Wolfarth Date

Functional Characterization of the Epithelial Protein, PRAP1, and Generation of Human Microbiota-Associated Mice to Model Bacterial Vaginosis

By

Alexandra A. Wolfarth
Doctor of Philosophy

Graduate Division of Biological and Biomedical Science
Immunology and Molecular Pathogenesis

_____

Andrew Neish
Advisor

_____

Augustine Rajakumar
Committee Member

_____

Sean Stowell
Committee Member

_____

Rabindra Tirouvanziam
Committee Member

_____

David Weiss
Committee Member

Accepted:

_____

Lisa A. Tedesco, Ph.D.
Dean of the James T. Laney School of Graduate Studies

_____

Date

# Functional Characterization of the Epithelial Protein, PRAP1, and Generation of Human Microbiota-Associated Mice to Model Bacterial Vaginosis

By

Alexandra A. Wolfarth
B.S., Northern Arizona University, 2012

Advisor: Andrew S. Neish, M.D.

An abstract of
A dissertation submitted to the Faculty of the
James T. Laney School of Graduate Studies of Emory University
in partial fulfillment of the requirements for the degree of
Doctor of Philosophy
in Immunology and Molecular Pathogenesis
2020

Abstract

Functional Characterization of the Epithelial Protein, PRAP1, and Generation of Human Microbiota-Associated Mice to Model Bacterial Vaginosis
By Alexandra A. Wolfarth

The microbiota maintains critical interactions with the host at the mucosa of both the gastrointestinal tract and the female reproductive tract. To understand the mechanisms by which certain members of the microbiota promote intestinal and reproductive health, we developed two independent projects. We first functionally characterize an under-studied protein, Proline-rich acidic protein 1 (PRAP1), induced by Lactobacilli in the gut epithelium. We found PRAP1 is a 17 kDa intrinsically disordered protein that prolongs the survival of mice after total body irradiation and prevents irradiation-induced apoptosis in the gut epithelium. We conclude that PRAP1 is an intrinsically disordered protein highly expressed by the gastrointestinal epithelium and functions at exposed surfaces to protect the barrier from oxidative insult. Second, to further understand the mechanisms by which the vaginal microbiota promote female reproductive health, we sought to improve current mouse models of the vaginal microbiota. We generated human microbiota-associated (HMA) mice using vaginal swabs collected from pregnant women with or without bacterial vaginosis (BV). Our goal was to generate mice that had a vaginal microbiota and birth outcome comparable to their respective human donors. There was considerable variability in the microbes that colonized each mouse, with no association to the microbiota of the donor. Although human mothers with BV had more frequent adverse birth outcomes, the vaginal microbiota was not predictive of adverse birth outcomes in mice. Together, these projects further our understanding of the mechanisms by which the microbiota promotes intestinal health and the potential uses and limitations of mouse models involving the female reproductive tract.

# Functional Characterization of the Epithelial Protein, PRAP1, and Generation of Human Microbiota-Associated Mice to Model Bacterial Vaginosis

By

Alexandra A. Wolfarth
B.S., Northern Arizona University, 2012

Advisor Andrew S. Neish, M.D.

A dissertation submitted to the Faculty of the
James T. Laney School of Graduate Studies of Emory University
in partial fulfillment of the requirements for the degree of
Doctor of Philosophy
in Immunology and Molecular Pathogenesis
2020

## Acknowledgements

**Chapter 2**

For assistance with Chapter 2, I would like to thank all of the co-authors for their help in carrying out experiments, discussing data and reviewing the manuscript. Additionally, I would like to thank my advisor, Dr. Andrew Neish, and my committee members for their guidance and support. I would also like to thank Dr. Jason Matthews, who provided constructive discussions and technical support that aided the development of this project. Finally, I would like to thank Dr. Victor Band for his participation in scientific discussions of the data and for his emotional support throughout the project.

**Chapter 3**

We are grateful to the women who generously agreed to participate in this research, to the research coordinators who interface with the participating women to carefully collect research data, and to the clinical providers, nursing and laboratory staff at the prenatal care clinics of Grady Memorial Hospital and Emory University Hospital Midtown without whose cooperation this research would not be possible. This study was supported in part by the Emory Gnotobiotic Animal (EGAC), which is subsidized by the Emory University School of Medicine and is one of the Emory Integrated Core Facilities. Additional support was provided by the Georgia Clinical & Translational Science Alliance of the National Institutes of Health under Award Number UL1TR002378. I would also like to acknowledge Caroline Addis and Amanda Metzger for their help in using the micro-isolator cages and the handling of germ-free mice. Finally, I would like to thank Dr. Rheinallt Jones for the opportunity to lead the experiments for this project and his help in drafting the manuscript.

## Table of Contents

# Chapter 1

## The Small Intestinal Epithelium: A Dynamic Barrier Critical to Human Health

### Introduction

The human gut harbors a substantial amount of bacteria, with initial colonizers acquired at birth. While some bacterial species such as *Clostridium difficile* are pathogenic and cause serious intestinal infections, the majority of bacteria found in the gut are commensal and thrive in harmony with the host [1]. It has become increasingly appreciated that not only does the colonization of beneficial bacteria prevent the ability of pathogenic bacteria to take hold and cause infection, but some taxa are in constant contact with the host epithelium and elicit beneficial host responses [2]. After sensing certain commensal bacteria, the intestinal epithelium can respond by secreting mucins and antimicrobial proteins [3]. These secreted factors are crucial in forming a selective barrier between the host epithelium and potential pathogenic bacteria. Contact with commensal bacteria also initiates several homeostatic processes such as proliferation, restitution and the expression of genes involved in protection from potential injury [4]. Understanding the many interactions and processes that contribute to a healthy gut epithelium has become increasingly important as the rates of inflammatory bowel diseases increase [5]. This importance is also underscored by the fact that many of the current treatments available for IBD are only successful for a fraction of IBD patients and an even lower fraction experience complete remission [6, 7]. As we continue to unravel the complex processes that promote a healthy gut barrier, the treatments for patients with chronic intestinal inflammation will improve. Ultimately, these enhanced treatments have the potential to improve the quality of life for over 1 million individuals [5].

**Microbial Composition and Epithelial Cell Types of the Small Intestine**

There are several physiological differences between the small intestine and colon which correspond with distinct compositions of bacteria in these two regions. Because the small intestine is located immediately after the stomach near the bile duct, the proximal small intestine is much more acidic, with the pH increasing distally towards the colon [8]. The small intestine also has a higher oxygen concentration compared to the colon [9]. In addition, Paneth cells are located almost exclusively in the small intestine, secreting high amounts of antimicrobial peptide into the mucus and luminal space. Lastly, the small intestine has a faster transit time and harbors different potential nutrients than the colon. All of these characteristics of the small intestine select for the survival of certain kinds of bacterial species. The most common bacteria found in the small intestine are fast growing facultative anaerobes that tolerate an acidic environment and are able to bind the mucus layer. Dominant bacterial families in the small intestine include Lactobacillaceae and Enterobacteriacea [10, 11]. Crucial to the colonization of these bacteria in the small intestine is their ability to bind mucins in the mucus layer initially by lectins and other membrane proteins. In order to penetrate the mucus and directly interact with the host epithelium, most commensal bacteria secrete mucinases and proteases [12, 13]. These enzymes degrade the mucus and allow commensal bacteria to penetrate the mucus layer and bind the host epithelium.

The small intestine is a unique organ of the body with a high amount of bacterial contact. This bacterial interaction occurs because it serves as the main site of nutrient absorption [14]. The potential for close contact with bacteria signifies the importance of maintaining a healthy gut epithelium to prevent translocation of bacteria, damaging inflammation and increased risk of IBD development. Because the main function of the small

intestine is to absorb nutrients exiting the stomach, it is important that the gut epithelium maintain a relatively thin layer of mucus (unlike the colon) and an epithelial barrier that is selectively permeable. In order to accomplish this, the host epithelium is comprised of a single cell layer that forms villus structures protruding towards the inner lumen and crypts that invaginate the mucosa and increase absorptive surface area. The cell type represented in 90-95% of the crypt-villus axis is the **absorptive epithelial cell** [15]. In order to carry out the important function of nutrient absorption, the absorptive epithelial cells express several types of glucose and amino acid transporters. The expression of these transporters are critical for the sensing and uptake of nutrients and their expression levels can change depending on the region of the small intestine and cell position within the crypt-villus axis [15]. At the base of the crypts are **intestinal stem cells**. These stem cells divide to replenish the constant turnover of epithelium and are the source of not only the absorptive epithelial cells, but additional epithelial cell types found within the epithelium: Paneth cells, goblet cells, enteroendocrine cells and tuft cells [16]. Located next to the intestinal stem cells at the base of the crypts are the **Paneth cells**. These cells function to secrete antimicrobial proteins and other survival signals that are crucial for maintaining a stem cell permissive environment [17]. This region of the crypt is referred to as the "crypt-stem cell niche" and is described in more detail later in this chapter. Another important secretory cell located throughout the epithelium of the small intestine and colon is the **goblet cell**. These cells secrete mucins to form the mucus layer, with a much more substantial mucus layer produced in the colon compared to the small intestine [18]. The importance of the mucus layer and details of its composition is provided in detail later in this chapter. Also scattered throughout the epithelial layer are **enteroendocrine cells**. These cells are capable of sensing nutrients and releasing hormones that have local and

systemic effects that are important for digestion and metabolism, including the control of gut motility, insulin release and satiety [19]. Finally there are **tuft cells**, which only make up about 0.4-1% of the epithelial cell population [20]. Tufts cells are most well known for their unique physical feature, displaying a prominent "tuft" of microvilli that extend into the gut lumen [21, 22]. There is a remarkable amount of heterogeneity found within the tuft cell population and they have been found in many mucosal sites outside of the small intestine [16, 21]. While their function seems to differ based on the tissue they are in, they are broadly defined as cells that sense chemical signals and respond by releasing a variety of biological mediators. In the intestine, tufts cells have been shown to express high levels of IL25, making them critical in the response to pathogens requiring a type-2 immune response, although their function in the gut certainly encompass much more than this [23, 24]. Despite their heterogeneity and presence in distant organs such as the thymus, lineage tracing has confirmed that intestinal tufts cells do indeed arise from Lgr5+ stem cells in the intestinal crypt [20]. In summary, the specialized cells that make up the gut epithelium act in concert to achieve the difficult task of nutrient sensing and absorption while maintaining physical separation between luminal antigens and the underlying sub epithelial compartment.

**Maintenance of the Epithelial Barrier**

While a variety of epithelial cell types can be found throughout the small intestinal epithelium, they all must act together to form a selectively permeable barrier capable of absorbing required nutrients while preventing translocation of unwanted solutes and antigens. To achieve this barrier, the plasma membrane of epithelial cells is impermeable to hydrophilic material, only allowing uptake by specific transporters [25]. In addition to regulating direct uptake by the epithelial cells, another critical and highly dynamic mechanism of barrier

maintenance is the presence of the apical junctional complex located in the paracellular space. Within this complex are tight junctions, adhererns junctions and the desmosome [26].

Starting at the basolateral region of the junctional complex is the desomosome, made of desmocollin, desmogelin and desmoplakin [27]. Above the desmosome are the adherens junctions, which are comprised of transmembrane cadherins that attach to α-catenin, β-catenin and actinomyosin filaments inside the cell [28]. Both desmosomes and the adherens junctions provide necessary adhesive forces that maintain cell-to-cell contact. At the apical end of the paracellular space are the tight junctions. These tight junctions are comprised of protein complexes that form both "pore" and "leak" pathways, achieving both size-and charge-selectivity [29]. The tight junctional claudins are responsible for forming pores while ZO-1, occludin and myosin light chain kinase (MLCK) are involved in the leak pathway [27]. Claudins that make up the tight junctions are thought to be the most important when determining the permeability of the barrier, as the modulation of claudin expression alone is able to change transepithelial resistance [30]. The importance of regulating claudin expression at the intestinal epithelium is underscored by the finding that mice lacking claudin 2 and 15 have improper luminal sodium levels and low nutrient absorption that ultimately leads to premature death [31]. While some claudins form pores important for nutrient absorption and ion flux, other claudins act to decrease permeability and create a tighter seal. The expression of claudins not only varies along the crypt-villus axis, but can be modulated by kinase activity and cytokine expression [27, 32]. Because the expression of claudins has such a direct effect on intestinal permeability, their dysregulation is thought to be a critical risk factor for the development of IBD in humans [25].

Another aspect of the intestinal epithelium that is critical to barrier maintenance but less understood is the highly controlled shedding of epithelial cells as they reach the villus tip. While epithelial cell shedding occurs at a rate of about 1 cell/minute, the barrier at the villus tip remains uncompromised [33]. Several hypotheses have been proposed to explain how the barrier is maintained during this process and may involve the cooperation of several mechanisms. Contraction of actin filaments to seal gaps in the barrier have been observed *in vitro*, tight junction formation under the extruding cell, contraction of subepithelial myofibroblasts and lastly, the observation of an unknown substance that fills gaps in the barrier that are devoid of cell cytoplasm and nuclei [34].

While formation of a highly selective epithelium is critical to forming an effective and functional intestinal barrier, the mucosa is often the first line of defense against microbes and potential pathogens. This requires additional specialized characteristics critical to the innate immune response.

## Innate Immunity at the Small Intestinal Epithelium

### *Mucus Layer*

Throughout the gastrointestinal tract is a mucus layer that not only prevents self-digestion but also serves as a significant physical barrier between luminal contents and the host epithelium. The mucus layer is composed of about 50 proteins, with the major component being the MUC2 mucin. MUC2 is composed of about 5,100 amino acids [35] and undergoes extensive polymerization before being secreted by goblet cells. After secretion the mucin expands immensely to form large nets [36]. In order for the mucin to unfold a high pH is required [37]. To achieve a high pH, adjacent enterocytes have been found to secrete bicarbonate [38]. Defects in mucin production are associated with spontaneous colitis [39] and

therefore play an important role in gut barrier function. While the mucus layer in the stomach and colon is very thick and has a dense inner layer and loose outer layer, the small intestine has only one layer of mucus on top of the glycocalix. The mucus layer in the small intestine has a larger pore size that allows bacteria to penetrate and gain proximity to the host epithelium [18]. Although the small intestine has a larger pore size and only a single layer, there are several factors which prevent most intestinal bacteria from reaching the host epithelium. As goblet cells produce and secrete mucin, the older mucin is pushed towards the lumen, creating a flow which makes it difficult for most bacteria to swim against [40]. Located at the base of the crypts in the small intestine are Paneth cells which secrete antimicrobial proteins. As these antimicrobials bind the mucins, their concentration is kept high near the host epithelium [41]. The intestinal mucus layer is important in barrier function because it physically separates microbes from the host epithelium while also binding and concentrating antimicrobial proteins released by the host, thereby controlling the microbiota composition.

***Epithelial sensing of Microbes***

Although a majority of bacteria in the gut is regulated and kept at bay, the gut epithelium expresses several receptors responsible for the recognition of and response to microbes in the case that microbes closely approach or breach the epithelium. It is extremely important that intestinal epithelial cells have multiple avenues to sense bacteria. This ensures that the host can regulate the bacteria present and quickly control any intestinal infection that would otherwise grow uncontrolled and become life threatening.

**Toll-like receptors (TLRs)** are a type of pattern recognition receptor (PRR) important for the sensing of bacterial macromolecules [42]. Ligand binding results in dimerization and activation of the TLR. Subsequent downstream signaling results in the transcription of

cytokines, chemokines and antimicrobial proteins. TLRs are most commonly found on immune cells but can also be expressed by the cells of the intestinal epithelium. Most notably, gut enterocytes express both TLR4 and TLR5 [43, 44], responsible for the recognition of LPS and flagellin, respectively. The sensing of either of these common bacterial ligands alerts the gut epithelium of a possible infection and the cell can then transcribe antimicrobial proteins and cytokines to recruit the appropriate immune cells needed to control an intestinal infection [45-48].

Although TLR activation is important in sensing and controlling an infection, it has also been shown to have an important role in the regulation of homeostatic processes at baseline. While most bacteria is kept some distance from the epithelium by mucus and antimicrobial proteins, some commensal bacteria are able to reach the epithelium and activate low levels of endogenous TLR4 signaling. This low level of commensal sensing has been shown to increase mucosal protection from injury [49]. The expression of TLRs in epithelial cells must be highly regulated to tolerate the abundance of potential TLR ligands present in the gut lumen. If not, TLR dependent sensing of commensal bacteria would lead to a loss of tolerance and damaging inflammation. To control TLR signaling in the gut, most TLR expression is polarized and more likely to be expressed on the basolateral side of the enterocyte [50]. Ligand binding from the basolateral side of the cell indicates that there has been a breach in the epithelium and the correct inflammatory signals ensue to control the infection [50].

**NOD-Like Receptors (NLRs)** are PRRs acting as intracellular sensors that are expressed in virtually all cell types. They are responsible for sensing a variety of ligands including microbial associated molecular patterns (MAMPs) and danger associated molecular

patterns (DAMPs). Upon ligand recognition, NLRs undergo a conformational change which then allows them to interact with downstream signaling proteins. This signaling results in the expression of inflammatory and antimicrobial genes [51-53]. In the intestine, NOD1 and NOD2 are NLRs of particular importance. NOD1 senses D-glutamyl-meso-diaminopimelic acid (DAP) found in gram-negative bacteria and some gram-positive bacteria. NOD2 senses muramyl-dipeptide (MDP), a common bacterial protein [54-56]. While NOD1 expression is found in a variety of cell types, NOD2 expression is limited to myeloid cells, lymphoid cells, intestinal epithelial cells and Paneth cells [57, 58]. NOD2 expression in the intestine is particularly important because the gene which encodes it was the first to be associated with Crohn's Disease susceptibility. Mutations in *NOD2* remain the strongest risk factor for developing Crohn's Disease [59, 60]. Several studies in mice have supported the hypothesis that NOD2 sensing and subsequent responses are a critical regulator of gut homeostasis. For example, when wildtype mice were administered NOD2 ligands such as peptidoglycan or MDP, they were protected from experimental colitis [61, 62]. In addition, not only do *NOD2* deficient mice spontaneously develop colitis, but if they are cohoused with wildtype mice, these wildtype mice also develop severe intestinal inflammation and barrier injury [63]. This finding suggests that NOD2 not only senses bacteria but plays a major role in regulating the composition of commensal bacteria, likely through the secretion of antimicrobial factors and shaping the immune response in the intestine.

**Formyl Peptide Receptors (FPRs)** are a seven membrane pass G protein linked surface receptor found on the cell membrane of a variety of cells, including phagocytes of the immune system and intestinal epithelial cells [64]. These receptors are activated by the binding of bacterial proteins containing an N-formyl group, such as the bacterial cell wall

component N-formyl-methionyl- leucyl-phenylalanine (fMLF). The activation of these receptors leads to downstream signaling that ultimately leads to the generation of reactive oxygen species (ROS) by an NADPH oxidase enzyme (Nox). While FPRs function to generate intracellular ROS, the consequence of this ROS generation is dependent on the cell expressing the receptor. While FPR activation on a phagocyte leads to high levels of ROS (respiratory burst) and subsequent killing of the engulfed bacteria [65, 66], FPR activation on the intestinal epithelia results in low levels of endogenous ROS [67]. This difference is due to the expression of different Nox enzymes within different cell types. While phagocytes express high levels of Nox2, the intestinal epithelia express high levels of Nox1, resulting in the generation of rapid, reversible physiological amounts of non-radical ROS [68].

This low level of FPR-dependent ROS generation in intestinal epithelial cells is thought to be an evolutionarily conserved mechanism of sensing and responding to bacteria and their products in the gut lumen, illustrated by the expression of a Nox ortholog in the *Drosophila* gut [67, 69, 70]. Non-radical ROS serves as an important second messenger, acting on regulatory enzymes containing oxidant-sensitive thiol groups. These sensory proteins can be involved in a wide array of signaling pathways, such as those involving NF-kB, MAP kinase and focal adhesion kinase [71-73]. The decreased enterocyte proliferation and restitution in germ-free mice underscores the importance of commensal bacteria in the promotion of several important host processes [74-76]. It has become increasingly appreciated that FPRs serve as a promising avenue by which commensal bacteria and their products are sensed by the gut epithelia to promote host processes critical in gut barrier maintenance.

**Microfold cells (M cells)** are a subset of intestinal cells which specialize in the sampling of luminal antigens. These cells are located in the follicle- associated epithelium

(FAE) of organized intestinal lymphoid tissue such as Peyers patches in the small intestine. M cells arise from Lgr5+ stem cells within dome associated crypts and their differentiation is dependent on the secretion of RANKL by stromal cells beneath the FAE [77]. Several characteristics make M cells efficient at antigen sampling: They have reduced microvilli, a thin glycocalyx layer, and express several receptors that mediate antigen uptake [78]. While the reduced microvilli and mucus layer allow close proximity between M cells and luminal contents, M cells also express several proteins that have been found to interact with potentially pathogenic bacteria. For example, M cells express several receptors such as glycoprotein 2 (GP2) and cellular prion protein which bind to FimH and Hsp60, respectively [79-82]. The expression of these receptors is important for efficient sampling of the gut microbiota.

In addition to the expression of receptors which detect a diverse range gut bacteria, M cells are also located strategically next to immune cells within the Peyers patch. This combination makes M cells critical in the early detection of pathogenic bacteria and subsequent control by the mucosal immune system. Beneath the M cells are macrophages, dendritic cells, B cells and T cells organized in a region known as the intraepithelial pocket [83, 84]. These immune cells are attracted to the intraepithelial pocket by several chemokines such as CCL20, CCL9, and CXCL16 and their close proximity to M cells promotes the efficient transfer of luminal antigens to mononuclear phagocytes (MNPs) [82, 85-87]. After uptake by MNPs, the adaptive immune response is alerted of any potential infection and lymphocytes within the mesenteric lymph nodes will home to the lamina propria to kill infected cells and produce secretory IgA specific for the inciting bacteria [79, 88]. This specific and early detection of potential pathogenic bacteria is made possible by the efficient sampling of luminal antigens by

M cells. This is underscored by the increase in susceptibility to several intestinal pathogens such as *Salmonella enterica* serovar Typhimurium when M cells are absent [88].

***Antimicrobial proteins***

A major component of intestinal innate immunity is the production and secretion of antimicrobial proteins by the gut epithelium. Antimicrobial proteins are peptides that target and kill bacteria, protozoa, viruses and fungi. Therefore, their secretion in the intestine plays a major role in the regulation of gut microbiota and protection against pathogens [89]. Antimicrobial proteins that are secreted by the epithelium are trapped by the overlying mucus layer, creating a gradient of antimicrobial concentration. It is has been shown that in the crypts of the small intestine where antimicrobial concentration is at its highest, concentrations of Paneth cell granule components can be over 1mM, in some cases exceeding the minimum inhibitory concentration (MIC) by 1,1000 times [90]. Major antimicrobial proteins of the human gut include lysozyme, Secretory phospholipase A2, defensins, Reg3α, galectins and cathelicidin **(Table 1)** [91-94]. The antimicrobial peptides found in the human intestine are small in size, with most less than 20kDa. Although these antimicrobials may bind and target different microbes, their known mechanisms of action are very similar. Most antimicrobial proteins are cationic and use electrostatic attraction to bind the negatively charged bacterial cell wall components [95]. Once bound to the bacteria, they usually use one of two mechanisms to disrupt the bacterial cell membrane. Antimicrobial proteins that have enzymatic activity such as lysozyme and phospholipase A2, hydrolyze the phospholipids of the bacterial cell membrane to disrupt the membrane and subsequently kill the bacteria [96, 97]. Other antimicrobial proteins such as defensins and cathelicidin dimerize or oligomerize on the bacterium's surface to form transmembrane pores. These pores lead to the loss of critical metabolites, decrease membrane

potential and ultimately lead the death of the cell [98]. In addition to direct bactericidal activity, some antimicrobials also have indirect mechanisms of regulating gut microbes. For example, HD-6 forms long oligomers that act as a net to entrap potential pathogenic bacteria in the mucus layer and prevent their translocation across the epithelium [99]. Lysozyme, which hydrolyzes components of the peptidoglycan layer, also has been shown to play a significant role in the activation of downstream innate immunity responses, such as inflammasome activation in response to *Staphylococcus aureus* [100].

Regulation of expression is unique among the different antimicrobials and factors such as cell type, tissue, cytokines and bacterial strain have all been shown to play an important role [101-105]. For example, human β defensins-1 (hBD1) is an antimicrobial expressed in several tissues of the body and was hypothesized to have an important role in the defense against pathogens. When the antimicrobial activity of hBD1 was initially tested, it had very low antimicrobial activity against multiple bacterial strains. It was only when hBD1 was treated with reducing agents that it began to show potent antimicrobial activity [106]. Reduction of the disulfide bonds within hBD1 is critical for its activity and reducing environments (as is found in the gut) regulate its activity.

Some antimicrobials are thought to be expressed constitutively by the gut epithelium to some degree. There are two major ways in which antimicrobial expression can be enhanced in the epithelium. The first way is through stimulation of epithelial cells with bacteria and/or their

**Table 1. Major Antimicrobial Proteins Found in the Intestine**

| Host Antimicrobial | Size [107] | Expressed By | Induced By | Mechanism Of Action | Targeted Microbes |
|---|---|---|---|---|---|
| **Lysozyme** | 16.5 | Secretory cells Macrophages Paneth Cells | Unknown | Hydrolysis of peptidoglycan components | Gram + bacteria |
| **Secretory Phospholipase A2** | 13-17 | Secretory cells Macrophages Paneth Cells | LPS | Electrostatic attraction, Hydrolysis of phospholipids | Gram + bacteria |
| **α Defensins (HD5 and HD6)** | 2-4 | Paneth Cells | NOD2 activation, Most highly expressed AMPs in intestine | Electrostatic attraction, transmembrane dimer-pore | Gram +/- bacteria, fungi, protozoa, enveloped viruses |
| **β Defensins** | 2-4 | Epithelia of small and large intestine | LPS, flagellin | Electrostatic attraction, transmembrane pores | Gram +/- bacteria, fungi, protozoa, enveloped viruses |
| **Reg3α/HIP/PAP (REG3γ in mice)** | 16 | Epithelia of small intestine, Paneth cells | TLR activation | Electrostatic attraction and hexamerix transmembrane pores | Gram + bacteria |
| **Galectins 4 and 8** | 36 | Epithelial cells | Unknown | Alters membrane integrity and motility | *E. coli* strains with carbohydrate structures mimicking BGA |
| **Cathelicidin (LL-37 in humans, CRAMP in mice)** | 18 | Epithelial cells, leukocytes | Butyrate, bile acids, Vitamin D, NOD2 | Electrostatic attraction, α-helices form membrane penetrating toroidal pore | Gram +/- bacteria, fungi |

products [108]. The second way is indirect and first involves the stimulation of immune cells by bacteria. Immune cells such as macrophages then release cytokines such as IL-1, enhancing expression of antimicrobials in epithelial cells [109, 110]. While most human data has involved exposing human skin to different stimuli and measuring the subsequent change in antimicrobial expression [111-113], some work has been done to investigate this regulation in the human gastrointestinal tract. For example, when compared to uninfected healthy controls, the mucosa of patients infected with *H. pylori* had a significant increase in expression of LL-37 (cathelicidin) [114].

To demonstrate whether an increase in antimicrobial expression contributes to protection of an intestinal pathogen, knockout mice have been generated to lack either certain antimicrobials or critical enzymes required for their processing. For example, a peroxisome proliferator-activated receptor gamma (PPARg) deficient mouse lacks beta defensin 10. These mice were more susceptible to several intestinal pathogens such as *Candida albicans*, *Bacteroides fragilis*, *Enterococcus faecalis* and *E. coli* [115, 116].

While many antimicrobial proteins are expressed throughout the small and large intestinal epithelial cells, some such as alpha defensins (HD-5 and HD-6) are exclusively stored and released by Paneth cells. Paneth cells are specialized secretory cells found at the base of crypts in the small intestine. The secretion of antimicrobial proteins by Paneth cells is critical for regulating the microbes in this region. This regulation plays a major role in protecting neighboring intestinal stem cells and maintaining a proper crypt-stem cell niche.

**The Crypt-Stem Cell Niche**

One of the many remarkable features of the gastrointestinal tract is its ability to replenish the epithelium with new cells every 4-5 days. This constant shedding of cells from the

top of the villi creates an enormous task for the intestinal stem cells which are responsible for providing their replacements. Any dysregulation in their function could lead to a suboptimal epithelial barrier and increases the risk of potential microbial antigens from breaching this barrier and causing chronic inflammation and disease. To ensure intestinal stem cells function properly, the region in which they reside has specialized cells that function to support and protect them. Intestinal stem cells, Paneth cells and stromal cells all reside in and near crypts of the small intestine, forming an extremely physiologically important region of the gut known as the crypt-stem cell niche.

**Intestinal Stem Cells (ISCs)** represent a self-renewing multipotent population of cells that reside in the crypts of the intestine [117, 118]. These ISCs proliferate in a Wnt-dependent manner giving rise to the transit-amplifying (TA) daughter cells that rapidly divide asymmetrically [119]. These TA cells migrate up the villus, differentiating into absorptive enterocytes, goblet cells or enteroendocrine cells. After about 4-5 days, they reach the top of the villi, undergo apoptosis ("anoikis") and are shed into the lumen [120]. In addition to migrating up the villi, some daughter cells will instead migrate down towards the base of the crypt to become Paneth cells. These Paneth cells secrete antimicrobials and other essential signals important for ISC protection and maintenance [121, 122].

While there is no question that ISCs represent the cells responsible for replenishing the intestinal epithelium, identifying the correct markers for this cell population has a controversial history. Through several lineage tracing techniques, it is becoming increasing appreciated that there are two populations of ISCs. One population, termed crypt base columnar (CBC) stem cells are located at the very base of the crypt among the Paneth cells. These CBC stem cells represent a rapidly dividing population responsible for baseline regeneration of the intestinal

epithelium [123]. The best known marker for these CBC stem cells is leucine-rich repeat containing G-protein coupled receptor (Lgr5) [119]. Sato et al. demonstrated that Lgr5+ cells are able to form self-renewing organoids in an *ex vivo* culture system while Lgr5+ low cells were not able to do so [124]. The second population of ISCs are the quiescent stem cells located at the +4 position from the base of the crypt termed label-retaining (LRC) stem cells. LRCs are thought to serve as a reserve of stem cells that are responsible for the regeneration of the intestinal epithelium after injury [125]. The best marker for LRCs is the Polycomb family member Bmil1 [126]. Although these cells may have a role in baseline regeneration, they are insensitive to Wnt signaling and are resistant to radiation injury [125]. The exact interplay between the CBC and LRC stem cells and their definitive contribution to epithelium regeneration is still not completely understood.

Among the ISCs are Paneth cells and stromal cells that are responsible for sensing and responding to environmental changes. These cells regulate ISC regeneration by providing several essential signals such as Wnt, Notch, bone morphogenetic proteins (BMPs) and hedgehog [127, 128]. Several studies have demonstrated the importance of these signals. For example, Wnt signaling promotes proliferation of ISCs and its signal is strongest near the base of the crypt and weakens as the cells migrate up the villus towards the lumen [129, 130]. When Wnt signaling is lost in a mouse model, proliferation in the crypts ceases and the epithelium is lost [131]. In addition, BMP signal decreases proliferation and its signal is thought to regulate proliferation of ISCs in the crypt. When mice lack the receptor for BMP (Bmpr1a), ISC proliferation goes uncontrolled resulting in hyperproliferation and crypt fission [132]. The proper balance of signals that form this crypt-stem cell niche are extremely important for ISC function and an optimal epithelial barrier.

**Paneth Cells** are specialized secretory cells located in the crypts of the small intestine. While most cells of the gut epithelium have a 4-5 day turnover, Paneth cells exist for about 60 days before being replaced [133]. They originate from the CBC stem cells but instead of migrating up the villi to differentiate into an absorptive enterocyte or goblet cell, they migrate downward to join the CBC stem cells at the base of the crypt. Paneth cells are most well known for being the main producers of antimicrobial peptides. These antimicrobials are stored in granules that are then released either constitutively or enhanced upon the sensing of microbial ligands [134, 135]. The most abundant antimicrobial secreted are the alpha defensins [136]. Defensin concentrations in the crypt lumen have been measured anywhere from 1-25 mg/mL [137]. Alpha defensins, lysozyme C, and sPLA4 are all secreted constitutively while REG3a and ANG4 (in mice) can have enhanced expression when induced by certain bacterial ligands [136]. The expression and secretion of these antimicrobials by Paneth cells serves the host in three important ways: (1) Keeps the lumen closest to CBC stem cells virtually free of microbes, (2) maintains a favorable microbial composition in the gut and (3) provides direct defense against enteric pathogens (Figure 1).

Because CBC stem cells are responsible for the maintenance of the epithelial gut barrier, it is extremely important that these stem cells function properly and remain unharmed by any potential pathogenic bacteria in the lumen. For this reason, Paneth cells secrete several antimicrobials that become concentrated by the mucus layer. Although the concentration of antimicrobials is high in the crypt, there has been evidence suggesting that these regions are not completely sterile. Some commensal bacteria are able to penetrate the mucus layer and are thought to resist attack from antimicrobials. These crypt associated bacteria were found to belong to the Acinetobacter and proteobacteria phyla [138, 139]. It has been suggested that

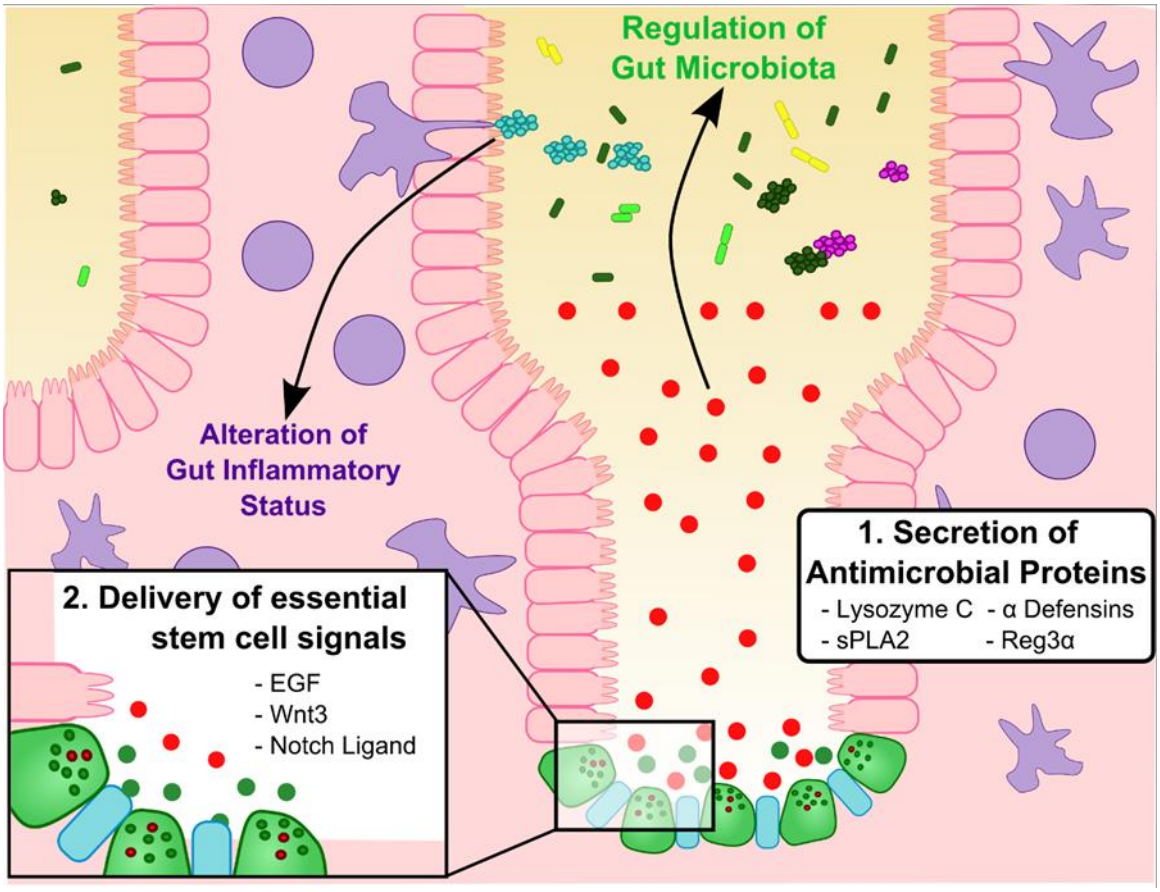


**Figure 1. Paneth cell function is critical for gut homeostasis.** Crypts in the small intestine contain crypt base columnar (CBC) stem cells. CBC stem cells rapidly proliferate and replenish the gut epithelium as intestinal enterocytes undergo rapid turnover. Located closely to the CBC stem cells are Paneth cells, which **(1)** secrete antimicrobial peptides and **(2)** provide several essential signals important for maintaining an optimal crypt stem cell niche. These signals (EGF, Wnt, and Notch ligand) promote CBC stem cell function and the proper replenishing of the gut epithelium [124].

crypt associated bacteria are responsible for reseeding the microbial community after various insults [138]. Although it is clear antimicrobial secretion by Paneth cells function to protect vulnerable cells such as intestinal stem cells, they are also capable of regulating which bacteria reside in the crypt. This regulation of microbial composition extends outside of the crypt region, having profound effects on the microbial population in the gut lumen and mucosa. In a mouse model lacking MMP7, the enzyme required for alpha defensin processing, changes in the major bacterial groups of the gut were observed. Compared to wildtype mice, the MMP7 deficient mice had an increased abundance of Firmicutes and a decrease in Bacteroidetes [89]. The opposite was true for transgenic mice expressing HD5. In addition, the total amount of bacteria in the gut remained unchanged [89]. This implies that Paneth cell secretion of antimicrobials function to regulate the dominant populations of bacteria in the gut. As alterations in microbial composition and dysbiosis are associated with the development of IBD, this underscores the importance of Paneth cells and their role in maintaining gut homeostasis. Lastly, antimicrobial secretion by Paneth cells is important for the defense against enteric pathogens. Again using the MMP7 deficient mice, the loss of alpha defensins rendered the mice more susceptible to *Salmonella* Typhimurium infection while the HD5 transgenic mouse had increased protection [116].

While antimicrobial secretion clearly plays a critical role in maintaining gut homeostasis, there has been a recent increase in appreciation for the role of Paneth cells in CBC stem cell function and numbers. Gene expression arrays confirm that Paneth cells produce large amounts of EGF, Wnt3, and Notch ligand Dll4 [17]. The importance of Paneth cell expression of these proteins is demonstrated in a minigut culture system. When sorted Lgr5+ CBC stem cells are grown ex vivo, they do not develop organoids. Organoids will only form if several

essential signals are added to the media. Remarkably, stem cells will also form organoids if they are co-cultured with Paneth cells [124]. This underlines the potential for Paneth cells to provide several essential signals for proper CBC stem cell function and proliferation. This relationship is further demonstrated by several *in vivo* models in which mice lacking Paneth cells also lack Lgr5+ stem cells [17, 122, 140].

When mutations in *NOD2* were discovered to have a high association with the development of Crohn's disease, much attention was placed on Paneth cells and their role in gut homeostasis- and rightfully so. Evidence suggests not only do these cells secrete antimicrobials that regulate the ever important gut microbiota, but they also provide essential help to the rapidly dividing stem cells that form the single cell membrane that separates the outside world from the rest of the human body **(Figure 1).**

Paneth cell secretion of antimicrobial proteins limits the amount of bacteria that survive in the crypt space and dictate the dominant phyla found in the small intestine [89]. Subsequently, Paneth cells can indirectly influence the systemic immune response [89]. Taken together, these contributions made by Paneth cells implicate their extreme importance in promoting gut homeostasis and the prevention of IBD.

**Inflammatory Bowel Disease**

Inflammatory Bowel Disease (IBD) is fundamentally characterized by inflammation of the gastrointestinal tract, resulting in pain, vomiting, diarrhea and weight loss. IBD encompasses two syndromes: Ulcerative colitis and Crohn's disease. The difference between these two syndromes relies mainly on the location and pattern of the inflammation. Ulcerative colitis involves acute inflammation restricted to the colon while Crohn's disease involves chronic, often granulomatous inflammation anywhere along the gastrointestinal tract. IBD has long been

associated with dysbiosis, or an unfavorable alteration in the microbial composition in the gut [141]. Usually this is characterized by a decrease in the diversity of microbial populations as well as the decrease in the amount of specific bacterial groups such as Clostridia [142-144]. Nonetheless, most bacteria implicated in the development of IBD have been species which are usually more closely associated with the epithelium and coated with secretory IgA [145]. Furthering this point, human studies have revealed that patients with IBD have an increased concentration of bacteria on the mucosal surface [146]. Although the unique bacterial compositions associated with IBD are a promising first step for developing treatments for IBD, it is still under question whether these differences initiate IBD pathogenesis or if they are a consequence of the disease [147].

Although it is unclear whether dysbiosis is a cause of IBD or a consequence, it is clear that Paneth cells play a major role in gut homeostasis and their dysfunction can lead to disease. Paneth cell dysfunction has the ability to cause IBD and they need to be considered when developing novel IBD therapies and preventatives. As discussed previously, mutations in *NOD2* are the strongest risk factor for the development of IBD [59, 60]. This bacterial sensor is highly expressed by Paneth cells and functions to regulate antimicrobial secretion and the expression of inflammatory cytokines. The importance of NOD2 in promoting gut homeostasis is made very clear in mouse models that spontaneously develop colitis in its absence. In addition to the link between NOD2 and development of disease, there is also strong evidence that Paneth cells regulate the composition of the gut microbiota. While transgenic HD5 mice display a significant shift in their dominant flora, they also lose SFB colonization after several hemizygous murine breading pairs [148]. Additionally, other models of Paneth cell dysfunction have increased levels of SFB colonization [148]. Taken

together, this demonstrates the importance of Paneth cell function on the microbial composition in the gut. Dysfunction in the sensing of microbes or secretion of antimicrobials can lead to an alternation in the gut flora. These alterations could lead to dysbiosis or the shift to pro-inflammatory bacteria such as SFB. As Paneth cells emerge as a pivotal player in both the regulation of the gut microbiota and the maintenance of CBC stem cells, their potential role in IBD pathogenesis is a topic of serious investigation.

The debilitating symptoms of IBD are the result of inappropriate immune responses to the commensal microbiota and the loss of tolerance to commensals [149, 150]. How one develops this loss of tolerance is under great debate and can clearly be different patient to patient. Potential factors include but are not limited to: diet, genetic background, immune system development following birth, and environmental insults [151]. While a majority of barrier damage seen with IBD is caused by immune cell infiltration in the gut, suboptimal epithelial barrier maintenance can also be a risk factor for developing the disease [152]. Increased paracellular permeability seen with the dysfunction in apical junctional complexes leads to increased levels of immune activation in the gut. Indeed, relatives of patients with Crohn's disease are more likely to have increased barrier permeability, but ultimately do not develop IBD [153]. It is proposed that barrier dysfunction is just one of the many risk factors that contribute to the development of disease [25].

Although there are several anti-inflammatory drugs that target the adaptive immune system, this sort of treatment is only sometimes successful for patients and only helps them manage their symptoms [7]. Improving current treatments should involve repair of the intestinal barrier and restoring proper function. To accomplish this, the field will need a much better understanding of how the human gut maintains an optimal barrier during homeostasis and after

injury. This chapter has introduced some of the most critical characteristics of the intestinal barrier, although our understanding of this complex yet ever-important epithelial lining is far from complete. Continuing to understand the complex mechanisms by which the gut barrier is maintained is a critical step in developing life-changing therapeutics for the 1+ million people living with IBD.

# Chapter 2

## Proline-rich acidic protein 1 (PRAP1) protects the gastrointestinal epithelium from irradiation-induced apoptosis

Alexandra A. Wolfarth[1], Xu Liu[2], Trevor M. Darby[3], Darra Boyer[1], Jocelyn B. Spizman[1], Joshua A. Owens[3], Bindu Chandrasekharan[1], Crystal R. Naudin[3], Krisztina Z. Hanley[1], Brian S. Robinson[1], Eric A. Ortlund[2], Rheinallt M. Jones[3,4], Andrew S. Neish[1,4,5]

Originally published in *CMGH,* Published online 7/3/2020, Pre-proof.

[1] Department of Pathology & Laboratory Medicine, Emory University, Atlanta, GA

[2] Department of Biochemistry, Emory University, Atlanta, GA

[3] Division of Gastroenterology, Hepatology and Nutrition, Department of Pediatrics, Emory University, Atlanta, GA

[4] Emory Microbiome Research Center, Emory University School of Medicine, Atlanta, USA.

[5] **Correspondence to**: Andrew S. Neish, Department of Pathology & Laboratory Medicine, Emory University, Atlanta, USA. Phone-404-712-4585; E-mail:aneish@emory.edu

**Abstract**

***Background & Aims:*** The intestinal epithelium must be resilient to physiochemical stress in order to uphold the physiological barrier separating the systemic compartment from the microbial and antigenic components of the gut lumen. Identifying proteins that mediate protection and enhancing their expression is therefore a clear approach to promote intestinal health. We previously reported that oral ingestion of the probiotic *Lactobacillus rhamnosus* GG (LGG) not only induced the expression of several recognized cytoprotective factors in the murine colon, but also many genes with no previously described function, including the gene encoding proline-rich acidic protein 1 (PRAP1). PRAP1 is a protein highly expressed in the epithelium of the gastrointestinal tract and we sought to define its function in this tissue.

***Methods:*** Purified preparations of recombinant PRAP1 were analyzed biochemically and PRAP1 antisera were used to visualize localization in tissues. *Prap1*$^{-/-}$ mice were characterized at baseline and challenged with total body irradiation and lastly, enteroids were generated to recapitulate the irradiation challenge *ex vivo*.

***Results:*** PRAP1 is a 17 kDa intrinsically disordered protein with no recognizable sequence homology. PRAP1 expression levels were high in the epithelia of the small intestine. While *Prap1*$^{-/-}$ mice presented only mild phenotypes at baseline, they were highly susceptible to intestinal injury upon challenge. After irradiation the *Prap1*$^{-/-}$ mice exhibited dramatically higher mortality rates with a significant increase in apoptosis and p21 expression in the small intestinal epithelium.

***Conclusions:*** PRAP1 is an intrinsically disordered protein highly expressed by the gastrointestinal epithelium and functions at exposed surfaces to protect the barrier from oxidative insult.

## Introduction

Induction of cellular protective pathways and the associated effector molecules is particularly important in tissues that are frequently exposed to environmental xenobiotics and oxidative stress, such as the gastrointestinal epithelium [4, 154, 155]. Such enterocytes are in intimate contact with the microbiota and their products as well as digestive components and ingested foodstuffs, requiring the epithelial cells perform their absorptive function while tolerating and responding to these exogenous stressors. When cells encounter exogenous insult that results in heightened oxidative stress and DNA damage, several pathways downstream of p53 activation determine cell fate and whether the cells will repair the DNA damage and continue in the cell cycle. In the case of overwhelming damage, they enact programmed cell death to safely eliminate injured cells [156, 157]. Improper response to exogenous insult can lead to compromised barrier integrity, allowing luminal components to traverse the epithelial layer to sub-epithelial compartments where they induce heightened localized or systemic inflammation that can result in a variety of pathological states [158-160]. Therefore, identifying proteins that promote proper epithelial response to exogenous insult and enhancing their expression is a subject of intense investigative focus.

It is increasingly appreciated that the normal resident gut microbiota plays a role in eliciting cytoprotection [161]. Corroborating this notion are studies showing that the intestines of germ-free mice that lack a microbiota are more susceptible to exogenous insult [4, 162]. Furthermore, ingestion of putatively beneficial bacteria, also known as ‘probiotics’, including *Lactobacillus rhamnosus* GG (LGG) are known to elicit cytoprotection in the gut [163]. To identify potential novel cytoprotective genes induced by LGG in the murine intestine, transcriptomic analysis was performed on the colon four hours after oral gavage. Among the

highest induced transcripts was a transcript coding for proline-rich acidic protein 1 (PRAP1) [4]. PRAP1 is a 17 kDa secreted protein with no recognizable sequence homology [164]. While *Prap1* was originally discovered to be highly expressed in the pregnant mouse uterus and later in the murine small intestine [165, 166], its function in the host remains largely unexplored. Studies using cultured transformed cell lines proposed that PRAP1 functions downstream of p53 signaling following DNA damage, with the disruption of PRAP1 function in this system rendering neoplastic cells more susceptible to chemotherapeutic agents [167]. Other studies described injection of pregnant mouse uteri with PRAP1 antisera and detected dysregulation in the expression of multiple proteins involved in apoptosis and inflammation, ultimately affecting embryo implantation [168]. While PRAP1 has been implicated in cell survival, apoptosis and response to injury, existing studies have yet to demonstrate *in vivo* PRAP1 function in the gastrointestinal tract.

We first aimed to characterize the structure and expression pattern of PRAP1 *in vivo*. We generated PRAP1 recombinant protein and PRAP1 antisera and found that PRAP1 is an intrinsically disordered protein highly expressed in the epithelia of the gastrointestinal tract in both mice and humans. To determine the function of PRAP1 we challenged germ line *Prap1*$^{-/-}$ mice with irradiation to show that PRAP1 protected the enterocytes from irradiation-induced apoptosis and that PRAP1 expression prolonged the survival of the mice after irradiation. Lastly, manipulation of PRAP1 expression in both enteroids and an epithelial cell line demonstrated PRAP1 significantly decreased epithelial expression of p21 and improved cell viability after irradiation. Together, these data show that PRAP1 functions *in vivo* to protect the gastrointestinal epithelium from oxidative insult.

## Results

### PRAP1 is an intrinsically disordered protein conserved in placental mammals

PRAP1 is a 17 kDa secreted protein comprised of 149 amino acids. The first 20 amino acids on the N terminus serve as a signal peptide while the remaining amino acids form the secreted portion of the protein (**Figure 1*A***). The amino acid sequence of the secreted protein does not have any detectable sequence homology with other proteins using the NIH Basic Local Alignment Search Tool (BLAST) analysis [164], and analysis of PRAP1 using PONDR-FIT (Predictors of Natural Disordered Regions) [169] predicts that PRAP1 has a high disordered score throughout the secreted portion of the protein and thus is predicted to be predominantly disordered (**Figure 1*B***). Analysis of recombinant PRAP1 on size exclusion chromatography revealed PRAP1 eluted at a considerably larger functional size than its predicted molecular weight (16,570 Da) (**Figure 1*C***). This suggests that PRAP1 is either multimeric or has an extended conformation which is a fundamental characteristic of intrinsically disordered proteins. We next used circular dichroism (CD) to identify secondary structures within PRAP1, which revealed a strong negative band near 200 nm, yet no significant signals around 208, 215 or 222 nm, indicating the absence of alpha helix or beta sheet in its secondary structure (**Figure 1*D***) [170]. Together, these data show that PRAP1 is intrinsically disordered, lacking any defined three-dimensional structure. To identify species that express PRAP1 orthologs, the human PRAP1 amino acid sequence was queried in the Comparative Genomics feature of Ensembl [171]. Of the 126 species considered, PRAP1 orthologs were present in 51 species, all of which were placental mammals **(Figure 1*E***). These data confirm that PRAP1 is indeed an intrinsically disordered protein, has no homology to other more functionally defined proteins and evolved relatively late in evolution, at the emergence of placental mammals.

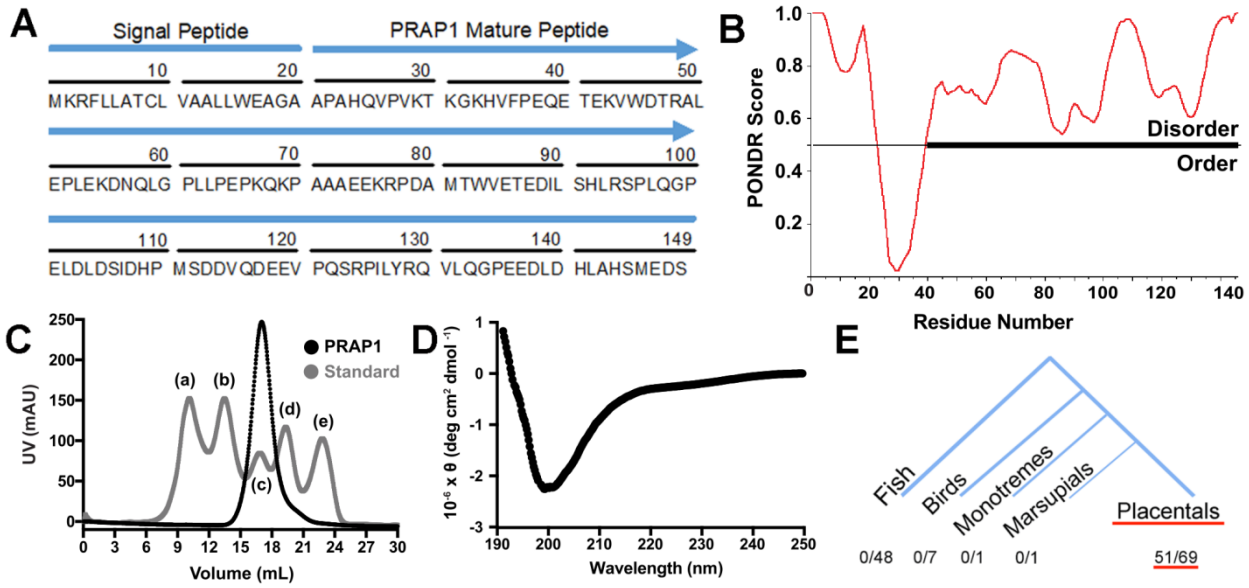


**Figure 1. PRAP1 is an intrinsically disordered protein conserved in placental mammals. (A)** Amino acid sequence of human PRAP1with signal peptide and secreted portion of the protein labeled. **(B)** Analysis of the PRAP1 amino acid sequence using the *Predictor* of Natural Disordered Regions (PONDR) software. The predicted ordered and disordered regions are plotted for each residue. **(C)** Size exclusion chromatogram of purified recombinant PRAP1 protein compared with a molecular weight standard: (a) Thyroglobulin (670,000 Da), (b) γ-globulin (158,000 Da), (c) Ovalbumin (44,000 Da), (d) Myoglobin (17,000 Da), and (e) Vitamin B12 (1,350 Da). **(D)** Circular dichroism spectra of recombinant PRAP1. **(E)** Analysis of the human PRAP1 amino acid sequence using the comparative genomics feature of Ensembl software. The number of PRAP1 orthologs identified in each taxonomic clade are indicated.

**PRAP1 is highly expressed in the epithelium of the gastrointestinal tract in mice and humans**

Before investigating the function of PRAP1, we first sought to define spatial and temporal PRAP1 tissue expression. We produced recombinant PRAP1 and generated highly specific PRAP1 antisera **(Supplemental Figure 1**). Immunoblot analysis and measurement of transcript levels in the mouse revealed that *Prap1* is highly abundant in the small intestine, with the relative abundance being 2-fold when compared to *β-actin* (**Figure 2*A* and *B***). *Prap1* expression was highest in the proximal small intestine with expression diminishing along the caudal axis, becoming nearly undetectable in the distal large intestine. Using PRAP1 antisera, we detected abundant PRAP1 protein expressed exclusively in the gut epithelium (**Figure 2*C***), with PRAP1 protein localization strongest in the perinuclear compartment of the cell (**Figure 2*D***). Tissue from *Prap1* whole-body knockout mice served as a negative control, confirming the specificity of our PRAP1 antisera. To determine whether the PRAP1 expression pattern was similar in both mice and humans, immunohistochemistry was performed on diagnostic biopsies of human ileum (**Figure 2*E***). Immunohistochemical (IHC) staining revealed high PRAP1 expression in the enterocytes of the human small intestine, consistent with the expression pattern we detected in mice. A human colonic biopsy served as a negative control and showed dramatically lower levels of PRAP1 staining in this tissue (**Figure 2*F***). Together, these data show that PRAP1 is highly expressed in the epithelium of the small intestine in both mice and humans.

In addition to high expression in the small intestine, qPCR analysis also detected highly variable *Prap1* expression in the murine uterus (**Figure 2*A***). To determine whether *Prap1*

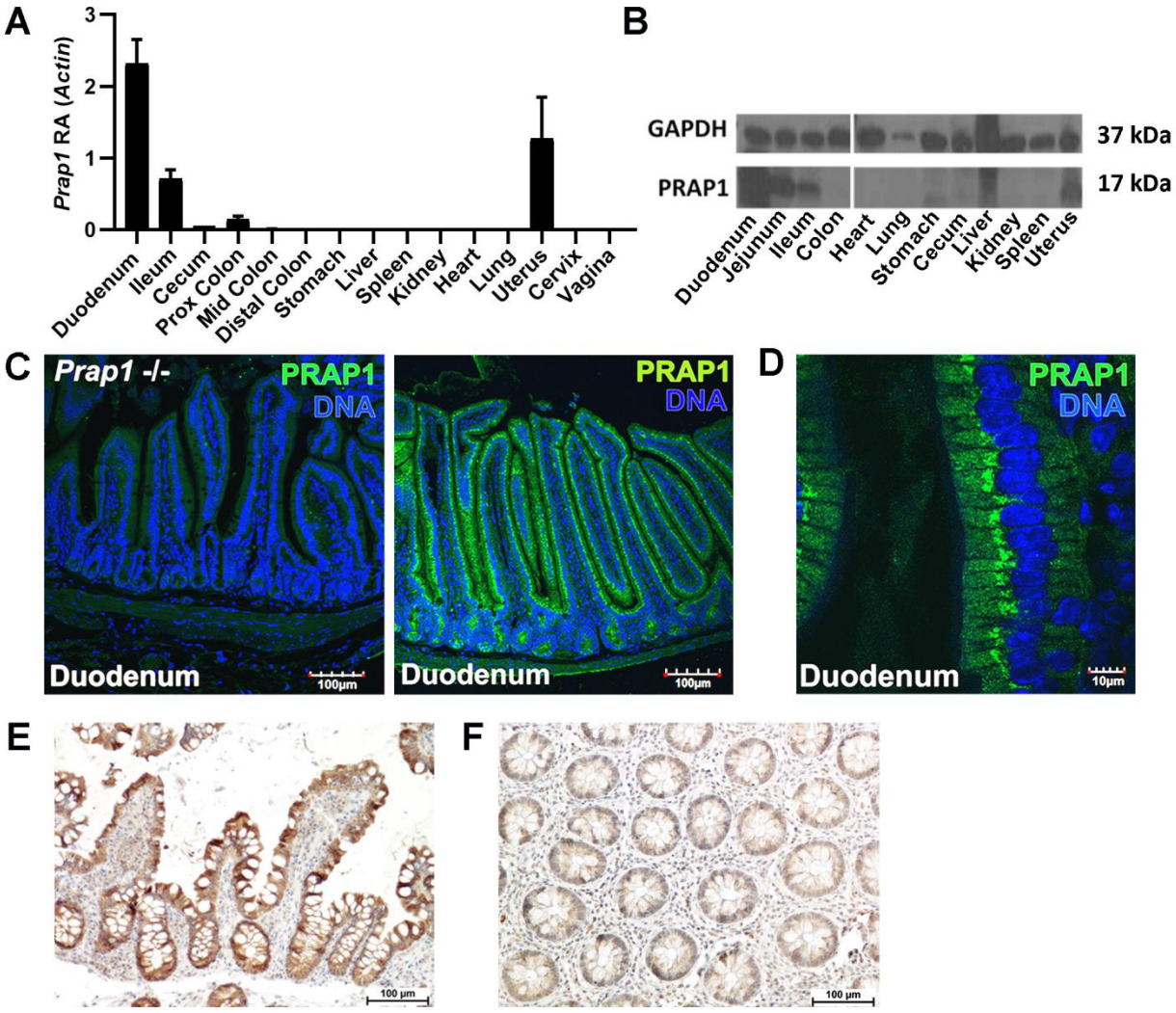
A
Prap1 RA (Actin)
3
2
1
0
Duodenum
Ileum
Cecum
Prox Colon
Mid Colon
Distal Colon
Stomach
Liver
Spleen
Kidney
Heart
Lung
Uterus
Cervix
Vagina
B
GAPDH
PRAP1
37 kDa
17 kDa
Duodenum
Jejunum
Ileum
Colon
Heart
Lung
Stomach
Cecum
Liver
Kidney
Spleen
Uterus
C
Prap1 -/-
PRAP1
DNA
Duodenum
100µm
PRAP1
DNA
Duodenum
100µm
D
PRAP1
DNA
Duodenum
10µm
E
100 µm
F
100 µm

(Legend for figure on previous page)

**Figure 2. PRAP1 is highly expressed by the epithelium of the gastrointestinal tract in mice and humans. (A)** Quantification of *Prap1* transcript measured via qPCR in the indicated tissues from 8-week-old wildtype C57BL/6 mice, n=3 mice. **(B)** Western blot analysis for the detection of PRAP1 protein abundance in the indicated tissues dissected from 8-week-old wildtype C57BL/6 mice. GAPDH was used as a loading control. Images are representative of three mice per tissue collected. **(C)** Immunofluorescence for the detection of PRAP1 (green) in the duodenum of 8-week-old wildtype C57BL/6 mice or *Prap1*$^{-/-}$ mice. Images are representative of the analysis of five mice per tissue collected. **(D)** Immunofluorescence staining of PRAP1 (green) in the duodenum of 8-week-old wildtype mice at 60X magnification. **(E and F)** Immunohistochemistry staining for the detection of PRAP1 [172] in the human ileum **(E)** and colon **(F)**. Image representative of 3 subjects.

expression changed during the hormonal cycle of the mouse, female wildtype mice were collected during each of the 4 hormonal stages: Proestrus, estrus, metestrus and diestrus. Both qPCR and western blot (**Supplementary Figure 2*A*, 2*B***) show PRAP1 extremely abundant only during the estrus stage of the cycle. This regulation of expression was also confirmed via immunofluorescence of murine uterine tissue, revealing abundant PRAP1 staining only in the estrus endometrium (**Supplementary Figure 2*C***). Visualization at high magnification confirm expression of PRAP1 in the endometrium of the uterus and abundant secretion into the luminal space (**Supplementary Figure 2*D***). We next sought to investigate this regulation in humans by obtaining sections of human endometrium curettings and staining them for PRAP1. Immunohistochemistry showed strong PRAP1 signal in the endometrium from women in the proliferative stage of their cycle, while PRAP1 staining was weaker in women during the secretory stage of their cycle (**Supplementary Figure 2*E***). Comparison of PRAP1 signal intensity during these two stages reveals a significantly higher PRAP1 signal during the proliferative stage, when the uterus is preparing for ovulation (**Supplementary Figure 2*F***). In summary, these data reveal that PRAP1 expression in the endometrium is conserved among mice and humans and is only expressed prior to ovulation.

### *Prap1*$^{-/-}$ mice have an altered gut microbiota and elevated inflammation

*Prap1* germline null mice were maintained in a specific pathogen-free barrier vivarium and monitored for any symptoms of spontaneous disease. *Prap1*$^{-/-}$ mice were successfully aged to 20 weeks and no spontaneous disease was apparent. At 10 weeks of age, the *Prap1*$^{-/-}$ mice displayed no difference in body weight, gut barrier architecture or in the expression levels of

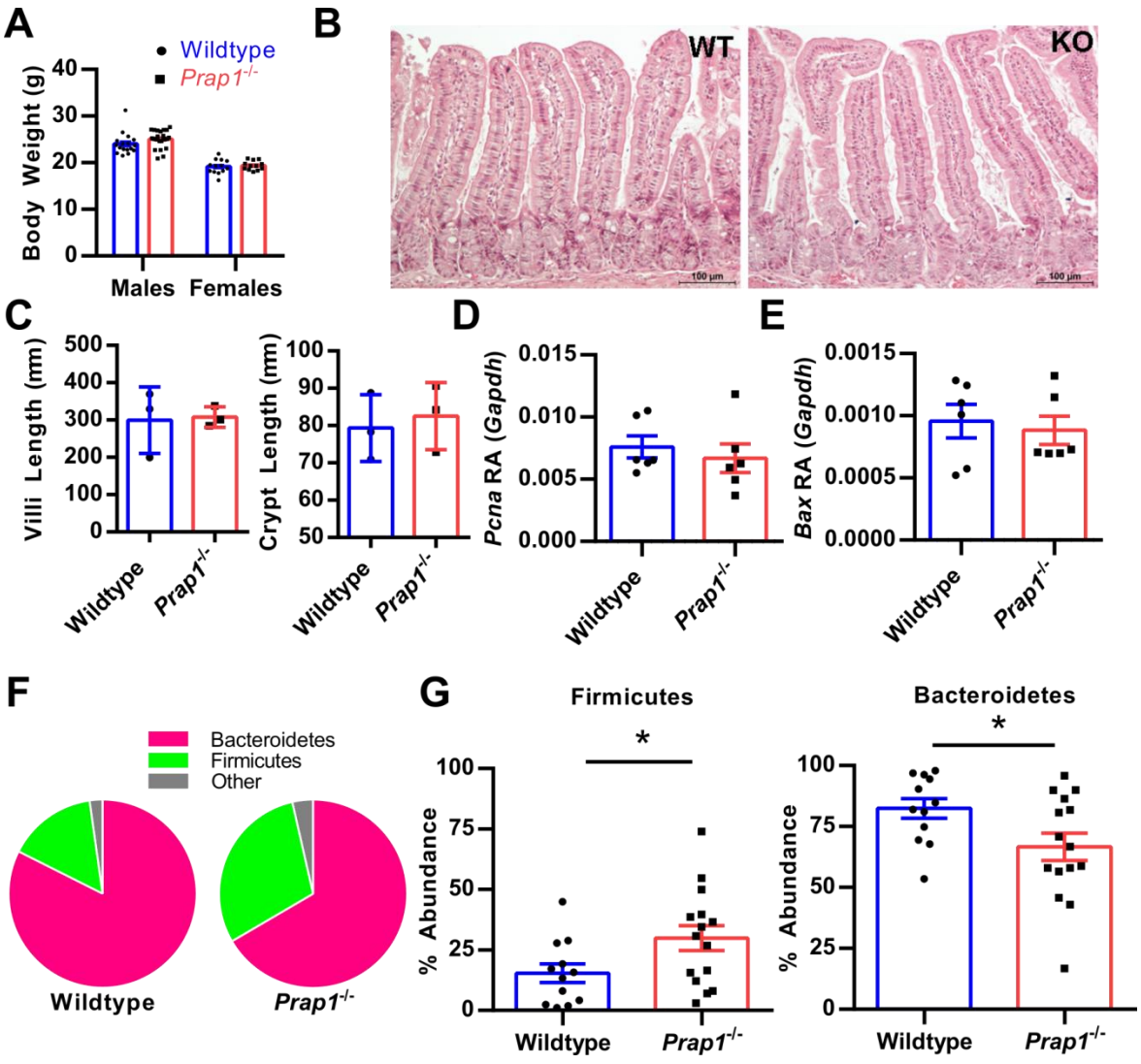
A
Wildtype
Prap1-/-
Body Weight (g)
40
30
20
10
0
Males
Females
B
WT
KO
100 µm
100 µm
C
Villi Length (mm)
500
400
300
200
100
0
Wildtype
Prap1-/-
Crypt Length (mm)
100
90
80
70
60
50
Wildtype
Prap1-/-
D
Pcna RA (Gapdh)
0.015
0.010
0.005
0.000
Wildtype
Prap1-/-
E
Bax RA (Gapdh)
0.0015
0.0010
0.0005
0.0000
Wildtype
Prap1-/-
F
Bacteroidetes
Firmicutes
Other
Wildtype
Prap1-/-
G
Firmicutes
*
% Abundance
100
75
50
25
0
Wildtype
Prap1-/-
Bacteroidetes
*
% Abundance
100
75
50
25
0
Wildtype
Prap1-/-

(Legend for figure on previous page)

**Figure 3. *Prap1*$^{-/-}$ mice have an altered microbiota in the small intestine. (A**) The body weight of wildtype and *Prap1*$^{-/-}$ littermates at 10 weeks old. **(B)** Hematoxylin and eosin staining of wildtype and *Prap1*$^{-/-}$ small intestine. Images representative of 3 mice per group. **(C)** Quantification of villi and crypt length in the small intestine of wildtype and *Prap1*$^{-/-}$ mice. Significance determined using unpaired t test, *=$p<0.05$. n= 3 mice. **(D and E)** qPCR analysis of *Pcna* **(D)** and *Bax* **(E)** expression in whole tissue from the small intestine of wildtype and *Prap1*$^{-/-}$ mice. Expression levels are relative to *Gapdh*. Significance determined using unpaired t test, *=$p<0.05$. n= 6 mice. **(F)** Pie chart comparison of the average Bacteriodetes:Firmicutes phyla ratio in the small intestine of wildtype and *Prap1*$^{-/-}$ littermates measured via 16S rRNA sequencing, n ≥12 mice. **(G)** Relative abundance of Firmicutes and Bacteroidetes in the small intestine of wildtype and *Prap1*$^{-/-}$ littermates. Significance determined using unpaired t test, *=$p<0.05$. n ≥12 mice. All data graphed as the mean ± SEM.

proliferative or pro-apoptotic proteins in the small intestine (**Figure 3*A*-*E***). To investigate whether the *Prap1*$^{-/-}$ mice have an altered gut microbiota, we sequenced the 16S rRNA gene from microbial DNA isolated from the small intestinal lumen of *Prap1*$^{-/-}$ and wildtype littermate controls. We detected a change in the ratio of Bacteriodetes:Firmicutes where wildtype mice had an average ratio of 82:15 and *Prap1*$^{-/-}$ mice had a statistically significant shift in this ratio, with an average ratio of 66:29 (**Figure 3*F* and 3*G***).

Because *Prap1*$^{-/-}$ mice had a significant shift in the abundances of dominant bacterial phyla, we next sought to determine whether the *Prap1*$^{-/-}$ mice had any significant inflammatory differences. To detect systemic inflammation at baseline, we measured the levels of pro-inflammatory cytokines in the sera using a multiplex ELISA that simultaneously detects the level of 10 proinflammatory cytokines. Sera collected from *Prap1*$^{-/-}$ mice had elevated levels of proinflammatory cytokines (**Figure 4*A***), with significantly higher IL-2, IL-4 and IL-12p70 (**Figure 4*B***). Along with elevated systemic cytokines, the *Prap1*$^{-/-}$ mice also had increased IL-12β transcript in colonic tissue (**Figure 4*C***). To determine the extent of local inflammation in the gut we measured the amount of secreted IgA and found there was no difference in the amount of secreted fecal IgA between wildtype and *Prap1*$^{-/-}$ littermates (**Figure 4*D***). To determine whether the altered microbiota and increased cytokine expression could be contributed to a defective gut barrier, we orally gavaged adult wildtype and *Prap1*$^{-/-}$ littermates with FITC dextran and collected the sera 4 hours later. There was no difference in serum FITC dextran, indicating no significant alteration in gut permeability (**Figure 4*E***). In summary, these data show that while *Prap1*$^{-/-}$ mice have an altered microbiota and elevated cytokine expression, they do not display any serious mucosal defects when unchallenged.

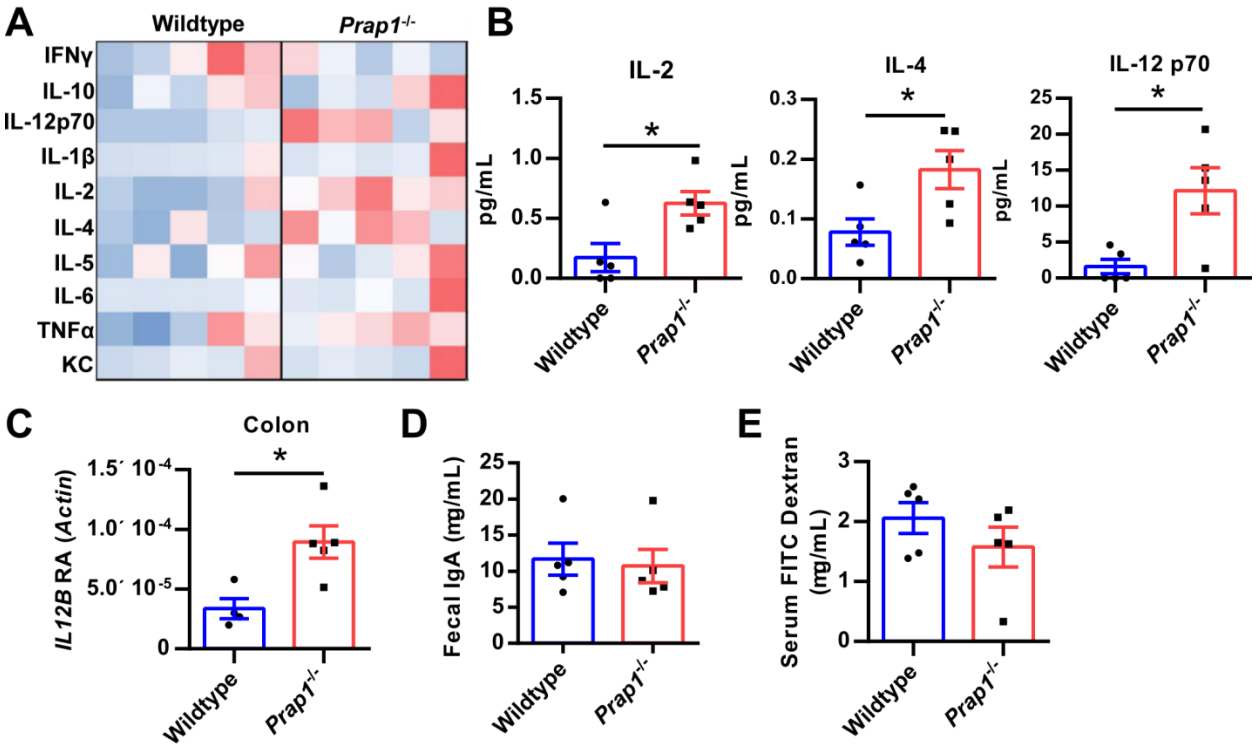


**Figure 4. *Prap1*$^{-/-}$ mice have elevated inflammation but no significant intestinal barrier defect. (A)** A multiplex ELISA was used for the detection 10 pro-inflammatory cytokines in sera of 10-week-old wildtype and *Prap1*$^{-/-}$ littermates. Data is displayed as a heat map, with red color indicating a higher than average concentration. Each column represents one mouse. **(B)** Graphical representation of significantly different cytokine levels shown in (A), including IL-2 (i), IL-4 (ii) and IL-12p70 (ii). Statistical significance determined using unpaired t test. *=$p<0.05$. n=5 mice. **(C)** Quantification of IL-12β transcript levels measured via qPCR in the colon of 10-week-old wildtype and *Prap1*$^{-/-}$ mice relative to the abundance of β-actin. Statistical significance determined using unpaired t test. *=$p<0.05$. n=5 mice. **(D)** Quantification of IgA levels in fecal pellets collected from 10-week-old wildtype and *Prap1*$^{-/-}$ mice, measured via ELISA. Statistical significance determined using unpaired t test. *=$p<0.05$. n=5 mice. **(E)** Quantification of FITC dextran in the sera of unchallenged 10-week-old wildtype and *Prap1*$^{-/-}$mice 4 hours after oral gavage with 4 kDa FITC dextran. Statistical significance determined using unpaired t test. *=$p<0.05$. n=5 mice.

***Prap1*$^{-/-}$ mice are more susceptible to radiological challenge**

Total body irradiation (TBI) introduces a significant amount of cellular oxidative stress that results in DNA damage and rapid apoptosis of dividing stem cells in the gastrointestinal epithelium. To investigate whether *Prap1*$^{-/-}$ mice were more susceptible to this exogenous insult, we challenged mice with a lethal dose of TBI. *Prap1*$^{-/-}$ females and males lost significantly more body weight when compared to wildtype littermate controls starting at 3 days after irradiation (**Figure 5*A***). Furthermore, *Prap1*$^{-/-}$ mice had significantly reduced viability after irradiation, with a median survival of 5 days while the wildtype controls had a median survival of 8 days (**Figure 5*B***). To compare early cellular injury in the small intestine of wildtype and *Prap1*$^{-/-}$ mice, apoptotic cells were labeled with TUNEL staining 6 hours after irradiation (**Figure 5*C***). At the tissue level, *Prap1*$^{-/-}$ mice had significantly more apoptotic cells per crypt compared to wildtype mice (**Figure 5*E***). To compare injury at a later time point, wildtype and *Prap1*$^{-/-}$ mice were sacrificed 72 hours after irradiation and the amount of apoptosis in the small intestine was measured via cleaved caspase-3 immunofluorescence. Again, the *Prap1*$^{-/-}$ mice had significantly higher levels of apoptosis in the epithelium of the small intestine compared to wildtype controls (**Figure 5*D* and *F***). By 96 hours after irradiation when *Prap1*$^{-/-}$ mice were approaching 75% initial body weight, their small intestine had a significantly higher amount of *Bax* expression, indicating a significant increase in apoptosis compared to wildtype controls (**Figure 5*G***). While the *Prap1*$^{-/-}$ mice had elevated apoptosis, they did not have any significant changes in *Pcna* expression, indicating no significant change in proliferation compared to wildtype controls (**Figure 5*H***). To determine whether the increased apoptosis in the *Prap1*$^{-/-}$ mice coincided with an increase in gut barrier permeability, we orally gavaged wildtype and *Prap1*$^{-/-}$ mice with FITC dextran 72 hours after TBI. Quantification of serum FITC dextran levels showed no difference

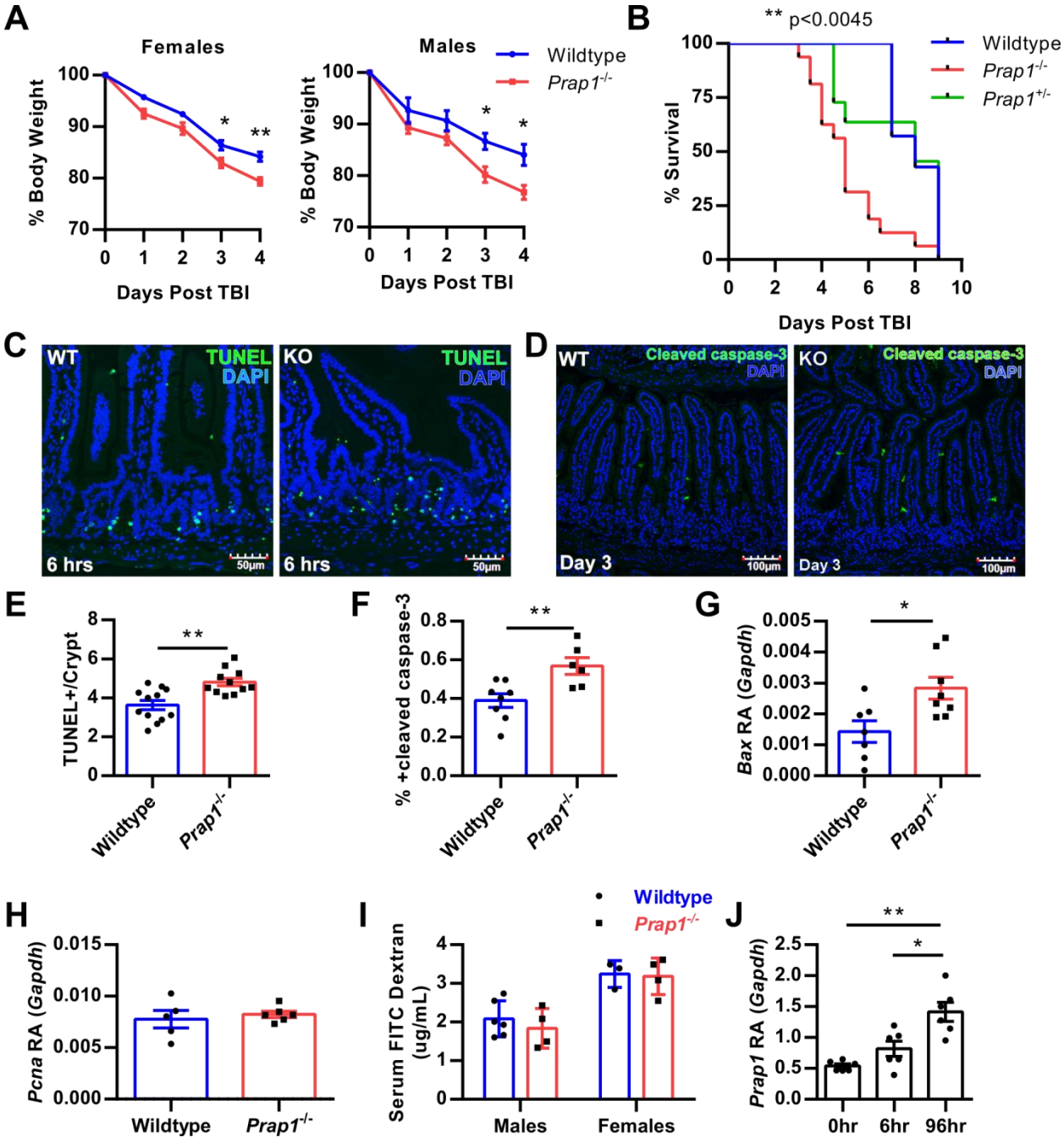
A
Females
Males
Wildtype
Prap1-/-
% Body Weight
Days Post TBI
B
** p<0.0045
Wildtype
Prap1-/-
Prap1+/-
% Survival
Days Post TBI
C
WT
KO
TUNEL
DAPI
6 hrs
50μm
D
Cleaved caspase-3
DAPI
Day 3
100μm
E
TUNEL+/Crypt
F
% +cleaved caspase-3
G
Bax RA (Gapdh)
H
Pcna RA (Gapdh)
I
Serum FITC Dextran (ug/mL)
Males
Females
J
Prap1 RA (Gapdh)
0hr
6hr
96hr

(legend for figure on previous page)

**Figure 5. *Prap1*$^{-/-}$ mice are more susceptible to radiological challenge and have increased apoptosis in the intestinal epithelium. (A)** Percent body weight loss of wildtype C57BL/6 and littermate *Prap1*$^{-/-}$ mice following 10 Gy total body irradiation (TBI). Statistical analysis represents comparison of wildtype vs. *Prap1*$^{-/-}$ on each respective day using Two-way ANOVA, Bonferroni's multiple comparisons test. *=p<0.05, **=P<0.01, n=4 mice. **(B)** Survival of wildtype, *Prap1*$^{+/-}$ or *Prap1*$^{-/-}$ mice following 10 Gy TBI. Statistical significance determined using the Log-Rank test, p=0.0045, n ≥11 mice. **(C)** Representative images of TUNEL-positive cells (green) within the small intestine of 8-week-old wildtype and *Prap1*$^{-/-}$ littermates 6 hours after receiving 10 Gy TBI. **(D)** Representative images of cleaved caspase-3 positive cells (green) within the small intestine of 8-week-old wildtype and *Prap1*$^{-/-}$ littermates 72 hours after receiving 10 Gy TBI. **(E)** Quantification of TUNEL-positive cells in (C). Significance determined using unpaired t test **=p < 0.005, n≥11 mice. **(F)** Quantification of cleaved caspase-3 positive cells in (F). Significance determined using unpaired t test **=p < 0.005, n≥6 mice. **(G)** Quantification of *Bax* transcript via qPCR on whole tissue from the small intestine of wildtype and *Prap1*$^{-/-}$ littermates 96 hours after 10 Gy TBI. Significance determined using unpaired t test *=p < 0.05, n=6 mice. **(H)** Quantification of *Pcna* transcript via qPCR on whole tissue from the small intestine of wildtype and *Prap1*$^{-/-}$ littermates 96 hours after 10 Gy TBI. Significance determined using unpaired t test, n=6 mice. **(I**) Quantification of serum FITC dextran in wildtype and *Prap1*$^{-/-}$ littermates after oral gavage with 4 kDa FITC dextran 72 hours after 10 Gy TBI. Significance determined using unpaired t test, n≥3 mice. All data graphed as the mean ± SEM. **(J)** Quantification of *Prap1* transcript via qPCR on whole tissue from the small intestine of wildtype mice at different time points following 10 Gy TBI. Significance determined using one-way ANOVA, Turkey's multiple comparisons test. **=p < 0.005, n=6 mice.

between wildtype and *Prap1*$^{-/-}$ mice, suggesting no significant change in gut barrier permeability at this particular time point (**Figure 5*I***). Lastly, wildtype mice significantly increased *Prap1* expression in the small intestine 96 hours after irradiation compared to unchallenged wildtype mice or mice 6 hours after irradiation (**Figure 5*J***). Taken together, these data show that PRAP1 expression protects the epithelium from irradiation-induced apoptosis 6 hours after challenge and this protection persists for days later, coinciding with increased expression of PRAP1 by the gut epithelium.

**PRAP1 protects enteroids from irradiation-induced apoptosis by limiting p21 expression**

To determine whether PRAP1 protection from irradiation could be observed in an isolated epithelial model, we harvested crypts from the small intestine of wildtype and *Prap1*$^{-/-}$ mice to culture enteroids *ex vivo*. On day 5 of culture, the enteroids were irradiated with 2 Gy and viability of the enterocytes was measured via the metabolic reduction of MTT to formazan. At 48 hours post-irradiation, the *Prap1*$^{-/-}$ enteroids had a significant decrease in the percent viability compared to wildtype controls (**Figure 6*A***). To determine whether this decrease in viability could be attributed to an increase in apoptosis, we stained the enteroids for cleaved caspase-3, 24 hours after irradiation (**Figure 6*B***). Enumeration of cleaved caspase-3 positive enteroids revealed *Prap1*$^{-/-}$ enteroids had a significantly higher percent undergoing apoptosis after irradiation (**Figure 6*C***). In summary, this data demonstrates that PRAP1 is capable of protecting the epithelium from irradiation-induced apoptosis in an isolated epithelial system.

Previous literature reports PRAP1 acts downstream of p53, protects neoplastic cells from chemotherapeutic agents and induces cell cycle arrest [167]. To further identify the mechanism by which PRAP1 protects cells from DNA damaging agents, we collected RNA from wildtype and *Prap1*$^{-/-}$ enteroids 24 hours after irradiation and compared expression of PRAP1 and multiple

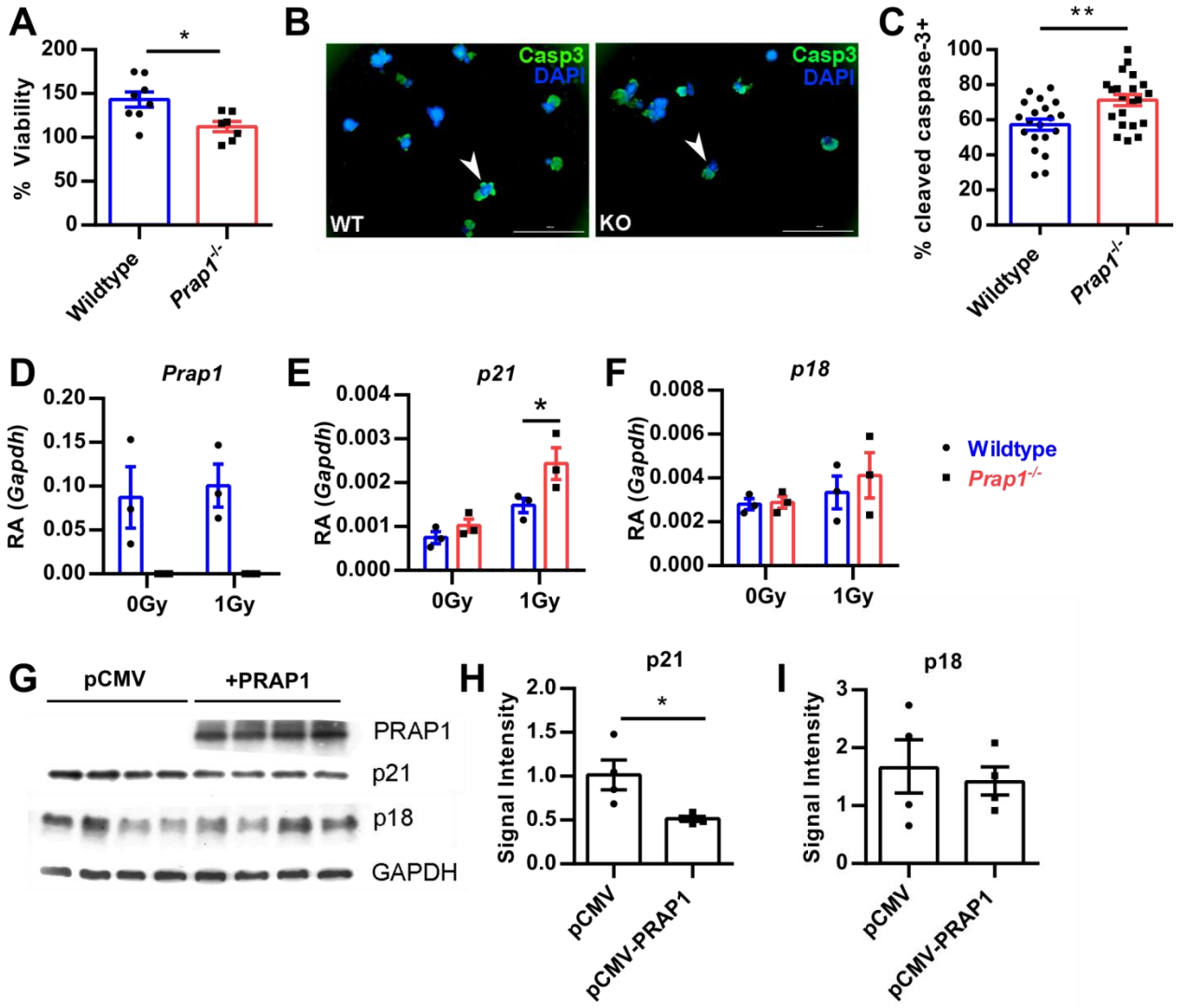
A
% Viability
200
150
100
50
0
*
Wildtype
Prap1-/-
B
Casp3
DAPI
WT
KO
C
% cleaved caspase-3+
100
80
60
40
20
0
**
Wildtype
Prap1-/-
D
Prap1
RA (Gapdh)
0.20
0.15
0.10
0.05
0.00
0Gy
1Gy
E
p21
RA (Gapdh)
0.004
0.003
0.002
0.001
0.000
*
0Gy
1Gy
F
p18
RA (Gapdh)
0.008
0.006
0.004
0.002
0.000
0Gy
1Gy
Wildtype
Prap1-/-
G
pCMV
+PRAP1
PRAP1
p21
p18
GAPDH
H
p21
Signal Intensity
2.0
1.5
1.0
0.5
0.0
*
pCMV
pCMV-PRAP1
I
p18
Signal Intensity
3
2
1
0
pCMV
pCMV-PRAP1

(legend for figure on previous page)

**Figure 6. PRAP1 protects enteroids from irradiation-induced apoptosis by limiting p21 expression.** **(A)** The percent viability of wildtype or *Prap1*$^{-/-}$ enteroids 48 hours after 2 Gy. Cell viability was measured using the addition of MTT and percent viability was calculated using the cell viability measured pre-irradiation. Significance determined using unpaired t test, *=$p < 0.05$, $n \geq 7$ wells. **(B)** Representative immunofluorescence images for the detection of cleaved caspase-3 in wildtype and *Prap1*$^{-/-}$ enteroids 24 hours after 2 Gy. Examples of cleaved caspase-3 positive enteroids are denoted with a white arrowhead. Scale bar = 1000 µm. **(C)** Quantification of cleaved caspase-3 positive enteroids in (B). Each data point represents the percent cleaved caspase-3 positive enteroids in a well. Data pooled from 4 independent experiments. Significance determined via unpaired t test, *=$p < 0.05$, n=4 mice per group. (**D-F**) Quantification of *Prap1* **(D)**, *p21* **(E)** and *p18* **(F)** transcript via qPCR in wildtype and *Prap1*$^{-/-}$ enteroids 24 hours after 0 Gy and1 Gy. Significance determined via unpaired t test, *=$p < 0.05$, each data point represents enteroids harvested from a unique mouse, n=3 mice per group. **(G)** Protein levels determined via western blot from epithelial cells transfected with pCMV (empty vector) or pCMV-PRAP1 48 hours after 8 Gy. **(H-I)** Quantification of p21**(H)** and p18 **(I)** protein levels in (G) determined via signal intensity relative to GAPDH. Significance determined using unpaired t test, *=$p > 0.05$, n=4. All data graphed as mean ± SEM.

other proteins known to be important for cell cycle arrest. As expected, the wildtype enteroids had strong PRAP1 expression both before and after irradiation (**Figure 6*D***). Interestingly, while both wildtype and *Prap1*$^{-/-}$ enteroids displayed an increase in *p21*$^{WAF1/Cip1}$ expression after irradiation, the *Prap1*$^{-/-}$ enteroids had significantly higher *p21* expression compared to wildtype controls (**Figure 6*E***). Expression of other proteins important for cell cycle arrest such as *p18*$^{Ink4c}$ was not different between wildtype and *Prap1*$^{-/-}$ enteroids (**Figure 6*F***). To determine whether this difference in p21 expression could be observed in a different epithelial model that was more conducive to the measurement of protein expression by western blot, we transiently overexpressed human PRAP1 in a human epithelial cell line. After 24 hours of PRAP1 overexpression, the cells were irradiated with 8 Gy and cell lysate was collected 48 hours later (**Figure 6*G***). Consistent with our findings in the enteroids, western blot analysis revealed the cells overexpressing PRAP1 had significantly less p21 protein after irradiation (**Figure 6*H***) and no difference in p18 (**Figure 6*I***). Taken together, these data show that PRAP1 protects the epithelium from irradiation-induced apoptosis by limiting the amount of p21 expression after challenge.

**Discussion**

We report for the first time that PRAP1 is an intrinsically disordered protein that is highly expressed in the small intestine of mice and humans. At homoeostasis, *Prap1* null mice exhibit mild physiological differences, with elevated cytokine levels and an altered gut microbiota. However, *Prap1* null mice are significantly more susceptible to oxidative insult by ionizing radiation, exhibiting increased mortality and enterocyte apoptosis. Additionally, *Prap1*$^{-/-}$ enteroids are more susceptible to irradiation-induced apoptosis and have elevated p21

expression. These data show that PRAP1 functions as an important component of the epithelial response to oxidative insult.

The study of intrinsically disordered protein (IDP) structure and function is inherently complex because the extended structure of IDPs is flexible and dependent on their environment and subcellular location [173]. Several IDPs have been shown to regulate cell signaling pathways, as their flexible conformation allows them to bind regulatory proteins with disparate functions. The ability of IDPs to weakly bind multiple proteins allows them to facilitate the assembly of cellular signaling complexes that control pathway signaling [173]. For example, p21 is a 21 kDa intrinsically disordered protein that has the ability to bind and regulate several Cdk-cyclin complexes and ultimately regulates cell cycle progression [174]. The ability to bind several proteins affords multiple functions and the regulation of a variety of complexes. Additionally, IDPs have also been implicated in the formation of hydrogels by regulating liquid phase transitions, as well as the formation of nonmembrane-bound intracellular granules [175]. Given the intracellular peri-nuclear localization of PRAP1 in the intestinal epithelial cells, it is possible that PRAP1 functions intracellularly to assemble proteins that function in cell signaling, ultimately regulating the cellular response to oxidative stress and cell cycle progression. In addition, there is a signal peptide on the N terminus of PRAP1, and our laboratory and others have found that PRAP1 is secreted at relatively high levels into the supernatant of cultured cells [176]. It may be possible that like many other IDPs, PRAP1 has multiple functions that are dictated by cellular location and the presence of interacting proteins.

The discovery of novel effector proteins that protect from exogenous insults is a challenging endeavor because the function of these proteins is not apparent *in vivo* at homeostatic conditions. For example, experimental rodents are generally maintained in

conditions that minimize exposure to xenobiotic agents or pathogenic microbes [177]. As a result, mice that are null for proteins that confer protection often do not exhibit any spontaneous phenotypes**.** Rather, it is only in response to exogenous insults that these null mice reveal phenotypes, typically manifested as increased susceptibility, or failure to recover following insult [178, 179]. Although *Prap1*$^{-/-}$ mice exhibited normal epithelial proliferation, apoptosis and gut permeability at baseline, there were signs of suboptimal intestinal function, as inflammatory markers were elevated and the upper GI microbiota was altered. After challenge with irradiation, underlying suboptimal intestinal functions were exaggerated with a significant increase in epithelial apoptosis, without corresponding increase in proliferation. While irradiation is not a naturally occurring challenge for the intestinal epithelium, the mucosa commonly encounters exogenous stressors that increase oxidative stress and this is especially true for the small intestinal epithelium where PRAP1 expression is highest. The small intestine must tolerate a myriad of stressors that are introduced by digestive processes, nutrient absorption and microbial contact [180]. Importantly, these stressors have the potential to significantly increase with a change in diet or gastrointestinal infection [181-183]. Discovering proteins critical to the epithelial response to oxidative insult has the potential to identify therapeutic targets to prevent tissue damage that ultimately results in a leaky gut phenotype. This occurs following the breakdown of the epithelial barrier of the gastrointestinal tract, increasing translocation of luminal antigens, microbes and their products which leads to increased local and systemic inflammation[184]. In this study, identifying a protective function for PRAP1 in the gut may allow for the development of effective therapeutics that augment the function of PRAP1, and thereby enhance protection against exogenous stressors.

Although this study focuses on PRAP1 function in the intestine, its function in the uterus remains to be described. PRAP1 is only found in placental mammals suggesting its function in the uterus is involved in a process specific to uterine implantation. Interestingly, PRAP1 was highly expressed in the uterus during estrus, when the female is ovulating and most receptive to mating. Estrus is a stage in the hormonal cycle when the epithelial lining of the uterus has just finished undergoing proliferation (proestrus) and starts to undergo apoptosis [185, 186]. Because PRAP1 expression in the uterine epithelium is so strongly correlated with dramatic changes in apoptosis and proliferation, it is plausible that PRAP1 has a role in protecting the uterine epithelial barrier during these processes. Further studies measuring apoptosis in the *Prap1*$^{-/-}$ uterus during the different cycle stages and after challenge will be extremely valuable in understanding PRAP1 function in the endometrium.

To elucidate the protective role of PRAP1 in the intestine, we used total body irradiation (TBI) as a model of exogenous challenge to the intestinal epithelium. TBI generates a large amount of oxidative stress, inducing rapid apoptosis of vulnerable proliferating cells in the bone marrow and intestinal crypts [172]. Loss of the cellular immune system and a compromised intestinal barrier is a combination that leads to rapid weight loss, lack of fluid retention and increases the risk of developing systemic bacterial infection [172, 187]. While we did not detect an increase in gut permeability 72 hours after irradiation via FITC dextran in the *Prap1*$^{-/-}$ mice, we did observe a significant increase in survival in the wildtype mice after a lethal dose of irradiation compared to the *Prap1*$^{-/-}$ littermates. It is probable that a significant defect in gut barrier due to excessive apoptosis immediately precedes necessary endpoints for humane euthanasia of the mouse, therefore making differences in gut permeability difficult to accurately measure. Although apoptotic cells in the epithelium can be quickly replaced by neighboring

epithelial cells [157], we did not see a corresponding increase in *Pcna* expression in the *Prap1*$^{-/-}$ tissue. Additionally, we found a significant increase in the expression of p21, a protein critical to regulating cell cycle regulation. In summary, the *Prap1*$^{-/-}$ epithelium exhibits increased apoptosis for days after irradiation in combination with dysregulation of a critical cell cycle regulating protein, ultimately affecting survival of the *Prap1*$^{-/-}$ mice.

The limitations of the current study are that the complete molecular mechanism whereby PRAP1 confers protection from irradiation remains enigmatic. Because PRAP1 is an IDP, it is likely that PRAP1 has multiple functions and has many interacting proteins based on the localization and disease context. In an *in vitro* model, others have shown PRAP1 to be downstream of p53 activation and that PRAP1 was required to arrest cells in the cell cycle following treatment with fluorouracil, ultimately resulting in less DNA damage and less caspase-dependent apoptosis [167]. Consistently, we observed decreased viability and increased apoptosis in the *Prap1*$^{-/-}$ enteroids following irradiation. Recapitulating the *in vivo* phenotype with *ex vivo Prap1*$^{-/-}$ enteroids reveals that the mechanism of PRAP1 protection is intrinsic to the epithelium and does not require other systemic host processes to function. Interestingly, both the enteroids and an epithelial cell line had decreased p21 expression in the presence of PRAP1 after irradiation. Although p21 has been shown to bind and affect several different signaling complexes and pathways (attributed to the fact that p21 is also an IDP [188]), existing literature consistently shows that p21 can have dual effects regarding the induction of apoptosis. In the context of UVB irradiation, overexpression of p21 led to increased apoptosis in keratinocytes [189]. Additionally, others have shown that p21 overexpression increased apoptosis of cancer cells and rendered them more susceptible to chemotherapeutic drugs [190, 191]. Here, our data shows that PRAP1 significantly limits p21 expression, thereby preventing irradiation-induced

apoptosis. Future studies involving the identification of PRAP1 interacting proteins in intestinal epithelial cells will be extremely valuable in defining the mechanism by which PRAP1 limits p21 expression and protects from oxidative insult.

## Methods

### Production of Recombinant PRAP1

The coding sequence for the secreted form of mouse PRAP1 protein (AA 21-149) was cloned into a pET28a vector with a 6xHis tag on the N terminus of the protein generating pET28a-6xHis-PRAP1. This plasmid was transformed into *E. coli* and expression of PRAP1 was induced using 1M Isopropyl β- d-1-thiogalactopyranoside (IPTG) at 30 °C for 4 hours. *E. coli* was lysed using 6M guanidine and solubilized with 10M urea. His6x-PRAP1 protein was purified using Ni-NTA agarose and buffered exchanged into PBS. For further purification and analysis, PRAP1 protein was loaded onto a size-exclusion chromatography column S200 10/300 at 0.5 ml/min and equilibrated in PBS. The S200 10/300 column was calibrated with a molecular weight standard containing Thyroglobulin (670,000 Da), γ-globulin (158,000 Da), Ovalbumin (44,000 Da), Myoglobin (17,000 Da), and Vitamin B12 (1,350 Da) (Biorad, Hercules, CA) (**Figure 1*C***).

### Circular Dichroism

Circular dichroism (CD) spectroscopy was monitored by a J-810 CD spectropolarimeter (Jasco, Easton, MD) to examine PRAP1 secondary structure. PRAP1 protein was dialyzed overnight in phosphate buffer (50 mM NaPO4, 15 mM NaCl, pH 6.8) at a concentration of 0.44 mg/ml for all measurements. The CD signal and molar ellipticity was measured from 190 to 260 nm with a 1 mm quartz cuvette at 25 °C. Data shown is the average of three spectral scans and after buffer subtraction.

**Quantitative RT-PCR Analysis**

Murine tissue was homogenized in TRIzol reagent (Invitrogen, Carlsbad, CA) and RNA was isolated using the phenol-chloroform extraction method. cDNA was made using the iScript Reverse Transcription Supermix (Biorad, Hercules, CA). Real-time PCR analysis was then performed using the iQ SYBR Green Supermix on a *MyiQ*™ Real time PCR system (Biorad, Hercules CA). *β-Actin* and *Gapdh* were used as housekeeping genes where indicated and all quantification is displayed as relative abundance to *β-Actin* or *Gapdh* using the delta-delta Ct analysis (ΔΔCT) method. The primer sequences used are below:

*Prap1* 5'-ATCTACAGCTTCGCCATTCG-3', 5'-GTTTGCCTTTGGTCTTGACAG-3'.

*Gapdh* 5'-TCTCCCTCACAATTTCCATCC-3', 5'-GGGTGCAGCGAACTTTATTG-3'

*Actin* 5'-ACCTTCTACAATGAGCTGCG-3', 5'-CTGGATGGCTACGTACATGG-3'

*Pcna* 5'-GGCTCTCAAAGACCTCATCAA-3', 5'-GAGTAAGCTGTACCAAGGAGAC-3'

*Bax* 5'-CAAGAAGCTGAGCGAGTGTC-3', 5'-GTCCACGTCAGCAATCATCC-3'

*IL-12* 5'-GATGTGTCCTCAGAAGCTAACC-3', 5'-CCAGTCCACCTCTACAACATAAA-3'

*p21* 5'-GTTCCTTGCCACTTCTTACCT-3', 5'-TCATCCTAGCTGGCCTTAGA-3'

*p18* 5'-TAGCCTGATGGAGGCAAATG-3', 5'-CGGACAGCCAACCAACTAA-3'

**Production of PRAP1 Antisera**

Full-length mouse PRAP1 recombinant protein was injected into rabbits for 70 days, whereupon antibodies were generated and serum was collected following the standard polyclonal package protocol undertaken by Pocono Rabbit Farms (Canadensis, PA). Rabbit PRAP1 antisera was aliquoted and stored at -80 °C. PRAP1 specificity was confirmed via immunofluorescence and immunoblot analysis of tissue samples from wildtype and *Prap1*$^{-/-}$ mice.

### *Prap1* Whole Body Knockout Mice

*Prap1* whole body knockout mice (Strain: B6;129S5-Prap1$^{tm1Lex}$/Mmucd, 032532-UCD), originally generated by Genentech, have all 5 exons of the *Prap1* gene targeted by homologous recombination. The mice were resuscitated by MMRRC-UC Davis (Davis, CA). *Prap1* heterozygous mice were then shipped from MMRRC-UC Davis and housed within a specific pathogen free facility at Emory University (Atlanta, GA). *Prap1* heterozygous mice were then backcrossed with wildtype C57BL/6 mice (Jackson Laboratories, Bar Harbor, ME) until the mice were determined to be fully congenic using the Speed Congenics 128 SNP Panel (Charles River, Wilmington MA). The *Prap1*$^{-/-}$ mouse colony was maintained with heterozygous breeding pairs to provide wildtype littermate controls for all experiments. All animal procedures were approved by the Institutional Animal Care and Use Committee of Emory University.

### Immunoblot Analysis

Immunoblot analysis using the PRAP1 antisera was performed on harvested murine tissues as previously described [192]. PRAP1 protein was detected using a 1:1000 dilution of PRAP1 antisera generated by the lab (see above) in 5% milk made in TBST.

### Immunofluorescence

Murine tissues were harvested and immediately fixed in methacarn solution to preserve any luminal material. Tissues were embedded in paraffin and sectioned at 5 microns. Sections were rehydrated in xylene and ethanol baths before undergoing a blocking step with 5% bovine serum albumin (BSA) in PBS. The primary antibody was diluted in 5% BSA and added to the section overnight at 4 °C. The secondary antibody conjugated to an Alexa Fluor was diluted 1:1000 in 5% BSA and added to the sections for 1 hour at room temperature. DAPI diluted 1:1000 in 5%

BSA was added as a counterstain for 5 minutes before the sections were mounted with Prolong Antifade Mountant (Invitrogen, Carlsbad, CA) and stored long term at -80℃. Slides were washed three times in PBS after each staining step. Images were captured on an FV1000 confocal microscope (Olympus, Tokyo, Japan).

**Hormonal Staging of Female Mice**

Wildtype C57/BL6 female mice at 8 weeks old were subjected to male bedding and monitored for hormonal cycling. The hormonal stage was determined by visual examination of the vaginal opening[193]. Upon sacrifice at each of the hormonal stages, the uterus and vagina were prepared for histology and the hormonal stage of each mouse was confirmed by hematoxylin and eosin staining.

**Immunohistochemistry Staining on Human Sections**

Diagnostic curettings of de-identified human tissue were obtained in collaboration with Dr. Krisztina Hanley and Dr. Brian Robinson (Emory University, Atlanta, GA). Immunohistochemistry was performed by the Cancer Tissue and Pathology Core at Emory University (Atlanta, GA). Human PRAP1 was visualized using a commercially available polyclonal antibody (Proteintech, Rosemont, IL) diluted 1:400. Quantification of PRAP1 signal in the endometrium was performed by measuring the average pixel intensity within the epithelium using ImageJ (National Institutes of Health, Bethesda, MD).

**Histological Assessment of Intestinal Architecture**

Murine proximal small intestine was fixed with formalin and embedded in paraffin before sectioning and staining with hematoxylin and eosin. Approximately 20 independent villi and crypt lengths were obtained from bright-field microscope images using ImageJ (National Institutes of Health, Bethesda, MD).

**Microbiota analysis**

Luminal content from the distal ileum of mice was collected and microbial DNA was isolated using the QIAmp Stool DNA mini kit (Qiagen, Hilden, Germany). Preparation of 16S samples was performed as reported previously[194]. PCR amplification of the 16S rRNA V4 region was performed using the 515F/806R primer pair (GTGCCAGCMGCCGCGGTAA and GGACTACHVGGGTWTCTAAT) with a unique 12-base Golay barcode on each reverse primer. DNA concentration was measured using a Qubit fluorometer (Thermofisher, Waltham, MA) and ran on a bioanalyzer to confirm a single 16S band. The DNA was pooled at equimolar ratios and then sequenced using an Illumina Miseq sequencer at the Emory Integrated Genomics Core (Emory University, Atlanta, GA). Read counts for each sample were generated by uploading the raw sequence files to Illumina's 16S Metagenomics Application on the BaseSpace Sequence Hub platform (San Diego, CA).

**Measurement of Cytokines and Fecal IgA**

Cytokine levels in whole serum from 10-week-old mice were measured using the V-PLEX Proinflammatory Panel 1 Mouse Kit (Meso Scale Discovery, Rockville, Maryland) following manufacturer's protocol with the help of the Emory Multiplexed Immunoassay Core (Emory University, Atlanta, GA). For Fecal IgA, fecal pellets were collected from adult mice and vortexed in PBS with 5mM EDTA to a final concentration of 0.1 mg feces/mL. The samples were then centrifuged at 6,000 g for 10 minutes and the supernatant was removed. An IgA ELISA kit (Invitrogen, Carlsbad, CA) was used to quantify the amount of mouse IgA present in the supernatant following manufacturers protocol.

**Measurement of Intestinal Permeability**

Adult mice (8 weeks old) were fasted for 12 hours and orally gavaged with 10 mg fluorescein isothiocyanate conjugated dextran (FITC-dextran, 4 KDa) dissolved in PBS. After 4 hours the mice were sacrificed and serum was diluted 1:4 with PBS. Quantity of FITC-dextran was determined by using a spectrophotometer capable of 485 nm excitation and 528 nm emission. Final concentration was calculated by comparing to a FITC-dextran standard curve. For irradiation experiments, mice were fasted for 4 hours on day 3 before oral gavage with FITC-dextran.

**Total Body Irradiation Challenge**

*Prap1*$^{-/-}$ and wildtype littermate controls at 8 weeks of age received 10 Gray of radiation (225 kV and 17.7mA) using a RS2000 X-ray irradiator (Rad Source Technologies, Buford, GA). Weight loss was monitored daily and the mice were sacrificed once they reached 75% of their initial body weight. Apoptotic cells were visualized in tissues sections collected 6 hours after radiation challenge using the In Situ Cell Death detection kit (Roche, Basel, Switzerland) and quantified by counting the number of positive cells per crypt in 10 random fields of view per mouse ($n \geq 9$ mice) at 400X total magnification on an FV1000 confocal fluorescence microscope (Olympus, Tokyo, Japan). Cleaved caspase-3 positive cells were visualized 72 hours after radiation challenge using the polyclonal cleaved caspase-3 antibody from Cell Signaling (Danvers, MA). Using a total magnification of 200X, the number of positive cells in 120 random villi was enumerated for each mouse ($n \geq 6$ mice) and assuming an average of 86 enterocytes per villi, the proportion of positive cells was calculated.

**Generation of Enteroids**

Enteroids from wildtype and *Prap1*$^{-/-}$ littermates were generated using the IntestiCult™ Organoid Growth Medium (Mouse) from StemCell Technologies (Vancouver, Canada) following manufacturer's provided protocol. Briefly, the entire length of the small intestine was dissected, washed and digested for the collection of small intestinal crypts. The crypts were enumerated and combined with a 1:1 ratio of Intesticult Organoid Growth Medium and Matrigel (Corning, Tewksbury, MA). Media was refreshed every 2 days and enteroids were passaged every 7 days. For irradiation experiments, enteroids were irradiated on day 4-5 of culture.

**Assessment of Enteroid Viability**

Enteroid viability was assessed by quantification of 3-(4,5-dimethylthiazol-2-yl)-diphenyltetrazolium bromide (MTT) reduction to formazan following the protocol described by Grabinger et al. [195]. Briefly, after treatment with either irradiation or a staurosporine positive control, sterile MTT was added at a final concentration of 500 ug/mL for 1 hour at 37 °C. Cell media was then replaced with 2% SDS to digest the matrigel and then DMSO was added to solubilize the formazan. Each well was then read at 563 nm using a spectrophotometer and the positive control OD was subtracted from each reading. The percent viability was calculated by dividing the OD of the treatment wells by the OD of untreated wells, multiplied by 100.

**Whole Mount Immunofluorescence Staining of Enteroids**

The immunofluorescence staining protocol was adapted from O'Rourke et al[196] and modified for staining and imaging in a 96 well plate. Enteroids were grown and treated in 96 well plates and on the day of staining, media was replaced with 80 µL 4% paraformaldehyde and fixed for 20 minutes at room temperature. Enteroids were then washed with IF buffer and permeabilized

for 20 minutes at room temperature with 80 µL 0.5% Triton X-100 in PBS. By this point, the matrigel is dissolved and the enteroids remain attached to the bottom of the well. After washing with IF buffer, the enteroids were blocked for 30 minutes at room temperature with 5% BSA in PBS. Primary antibody specific for cleaved caspase-3 (Cell Signaling, Danvers, MA) was diluted 1:100 in blocking solution and incubated overnight at 4 °C. After washing with IF buffer, secondary antibody specific for rabbit IgG was diluted 1:1000 in blocking buffer for 1 hour at room temperature protected from light. Secondary antibody was removed and DAPI diluted 1:1000 in PBS was added for 10 minutes protected from light. The enteroids were then washed with IF buffer and then with PBS. PBS was left in the well during imaging on a Lionheart FX Auotmated Microscope (BioTek, Winooski, VT).

**Preparation of Enteroids for RNA Isolation**

Enteroids were grown in 24 well plates and collected using 1 mL ice-cold PBS. Enteroids from at least 4 wells were pooled into a 15 mL conical tube and spun at 500 g for 5 minutes, 4 °C. The supernatant was carefully collected while also collecting as much matrigel as possible above the enteroid pellet. 1 mL of fresh, cold PBS was slowly added to the tube to lift any remaining matrigel off the enteroid pellet. All remaining PBS/matrigel was carefully collected, leaving the enteroid pellet undisturbed. The enteroid pellet was collected with 300 µL Trizol and transferred to a 1.7 mL Eppendorf tube. The enteroids were sonicated twice for 5 seconds, resting on ice in between. The RNA was isolated and qPCR was carried out as described above.

**Overexpression of Human PRAP1**

A human colonic epithelial cell line (SK-CO15) was grown to confluence in a 24 well plate before the addition of 2 µL Lipofectamine 2000 (Invitrogen, Carlsbad, CA) with 1 µg plasmid DNA. Cells were transfected with either an empty vector control (pCMV-myc), pCMV-PRAP1-

myc to transiently overexpress human PRAP1, or pCMV-GFP to monitor the success of the transfection. After an overnight transfection, media was refreshed and 6 hours later subjected to 8 Gray [197] of radiation (225 kV and 17.7mA) using a RS2000 X-ray irradiator (Rad Source Technologies, Buford, GA). After 48 hours the cells were washed with cold PBS and collected with RIPA buffer (Thermo Fisher Scientific, Waltham, MA) and western blot was performed as previously described [192]. PRAP1 was detected by immunoblot with the commercially available anti-PRAP1 antibody (Proteintech, Rosemont, IL) diluted 1:1000 in 5% milk and TBST. GAPDH was detected using a rabbit monoclonal antibody (Cell Signaling, Danvers, MA) diluted 1:5000 in 5% milk and TBST while all other proteins were detected using the Cell Cycle Regulation Antibody Sampler Kit from Cell Signaling (Danvers, MA) following manufacturer's protocol. Quantification of bands was performed by measuring signal intensity using ImageJ (National Institutes of Health, Bethesda, MD) and calculated as signal intensity relative to GAPDH.

**Statistical Analysis**

Cumulative data was graphed as mean ± SEM, with significance determined via Student's unpaired t test or ANOVA if comparing more than two groups. Multiple comparisons used either Turkey's multiple comparisons test or Dunnett's multiple comparisons test when appropriate. Survival curves were compared using the Log-rank (Mantel-Cox) test. All statistical tests were performed using GraphPad Prism 8.0.1 (San Diego, CA). A p value of $\leq 0.05$ was considered significant.

## Supplemetal Figures

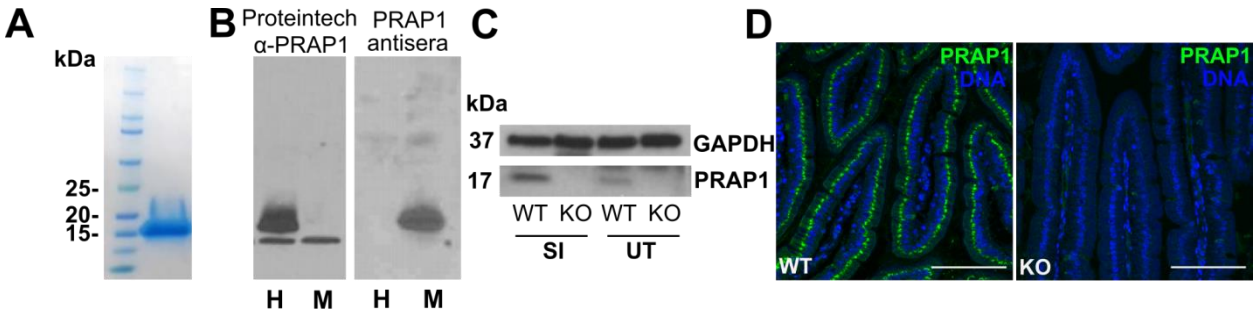


**Supplemental Figure 1. Generation and validation of PRAP1 recombinant protein, PRAP1 antisera and Prap1-/- mice. (A)** SDS-PAGE with Coomassie staining of recombinant 6xHis-PRAP1 expressed in *E. coli* and purified by Ni-NTA affinity chromatography column followed by a size exclusion column. **(B)** A human colonic epithelial cell line (SK-CO15) was transfected to overexpress human (H) and mouse (M) PRAP1. Cell lysates were blotted with a commercially available antibody specific for human PRAP1 (Proteintech, first blot) or with PRAP1 rabbit antisera generated using 6xHis-PRAP1 (second blot). **(C)** Western blot of small intestine and uterine whole tissue from wildtype and *Prap1*$^{-/-}$ mice, blotted with PRAP1 antisera introduced in (B). **(D)** Immunofluorescence staining of wildtype and *Prap1*$^{-/-}$ duodenum using PRAP1 antisera. Whole body knockout mice were procured from MMRRC-UC Davis and backcrossed to obtain a fully congenic C57BL/6 background.

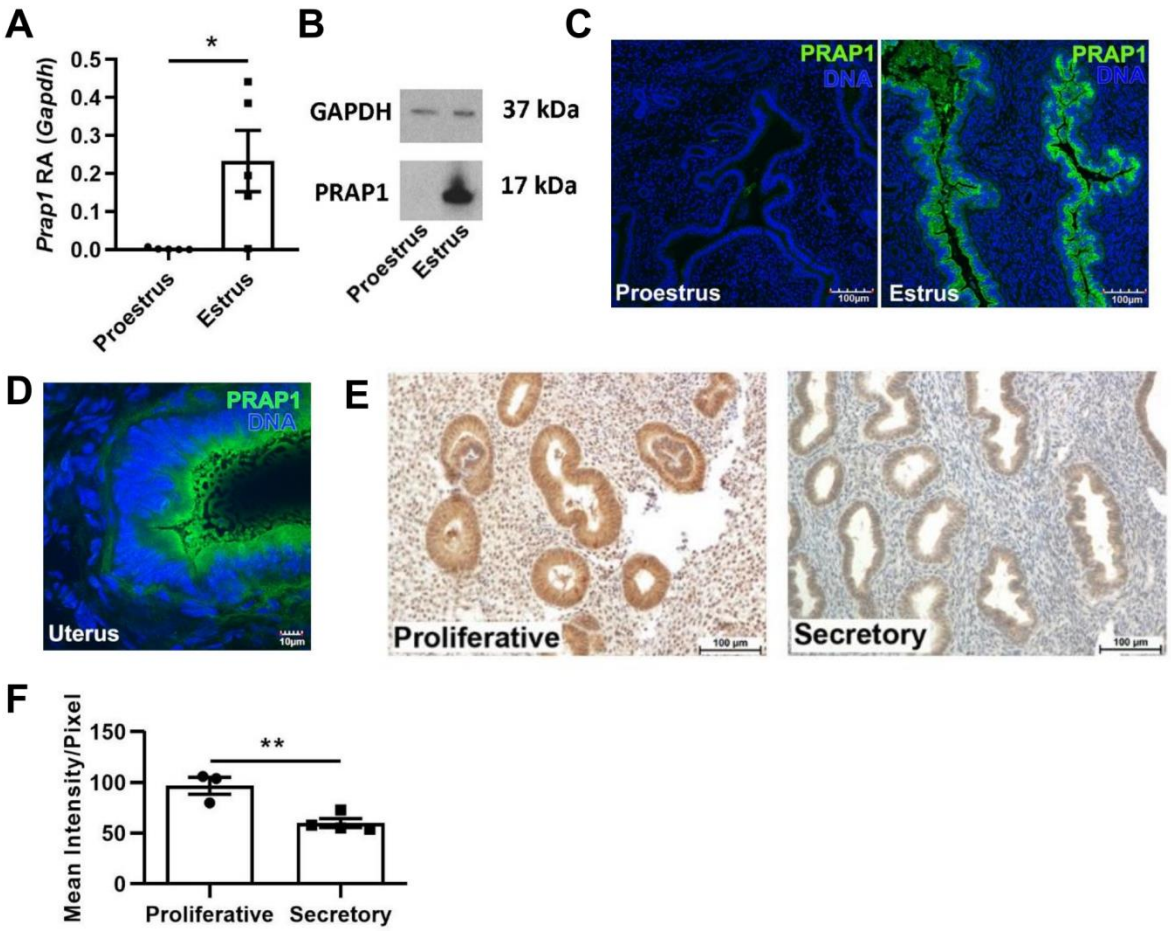
A
*
Prap1 RA (Gapdh)
0.5
0.4
0.3
0.2
0.1
0.0
Proestrus
Estrus
B
GAPDH
37 kDa
PRAP1
17 kDa
Proestrus
Estrus
C
PRAP1
DNA
Proestrus
100μm
PRAP1
DNA
Estrus
100μm
D
PRAP1
DNA
Uterus
10μm
E
Proliferative
100 μm
Secretory
100 μm
F
**
Mean Intensity/Pixel
150
100
50
0
Proliferative
Secretory

(legend for figure on previous page)

**Supplementary Figure 2. PRAP1 is highly expressed in the murine and human endometrium. (A)** Quantitative RT-PCR analysis detecting the relative abundance of *Prap1* transcript in whole uterine tissue harvested from 8-week-old wildtype C57BL/6 mice at proestrus and estrus. Statistical significance determined using unpaired t test, *=$p<0.05$, n=5. Data graphed as the mean ± SEM. **(B)** Western blot analysis for the detection of PRAP1 protein abundance in whole uterine tissue harvested from 8-week-old C57BL/6 female females during the indicated stages of the hormonal cycle. Images are representative of the analysis of five mice per tissue collected. **(C)** Immunofluorescence staining to detect PRAP1 (green) in the uterine horns of 8-week-old wildtype C57BL/6 female mice collected at proestrus and estrus. Images are representative of the analysis of five mice per hormonal cycle stage. **(D)** Immunofluorescence staining showing PRAP1 (green) of the wildtype murine endometrium during estrus at 100X magnification. **(E)** Immunohistochemistry for the detection of PRAP1 in human endometrium tissue during the proliferative and secretory stages of the hormonal cycle. Images are representative of the analysis of 3 subjects per hormonal cycle stage. **(F)** Quantitative measurement of the intensity of PRAP1 signal in the endometrium of women during the proliferative and secretory stages of the hormonal cycle presented in (E). Statistical significance determined by student's t test (alpha = 0.05), $n \geq 3$. Data graphed as the mean ± SEM.

# Chapter 3

## A human microbiota-associated murine model for assessing the impact of the vaginal microbiota on pregnancy outcomes

Wolfarth AA[1], Smith TM[1], VanInsberghe D[1], Dunlop AL[2], Neish AS[1], Corwin EJ[2], and Jones RM[3]*

Currently In Review at *Frontiers in Cellular and Infection Microbiology*, July 2020.

[1] Department of Pathology

[2] Emory University Nell Hodgson Woodruff School of Nursing

[3] Division of Pediatric Gastroenterology, Hepatology, and Nutrition, Department of Pediatrics, Emory University School of Medicine, Atlanta GA, 30322.

***Corresponding Author:** Rheinallt M. Jones, Division of Pediatric Gastroenterology, Hepatology, and Nutrition, Department of Pediatrics, Emory University School of Medicine, 615 Michael Street, Atlanta GA, 30322, (rjones5@emory.edu) Tel: (404) 712-7231, Fax: (404) 727-8538

**Abstract**

Disease states are often linked to large scale changes in microbial community structure that obscure the contributions of individual microbes to disease. Establishing a mechanistic understanding of how microbial community structure contribute to certain diseases, however, remains elusive thereby limiting our ability to develop successful microbiome-based therapeutics. Human microbiota-associated (HMA) mice have emerged as a powerful approach for directly testing the influence of microbial communities on host health and disease, with the transfer of disease phenotypes from humans to germ-free recipient mice widely reported. We developed a HMA mouse model of the human vaginal microbiota to interrogate the effects of Bacterial Vaginosis (BV) on pregnancy outcomes. We collected vaginal swabs from 19 pregnant women with and without BV (diagnosed per Nugent score) to colonize female germ-free mice and measure its impact on birth outcomes. There was considerable variability in the microbes that colonized each mouse, with no association to the BV status of the microbiota donor. Although human mothers with BV had more frequent adverse birth outcomes, the vaginal microbiota was not predictive of adverse birth outcomes in mice. However, elevated levels of pro-inflammatory cytokines in the uterus of HMA mice were detected during pregnancy. Together, these data outline the potential uses and limitations of HMA mice to elucidate the influence of the vaginal microbiota on health and disease.

## Introduction

The vagina houses a numerically immense and functionally consequential microbiota [198, 199]. Distinct anatomic regions within the female reproductive tract house a dynamically changing microbial community of vastly different numbers and taxonomic composition. For example, it is well known that the vagina maintains a numerically vast microbiota while the uterus (pregnant and non-pregnant) is normally colonized with very limited microbiota [200, 201]. Lactobacilli are the dominant taxa of the human vaginal microbiota and are the one of the first bacteria to which neonates are exposed. The origin and consequences of the unique lactobacilli-dominant community structure remains enigmatic, though it is generally accepted that lactate produced by these bacteria results in the characteristic acidic pH of the healthy vagina. This is a result of direct or syntrophic fermentation of the abundant glycogen found in apical squamous epithelia of the vagina [202, 203]. This low pH is generally assumed to have intrinsic bacteriostatic effects and is a prime example of the innate defenses of the female reproductive tract. Thus, the female reproductive tract has a highly adapted microbiota with known beneficial effects including colonization resistance against pathogens [204].

In support of this notion, a study that characterized the diversity of bacterial taxa within the vaginal microbiome of nearly 400 multi-ethnic reproductive age women discovered that the vaginal microbiota clustered into community state types (CSTs) [205, 206]. Indeed, about 25% of the women sampled clustered into a group (designated CST IV) where lactobacilli was not the dominant taxon. This group was associated with a less acidic pH and higher indices associated with bacterial vaginosis (BV). Intriguingly, African American and Hispanic women were overrepresented among CST IV. Additionally, African Americans are also at a higher risk for adverse pregnancy outcomes, including preterm birth [207]. Considering the association between

BV and preterm birth [208, 209], investigating the microbiota of the reproductive tract in this context may offer a path toward refined associations and molecular mechanisms underlying the development of adverse pregnancy outcomes in this population of women.

BV is a common clinical syndrome seen in gynecological practice. African American women are more commonly affected by BV, with prevalence estimates of 51.4% for African American women compared to 23.2% for US white women of reproductive age [210]. This condition is best conceptualized as an ecological disorder characterized by the displacement of a lactobacillus-dominant microbiota (and loss of acidic pH) by a variable mix of facultative organisms often including *Gardnerella vaginalis* [211]. Interestingly, BV can result in the formation of endometrial biofilms with *G. vaginalis*, observed in 50% of patients with BV, including both pregnant and non-pregnant patients [212], indicating abnormal microbial community structure can result in ascending infection. Furthermore, a consequence of reduced lactobacilli abundance in the vaginal canal is associated with reduced implantation efficiency in humans [213]. These observations suggest that specific commensal taxa such as lactobacilli within the female reproductive tract mediate colonization resistance against pathogens and positively influence pregnancy outcomes.

Despite the known complications in patients with BV, animal models for human BV remain underdeveloped. To address this void, we aimed to develop a human microbiota-associated (HMA) mouse model of BV using germ-free mice. While the natural microbiota of mice differs greatly to that of humans [214], HMA mice allows microbial colonization of germ-free mice with the relevant human microbiota and later studied. Colonizing germ-free mice with bacteria from human donors aims to maintain a microbiota diversity and profile similar to the human donor and thus may be a faithful model to examine the role of the human vaginal

microbiota in diseases of the reproductive tract and adverse pregnancy outcomes [215]. Furthermore, housing of HMA mice in a hermetically sealed bio-exclusion cage system means that no further bacteria from the environment will enter and alter the diversity of the humanized mouse [216].

Herein, we describe the generation of HMA mice harboring the microbiota collected from the vaginal tract of pregnant women and describe the extent to which the human vaginal microbiota can colonize the vaginal tract of germ-free mice. We show that pregnant women with BV harbor a distinct microbiota and carry elevated risk for adverse pregnancy outcomes. Further, we observed substantial variation in pregnancy outcomes and pro-inflammatory cytokine production among HMA mice, despite donor microbiota being a poor predictor of these properties. Together, these data outline the potential use and limitations of using HMA mice harboring the microbiota collected from the human vaginal tract to elucidate the impact of the vaginal microbiota on pregnancy outcomes.

## Results

### Pregnant women with BV harbor a distinct microbiota community structure.

To employ a rigorous experimental approach to generate HMA mice, it is essential to establish a well-characterized cohort of patients with well-characterized disease states as donors of human microbiota. To this end, 19 pregnant African American women were recruited and information pertaining to Nugent score of vaginal swab were collected at the same time as the microbiota sample (for gold standard diagnosis of BV), while patient demographics, health status, pregnancy complications and birth outcomes were recorded as well (**Table 1**). Specifically, seven women presented with a normal Nugent score between 0 and 3, four women presented with an intermediate Nugent score between 4 and 6, and eight women presented with a Nugent score of 7 or higher indicative of BV (**Table 1**). The vaginal and rectal microbiota community structures were characterized for each of the nineteen patients. Healthy patients with a low Nugent score harbored a microbiota diversity typical of that previously detected in heathy women[217] where the microbial community is dominated by lactobacilli (**Figure 1A**). However, patients with an intermediate or high Nugent score harbored a dysbiotic vaginal microbiota community structure, typified by the diminishment in the relative abundance of lactobacilli and an expansion in the relative abundance of bacteria of genera Prevotella, Gardernella and Shuttleworthia (**Figure 1A**). Furthermore, beta diversity analysis of the vaginal microbiota revealed distinct separation of patients with respect to their Nugent scores (**Figure 1C**). By contrast, characterization of the fecal microbiota diversity of these patients did not reveal any salient differences in either relative bacterial abundances (**Figure 1B**), nor in beta diversity, with no detectable separation of patients clustering with respect to their Nugent score (**Figure 1C)**. The Shannon diversity index of the vaginal microbiota of each patient was also

**Table 1. The clinical parameters of the 19 pregnant women used for HMA mouse generation**.

| Characteristics | Subjects (n=19) |
|---|---|
| Age, years (mean±sd) | 25.1±5.06, |
| Race/Ethnicity | |
| African American | 19 (100%), |
| Educational level | |
| Less than high school | 6 (31.6%) |
| High school or GED | 6 (31.6%) |
| Some college | 6 (31.6%) |
| College graduate | 1 (5.3%) |
| Prenatal Insurance, n (%) | |
| Medicaid | 17 (89.5%) |
| Private | 2 (10.5%) |
| Nugent Score, n (%) | |
| Normal (0-3) | 7 (36.8%) |
| Intermediate (4-6) | 4 (21.1%) |
| BV (7+) | 8 (42.1%) |
| Gestational Hypertension | 1(5.3%) |
| Gestational Diabetes | 1(5.3%) |
| Obstetrical history, n (%) | |
| Prior term birth | 11 (57.9%) |
| Prior preterm birth | 3 (15.8%) |
| Birth Outcome*, n (%) | |
| Full term | 10 (52.6%) |
| Early term | 6 (31.6%) |
| Preterm | 1(5.3%) |
| Spontaneous abortion | 1(5.3%) |
| Exposure to antibiotics in the month prior to microbiota sampling, n (%) | |
| Yes | 7 (36.8%) |
| No | 12 (63.2%) |

* Full term (39 weeks≥), Early term (39 weeks<x≤36 weeks), Preterm (36 weeks<)

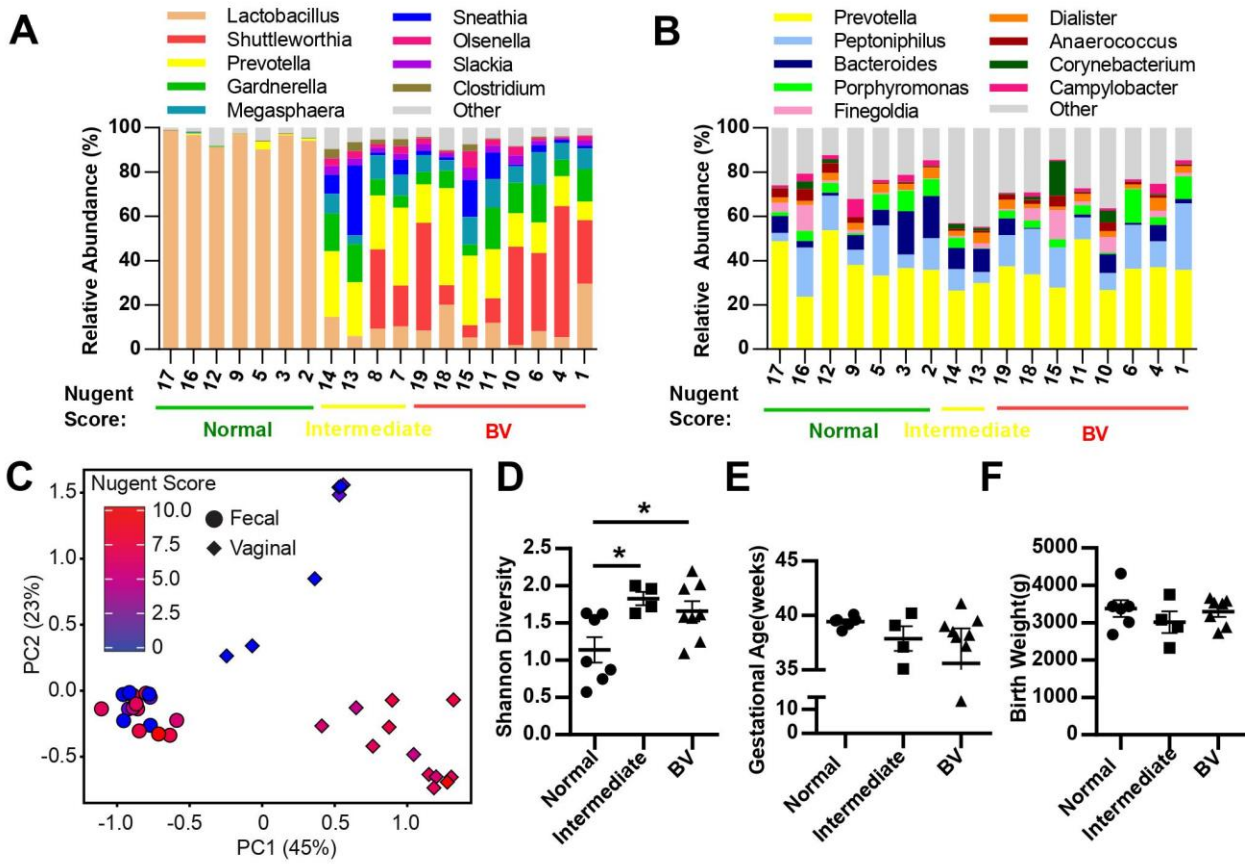
A
Lactobacillus
Shuttleworthia
Prevotella
Gardnerella
Megasphaera
Sneathia
Olsenella
Slackia
Clostridium
Other
Relative Abundance (%)
Nugent Score:
Normal
Intermediate
BV
B
Prevotella
Peptoniphilus
Bacteroides
Porphyromonas
Finegoldia
Dialister
Anaerococcus
Corynebacterium
Campylobacter
Other
C
Nugent Score
Fecal
Vaginal
PC2 (23%)
PC1 (45%)
D
Shannon Diversity
E
Gestational Age(weeks)
F
Birth Weight(g)

(legend for figure on previous page)

**Figure 1. Pregnant women with bacterial vaginosis harbor a distinct microbiota community structure. (A-B)** Relative abundance of bacterial genera within the vaginal tract **(A)** and rectum **(B)** of pregnant women assigned as Normal, Intermediate or BV by Nugent score described in Table 1. Data represents the top 10 most abundant bacterial genera detected. Each column represents one patient. **(C)** Principal Component Analysis (PCA) plot depicting the beta-diversity of the microbiota community structure within the vaginal tract and the rectum of pregnant patients described in Table 1. **(D)** Shannon diversity index of patient vaginal microbiota determined via 16S rRNA gene sequencing according to patient Nugent score. Data graphed as mean ± SEM. **(E)** Gestational age of delivery for pregnant patients described in Table 1 with either a normal, intermediate or BV Nugent score. Data graphed as mean ± SEM. **(F)** Birth weight of infant delivered by patients described in Table 1 with a normal, intermediate or BV Nugent score. Data graphed as mean ± SEM. Statistical significance determined via One-way ANOVA, Turkey's multiple comparison test (D, F) or Kruskal-Wallis test, Dunn's multiple comparisons test (E). *=$p<0.05$. n=19 patients.

plotted with respect to the grouped Nugent score, and revealed that patients with a normal Nugent score between 0 and 3 had significantly lower microbiota diversity (Shannon diversity index) compared to patients with an intermediate Nugent score between 4 and 6, or compared to patients with a Nugent score of 7 or higher (**Figure 1D**). The gestational age and birthweight of each infant was also collected and revealed that patients with an intermediate or high Nugent score in this cohort trended towards a pre-term-birth and a lower birthweight (**Figure 1E and 1F**). Together, these data establish a cohort of normal and disease patients with defined and quantifiable disease activity for use in the generation of HMA mice.

**Generation of human microbiota-associated (HMA) mice harboring the microbiota collected from the vaginal tract of pregnant women with bacterial vaginosis**

The patients' vaginal microbiota was swabbed at the hospital and the swabs were transported immediately to the Emory Gnotobiotic Animal Core (EGAC). The vaginal tract of female germ-free C57BL/6 mice was inoculated by physically wiping the vaginal swab on the mouse, concentrating the swab to the vaginal opening. This process was typically completed within 2 hours of collecting the vaginal swab from the patient. Mice were then housed within bioexclusion husbandry cages for the vaginal microbiota to establish and colonize. After 2 weeks, a male germ-free mouse was introduced into the bioexclusion cages of each HMA female mouse, and conception date recorded by the appearance of a viscous copulatory plug. At 18.5 days post-coitum (18.5 dpc) and before delivery of litters, mice were sacrificed and the uterus, vagina, and fecal pellet collected under sterile conditions (**Figure 2A**). Characterization of the vaginal microbiota in HMA mice using 16S rDNA amplicon sequencing revealed that although each HMA mouse became colonized by microbes from the donor sample, the proportional abundance of those taxa in the HMA mice was very different from the donor sample (**Figures**

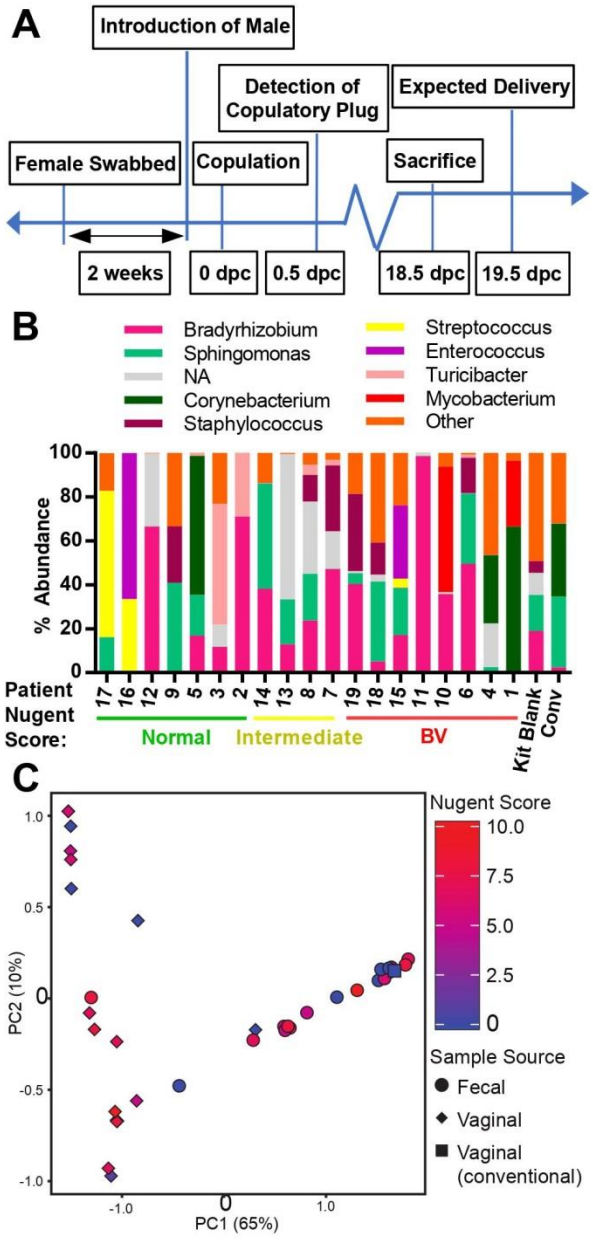
A
Introduction of Male
Detection of Copulatory Plug
Expected Delivery
Female Swabbed
Copulation
Sacrifice
2 weeks
0 dpc
0.5 dpc
18.5 dpc
19.5 dpc
B
Bradyrhizobium
Sphingomonas
NA
Corynebacterium
Staphylococcus
Streptococcus
Enterococcus
Turicibacter
Mycobacterium
Other
% Abundance
100
80
60
40
20
0
Patient
Nugent Score:
17 16 12 9 5 3 2 14 13 8 7 19 18 15 11 10 6 4 1 Kit Blank Conv
Normal
Intermediate
BV
C
Nugent Score
10.0
7.5
5.0
2.5
0
Sample Source
Fecal
Vaginal
Vaginal (conventional)
PC2 (10%)
PC1 (65%)
1.0
0.5
0
-0.5
-1.0

(legend for figure on previous page)

**Figure 2. Generation of human microbiota-associated (HMA) mice harboring the microbiota collected from the vaginal tract of pregnant women with bacterial vaginosis. (A)** Graphical depiction of experimental approach to generate human microbiota-associated (HMA) mice harboring the microbiota collected from the vaginal tract of pregnant patients described in Table 1. Swabs were collected from the vaginal tract and immediately transported to the Emory Gnotobiotic Animal Core (EGAC). The vaginal tract of female germ-free C57BL/6 were inoculated by physically wiping the swab on the vaginal opening of the mouse. Mice were then housed in Tecniplast ISOcageP Bioexclusion cages for the microbiota to colonize. After 2 weeks, a male germ-free mouse was introduced to the HMA female mouse and conception monitored. On 18.5 dpc (days post-coitum), pregnant female mice were sacrificed under sterile conditions for sample collection and analysis.**(B)** Relative abundance of the bacterial genera detected via 16S analysis in the vaginal tract of HMA mice on 18.5 dpc. Data represents the top 10 bacterial genera detected and each stacked column represents one mouse. Data is separated by BV status of the corresponding human donor. **(C)** Principal Component Analysis (PCA) plot depicting the beta-diversity of the microbiota community structure within the vaginal tract and gastrointestinal tract of HMA mice on 18.5 dpc. Symbols are colored by the Nugent score of the corresponding human donor.

**1A and 2B)**. Importantly, the lactobacilli from the normal Nugent score patients did not efficiently colonize the mouse vaginal tract (**Figure 2B**). Furthermore, there was high variability in the colonizing microbiota of each HMA mouse, and similarity between the microbiota of HMA mice was not driven by the BV status of the donor sample (**Figure 2C**). We also detected no significant differences in the fecal microbiota of the HMA mice and no separation based on patient Nugent score (**Figure 2C**). These results suggest that while the vaginal canal of germ-free mice provides a competition-free niche for bacteria in a donor sample, the vaginal microbiota of HMA mice generated using this approach does not closely resemble the community present in donor samples.

**Pregnancy outcomes in human microbiota-associated (HMA) mice harboring the microbiota collected from the vaginal tract of pregnant women with bacterial vaginosis**

Despite limited similarity between donor and HMA mouse vaginal microbiota, we recorded considerable differences in pregnancy outcomes among the HMA mice and sought to determine whether the microbiota harbored in the vaginal canal correlated with any adverse outcomes. We correlated pregnancy outcome in HMA mice by recording the number of pups within the uterine horns at 18.5 dpc. This was done before birth in order to obtain a faithful count of viable pups and to mitigate the prospect that the new moms' cannibalize their newborn offspring, which often occurs postpartum in C57BL/6 mice and could affect our data. We compared the litter size at 18.5 dpc with the Nugent score of the corresponding patient described in table 1 used for inoculation and detected a considerable amount of variation in litter size, with a trend towards smaller litter sizes in the BV inoculated group (**Figure 3A**). We also compared the litter size of HMA mice with the Shannon diversity index of their vaginal microbiota and found that mice with smaller litter sizes did not have a significant difference in vaginal

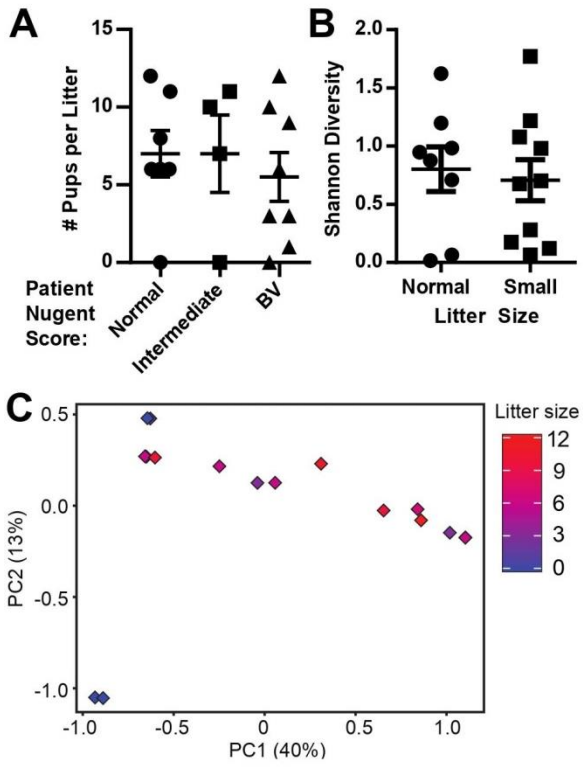


**Figure 3. Pregnancy outcomes in human microbiota-associated (HMA) mice harboring the microbiota collected from the vaginal tract of pregnant women with bacterial vaginosis.**

**(A)** The number of pups detected in the uterine horns of HMA mice on 18.5 dpc separated by the Nugent score of the corresponding donor. Data graphed as mean ± SEM. **(B)** Shannon diversity index of the mouse vaginal microbiota determined via 16S analysis on 18.5 dpc separated by litter size of the pregnant HMA mouse. Less than 7 pups on 18.5 dpc is considered a small litter, while 7 or more pups is considered a normal litter. Data graphed as mean ± SEM. **(C)** Principal Component Analysis (PCA) plot depicting the beta-diversity of the microbiota community structure within the vaginal tract of HMA mice on 18.5 dpc. Symbols are colored by the litter size on 18.5 dpc.

diversity **(Figure 3B)**. Lastly, a PCA plot comparing the beta diversity of the mouse vaginal microbiota and the corresponding litter size (**Figure 3C**) shows that the vagina microbiota of the HMA mice did not have a significant influence on litter size.

**Altered pregnancy outcomes in human microbiota-associated (HMA) mice is associated with elevated levels of pro-inflammatory cytokines in the uterus of mice during pregnancy.**

Inflammation in the uterus, or endometritis is commonly associated with pregnancy complications. We examined the extent to which the colonizing microbes influenced levels of inflammation in the uterus of HMA mice. Although the uterus has considerably lower levels of bacteria compared to the vaginal tract, it may be possible that certain bacterial species in the vaginal tract have negative impacts on the physiology of the entire reproductive system. A comprehensive analysis of cytokine concentrations in the uterus of HMA mice described in figure 2 revealed significantly higher levels of IL-12 and IL-4, and trending higher levels of IFNγ in the uteri of mice with smaller litter sizes, whereas a significantly higher level of TNFα in the uterus was associated with a larger litter size (**Figure 4A**). To determine the extent to which certain murine vaginal microbial communities were associated with altered uterine cytokine levels during pregnancy, we conducted PCA analysis comparing cytokine levels and the vaginal microbiota community. However, our analysis revealed that the HMA mouse vaginal microbiota did not group with any alterations in uterine cytokine levels and had no correlation with BV status of the patient (**Figure 4B**).

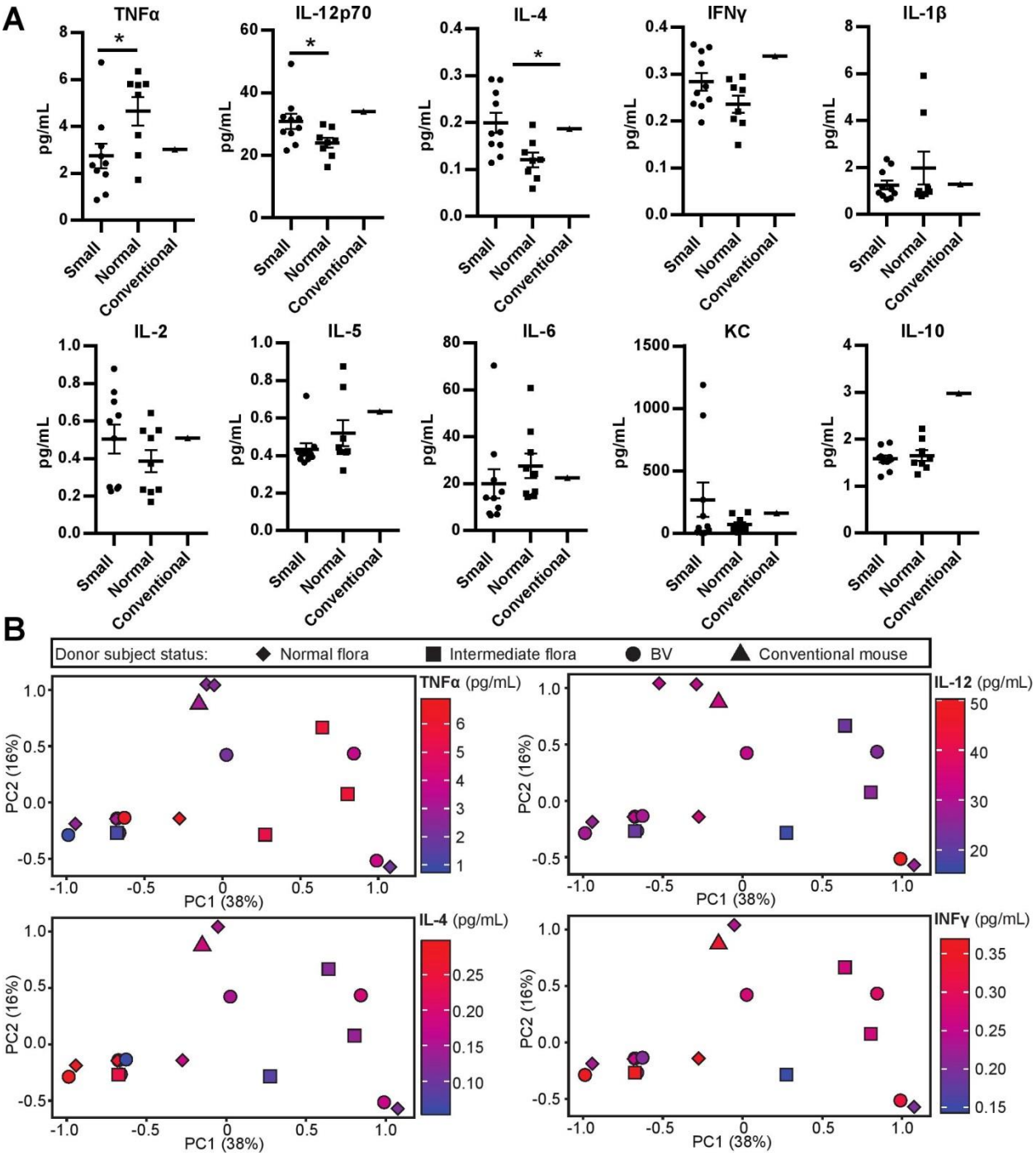
A
TNFα
IL-12p70
IL-4
IFNγ
IL-1β
IL-2
IL-5
IL-6
KC
IL-10
pg/mL
Small
Normal
Conventional
*
B
Donor subject status:
Normal flora
Intermediate flora
BV
Conventional mouse
TNFα (pg/mL)
IL-12 (pg/mL)
IL-4 (pg/mL)
INFγ (pg/mL)
PC1 (38%)
PC2 (16%)

(legend for figure on previous page)

**Figure 4. Pregnancy outcome in human microbiota-associated (HMA) mice is associated with altered uterine cytokine levels during pregnancy. (A)** Cytokine concentrations in the uterus of HMA mice on 18.5 dpc. Cytokine levels are plotted with respect to the litter size. Less than 7 pups on 18.5 dpc is considered a small litter, while 7 or more pups is considered a normal litter. Statistical significance determined using unpaired t test. *=$p<0.05$. $n\geq8$. Data graphed as mean ± SEM. **(B)** Principal Component Analysis (PCA) analysis depicting the correlation between cytokines concentrations in the uterus that were significantly altered or trending towards significance in (A), the HMA mouse vaginal microbiota community, and the Nugent score of the corresponding donor patient.

**Discussion**

In order to better understand the effect of the vaginal microbiota on health, we assessed the utility of the HMA mouse approach, which has been widely employed in the study of host cell and intestinal microbe interactions [218, 219]. Studies using HMA mice have not only attributed causality of specific microbial community structures in the development of many chronic diseases such as metabolic syndrome, but have also helped to unravel the mechanisms behind these associations- an approach that is unfeasible in human subjects [220]. While mice with a humanized microbiota have offered an invaluable model for the study of the gastrointestinal microbiota and its role in human health, the same mouse model for the human vaginal microbiota has not been fully established [221]. We first collected patient data on a cohort of pregnant women, including Nugent scores for the assessment of BV in patient. Using vaginal swabs from these patients, we generated HMA mice harboring the microbiota collected from the vaginal tract of pregnant women with BV. Comparison of the vaginal microbiota of BV patients and HMA mice revealed only modest similarity. In addition, there was no correlation detected between the number of pups within pregnant HMA mice and Nugent scores from BV patients. Significantly elevated levels of pro-inflammatory cytokines in the uterus of mice were detected during pregnancy, although there was no clear correlation between the murine vaginal microbiota, Nugent scores from BV patients and pro-inflammatory cytokine levels.

In both mice and humans, the uterus functions to nurture a fertilized egg until the fetus, or offspring, is ready to be delivered. However, the anatomy of the mouse female reproductive tract has clear differences compared to humans. The murine uterus is bicornuate, forming two uterine horns that help accommodate large litter sizes, with an average of 8.5 newborns per litter [222]. By comparison the human uterus is simplex, an inverted pear-shaped muscular organ, located

between the bladder and the rectum, and typically harbors only one infant. Importantly, both humans and mice have a cervix which forms a tight physical barrier between the vagina and uterine cavity. The cervix plays a critical role in preventing vaginal bacteria from ascending into the uterus [223, 224]. As in humans, mice have a resident commensal vaginal microbiota and virtually undetectable numbers of microbes in the uterus [225, 226]. As in humans, mice also undergo a hormonal cycle regulated by steroid hormones, with their cycle being much shorter, about 4 days in total, compared to a human's 28 day cycle [227]. Interestingly, mice also do not undergo menstruation and instead only decidualize if fertilization occurs [228]. The lack of menstruation may be a governing determinant in the establishment of the microbiota community structure within the mouse reproductive tract. Indeed, the composition of the vaginal microbiota differs greatly between mice and humans. In fact, humans have a distinct vaginal microbiota compared to most other mammalian species sampled including even non-human primates [229]. Humans are the only species to have a vaginal microbiota dominated by lactobacilli, while all other mammals have a considerably more diverse vaginal microbe community structure [230, 231]. The teleological explanation for the specific nature of the human vaginal microbiota diversity in terms of the purpose it serves remains enigmatic, with progress in our understanding perhaps hindered by the very fact that there is no suitable animal to model the human vaginal microbiota [232]. Establishing an HMA animal model would greatly enhance our understanding of how the vaginal microbiota affects the development of several human reproductive diseases, many of which cause pre-term births, and may facilitate the development of novel therapies that are desperately needed for millions of women.

Preterm labor is defined as labor that begins prior to the $37^{th}$ week of pregnancy, and is associated with nearly 12% of infants born in the US, and >15% of those born in the developed

world [233-235]. Importantly, however, according to the National Center for Health Statistics recent natality data (Retrieved June 03, 2020), when broken down by race, the average preterm birth rate among African American women during the years 2016-2018 was 13.8%, or 50% higher than the 9.1% average among white women during the same time period. The sequelae of preterm birth accounts for a burden of up to 70% of all perinatal morbidity and mortality, specifically intracranial hemorrhage and periventricular leukomalacia, bronchopulmonary dysplasia, cerebral palsy, and retinopathy of prematurity, consequences which overall are more common among African American infants and which may be lifelong. The incidence and severity of these complications are inversely associated with gestational age, with the most deleterious outcomes occurring in infants delivered close to the 24-week limit of viability. Despite this medical, social and economic toll, there remains a major gap in understanding the biological mechanisms that lead to preterm birth, as well as the health disparity experienced by African American families.

While there are multiple risk factors for preterm birth, including premature rupture of membranes, placental abruption, multiple gestation, smoking and hypertensive disorders of pregnancy, the major cause is chorioamnionitis/uterine inflammation [233, 234, 236, 237]. Chorioamnionitis, also known as intra-amniotic infection (IAI) is an inflammation of the fetal membranes (amnion and chorion) due to a bacterial infection [238]. Up to 40% of preterm births are clinically associated with intrauterine infections [239]. An objective histopathological analysis of a large cohort (3928 patients) of preterm (20-34 weeks) placentas detected active chorioamnionitis in 66% of cases at 20-24 weeks and 16% at 34 weeks [240]. Thus, preterm labor and delivery is a common and important complication of otherwise normal pregnancy, and is most often caused by infection of the uterus.

The biological mechanisms by which the normal gravid uterus protects itself from ascending infection are not fully known. Recently, it has been established that the indigenous microbiota residing on host mucosal surfaces act in concert with the host to prevent pathogenic microbial colonization in a process called colonization resistance. The colonization resistance offered by the lactobacilli rich microbiota combined with the physical barrier of the cervix is considered to be a major defense against ascending uterine infections. Furthermore, there is increasing literature describing the influence of microbial diversity within the female reproductive tract on uterine health and disease. Indeed, our approach did discover significant variation in uterine cytokine levels of HMA mice and large range of litter sizes, despite the colonizing communities bearing limited similarity to their donor sample. In that way, the approach we describe in this study could still be a valuable method for interrogating the mechanistic details through which microbes and microbial consortia influence reproductive health. Further, although we report limited similarity based on 16S rDNA amplicon sequencing, assessing microbial community composition using metagenomics and metatranscriptomics could reveal more meaningful similarities among the colonizing microbes in HMA mice. That is, it is possible that the HMA mice with more similar litter sizes and levels of inflammatory cytokines were disproportionately colonized by microbes enriched with similar metabolic capabilities. Ultimately, the HMA mouse model we describe here is a valuable step towards developing new methods that can provide mechanistic insight into how microbe-host interactions affect reproductive health.

## Methods

### Patient recruitment and swab collection

Women who participated in this study were part of the Emory University African American Vaginal, Oral, and Gut Microbiome in Pregnancy Cohort Study [241]. During the recruiting period for this study (7/31/2018 through 11/15/2018), women who were recruited for the parent study were offered the option of collecting an additional vaginal and rectal swab for participation in the present study. The study protocol was carried out in accordance with the review and approval of the Emory University Institutional Review Board and the Grady Research Oversight Committee. All women participating in this study provided written informed consent in accordance with the Declaration of Helsinki.

Pregnant women were recruited to participate in this study from the prenatal care clinics of two metropolitan hospitals in Atlanta, GA, affiliated with Emory University Woodruff Health Sciences Center: Grady Memorial Hospital, a county-supported hospital that serves as a safety net for low-income patients; and Emory University Hospital Midtown, a private hospital that serves patients from a wide economic range. Inclusion criteria were that each participant is: 1) African American by self-report; 2) Between 8 and 14 weeks' gestation (verified by clinical record) and expecting a singleton pregnancy; 3) Able to comprehend written and spoken English; 4) Between 18 and 40 years of age; 5) Experiencing no chronic medical condition or taking prescribed chronic medications (verified by prenatal record). For enrolled women, data collection consisted of completing a sociodemographic questionnaire as well as self-collecting vaginal and rectal swabs during the study visit and giving permission to complete a medical record abstraction at the end of the pregnancy.

For the swab collection, participants were provided verbal and pictorial instructions directing them to obtain (in a private exam room) self-collected vaginal swabs (one for Gram staining according to Nugent's score, one for DNA extraction and 16S rRNA gene sequencing, and one for inoculation of the mouse model) and rectal swabs (one for DNA extraction and 16S rRNA gene sequencing, and one for inoculation of the mouse model). The swabs for microbiota sequencing were Sterile Catch-All™ Sample Collection Swabs (Epicentre Biotechnologies, Madison WI) which were immediately plunged into MoBio bead tubes (MoBio Laboratories, Inc., Carlsbad, CA) and frozen upright on dry ice until transported to the lab, to be stored at −80 °C until DNA extraction and preparation for vaginal microbiota measurement occurs. The swabs for vaginal Gram staining were dacron swabs that were stored in a sterile tube until transport to the Emory Clinical Microbiology Laboratory for Gram staining for Nugent criteria scoring for evaluation of BV [242]. Well-designed studies support that vaginal self-collection swabs sample the same microbial diversity as physician-collected swabs of the mid-vagina and have high overall morphotype-specific validity compared with provider-collected swabs based on microbiome analysis [243].

Maternal Medical Chart Abstraction was completed by the research team using a standardized chart abstraction tool to ascertain for the following: *Gestational age at birth*. All participants receive early pregnancy dating by last menstrual period (LMP) and/or early ultrasound, given enrollment criteria. Gestational age at birth is determined from the delivery record, based upon the date of delivery in relation to the estimated date of confinement established during the 8–14 week prenatal visit. Gestational diabetes, preeclampsia/eclampsia, etc., type and mode of delivery are ascertained from record review after delivery and defined according to standard clinical definitions of the American College of Obstetricians and

Gynecologists. *Medication use*, including any antibiotic use, in the month prior to sampling was also ascertained.

**Generation of human microbiota-associated mice**

After collection of the human vaginal swabs by hospital staff the swabs were immediately transferred to research staff who inoculated a germ-free female single-housed in a bioexclusion microisolator cage at the Emory Gnotobiotic Animal Core (EGAC). Inoculation was achieved by physical wiping of the vaginal swab at the vaginal opening of the mouse for several seconds, ensuring adequate transfer of microbes from the swab onto the vaginal opening of the mouse. Inoculated females were housed for 2 weeks before introduction of a germ-free male. Evidence of copulation was monitored by inspection for a vaginal copulatory plug every morning after inoculation. Observance of a vaginal plug was designated as 0.5 days post-coitum (dpc). After identification of a vaginal plug the male mouse was removed to prevent the possibility of multiple copulations. The day before expected delivery (18.5 dpc) the female mouse was sacrificed and the uterine horns, vagina and fecal pellet were collected under strict sterile conditions. The number of developing pups in the uterus were enumerated and removed. The vaginal canal was immediately processed for microbial DNA isolation and the uterine horn was flash frozen for future cytokine analysis.

**Microbial DNA isolation and 16S Analysis**

After sterile collection the vaginal canal from the HMA mouse was placed in a MagnaLyser tube [190] with 1mL sterile PBS. The tube was vigorously vortexed three times for 10 seconds each to remove the mucosa and bacteria from the vaginal tissue. The 1mL of PBS containing the vaginal mucosa and bacteria was collected and the microbial DNA was isolated using the QIAamp DNA microbiome kit (Qiagen, Hilden, Germany). Adequate and faithful amplification

of the 16S rRNA V4 region required an initial PCR amplification of the near full length 16S rRNA genes using the 27F (5'- AGAGTTTGATCMTGGCTCAG -3') and 1492R (5'-TACGGYTACCTTGTTACGACTT-3') primer pair for 25 cycles. The resulting amplicon was then used as template for amplification of the V4 region using the 515F/806R primer pair (GTGCCAGCMGCCGCGGTAA and GGACTACHVGGGTWTCTAAT) for 30 cycles in triplicate. Each 806R primer had a unique 12 base golay barcode. The PCR products were quantified using a Qubit fluorimeter (Invitrogen, Carlsbad, CA) and ran on a bioanalyzer to confirm the presence of a single band at 350bp and no band for the "kit-ome" control. DNA samples were pooled and sequenced using the Illumina MiSeq at the Emory Integrated Genomics Core. Sequencing data was processed using the analysis pipeline developed by VanInsberghe et al [244]. Briefly, primers were trimmed, allowing up to one mismatch and discarding all sequences without primers, and Dada2 was used to infer the Amplicon Sequence Variants (ASVs) [245].

**Measurement of uterine cytokine levels**

The uterus from HMA mice at 18.5 dpc was collected and the pups were carefully removed. The uterine wall was flash frozen with liquid nitrogen. To ensure adequate representation of the uterine tissue in subsequent cytokine analysis, the uterine tissue was ground while frozen with mortar and pestle. 50 mg of tissue was then added to homogenization buffer in a Magnalyser tube and homogenized twice for 30 seconds at 6,500 rpm using a Magnalyser (Roche, Basel, Switzerland). Protein concentrations were quantified using the Pierce BCA assay kit and the protein concentrations were diluted and normalized for cytokine quantification using the V-PLEX Proinflammatory Panel 1 Mouse Kit (Meso Scale Discovery, Rockville, Maryland)

following manufacturer's protocol with the help of the Emory Multiplexed Immunoassay Core (Emory University, Atlanta, GA).

# Chapter 4

# Discussion

## The Role of PRAP1 in the Epithelial Response to Irradiation

Exposure to irradiation injures cells by inducing high amounts of reactive oxygen species resulting in oxidative DNA damage [246]. The stem cells in the gastrointestinal epithelium, along with hematopoietic cells in the bone marrow, are highly sensitive to DNA damage because of their high proliferative capacity and therefore are the first cells that undergo apoptosis following irradiation. Irradiation-induced apoptosis is dose dependent, with apoptosis observed in levels as low as 0.02 Gy and increases with higher doses [247]. When a mouse is exposed to a high irradiation dose around 10-12 Gy, there is maximum apoptosis that occurs in the crypts of the small intestine and there is failure of recovery of the gastrointestinal epithelium [248]. While many stem cells in the crypt are lost to apoptosis following irradiation, the remaining epithelial cells continue to mature and migrate, eventually shedding from the villus tip. Because high doses of irradiation significantly hinder the proliferative capacity of the small intestinal epithelium, severe villus blunting and atrophy is observed days after the initial injury [248, 249]. This occurs because the epithelium has lost its ability to replenish the high turnover of enterocytes. The loss of viable crypts and shortening of the villi structures leads to decreased absorption of critical nutrients and failure of the epithelial barrier. This acute injury in the gut after high doses of whole body irradiation is referred to as acute radiation enteritis and can lead to death of the animal within 10 days [250, 251].

After enduring DNA damage following irradiation, the fate of the cell is largely dependent on the expression and downstream signaling initiated by the tumor suppressor gene, p53 [252]. This “guardian of the genome” is thought to be critical to a cell’s response to DNA

damage and can induce apoptosis of a cell that has undergone extensive DNA damage, therefore preventing survival of cells with dangerous oncogenic mutations [247]. The importance of p53 is underscored by studies that show p53 expression is increased in cells after exposure to irradiation and p53 null mice lack the expected apoptosis in the small intestine following irradiation [253]. While the expression of p53 coincides with increased apoptosis after injury, it is also capable of promoting survival by inducing the expression of proteins such as p21, which induce cell cycle arrest and allow the cell to undergo DNA damage repair before resuming mitosis [254]. The induction of cell cycle arrest and/or apoptosis is largely dependent on the amount of initial injury and the expression levels of other proteins important for determining cell fate [255]. Expression levels of oncogenes and pro-apoptotic proteins within a cell will determine whether a cell survives injury, with many of these proteins downstream of p53 activity.

In Chapter 2, we introduce an understudied protein, PRAP1, highly expressed by the epithelium of the small intestine and investigate its role in the response to irradiation injury. Previous studies on PRAP1 expression *in vitro* demonstrate that PRAP1 expression is induced after exposure to gamma-irradiation and chemotherapeutic agents [167]. This increased PRAP1 expression helped promote survival of cells following DNA damage by inducing cell cycle arrest. It was also confirmed that the promotor of PRAP1 contains a p53-response elements and that PRAP1 expression was downstream of p53 activity [167]. While this provides strong evidence that PRAP1 functions in response to DNA damage, the function of PRAP1 expression in the gastrointestinal epithelium remained unexplored.

Although PRAP1 expression is always impressively high in the small intestine, the *Prap1*$^{-/-}$ mice displayed no spontaneous disease and histological analysis of the intestinal epithelium appeared normal. It was only after 10 Gy TBI that the *Prap1*$^{-/-}$ mice displayed an

obvious phenotype with accelerated death and increased apoptosis of the epithelial cells. While apoptosis of epithelial cells after irradiation is an important mechanism for the elimination of damaged cells, increased apoptosis in the crypts can have lasting effects on the ability of the epithelium to restore normal function, leading to acute radiation enteritis and death [248]. Indeed, *Prap1*$^{-/-}$ mice had increased apoptosis in the crypts of the small intestine, making them more susceptible to acute radiation enteritis. In addition to increased apoptosis in the crypts 6 hours post-irradiation, the *Prap1*$^{-/-}$ mice displayed increased apoptosis 3-4 days after irradiation. This increased level of late apoptosis coincided with increased expression levels of the pro-apoptotic gene, *Bax*. The cells undergoing apoptosis days after irradiation were located outside the crypt and were likely much lower and perhaps inside the crypt when irradiation took place. Apoptotic cells found days after irradiation in the intestinal epithelium are less understood with few studies describing their presence. One study did observe additional apoptosis 24 hours and 40 hours after irradiation and this apoptosis was concluded to be independent of p53 expression [256]. The p53 null mice displayed very little early apoptosis shortly after irradiation but had comparable apoptosis at these later time points compared to wildtype mice. The apoptosis observed at later time points was only observed in mice that received high amounts of DNA damage and are presumed to be cells that escaped DNA damage repair and experience mitotic catastrophe, undergoing apoptosis induced by an unknown p53-independent mechanism. The increased apoptosis and accelerated death of *Prap1*$^{-/-}$ mice after irradiation implicates PRAP1 as an important mediator in determining cell fate after irradiation and it is likely that PRAP1 activity is involved in the downstream activity of p53 at early time points after irradiation.

To investigate the mechanism by which PRAP1 could influence cell fate after irradiation we measured the expression of cell cycle arrest proteins in an isolated *ex vivo* epithelial model

before and after irradiation. These isolated primary epithelial cells were derived from a harvest of intestinal crypts from wildtype and *Prap1*$^{-/-}$ mice, forming enteroids with or without PRAP1 expression. The enteroids were extremely sensitive to irradiation, displaying considerable amounts of apoptosis after a 2 Gy dose of irradiation. Following irradiation, all enteroids had increased expression of p21, as expected. This increase in p21 expression is important for the inhibition of cyclin-CDK activity, promoting cell cycle arrest and allowing for important DNA damage repair and cell survival [257]. Interestingly, the *Prap1*$^{-/-}$ enteroids had a significantly higher expression of p21, coinciding with increased rates of apoptosis. This increased p21 expression in the *Prap1*$^{-/-}$ mice was further validated with a decrease in p21 protein after PRAP1 overexpression in an epithelial cell line. While p21 activity has been shown to increase survival after irradiation due to cell cycle arrest [258], multiple studies have shown that p21 can have dual function regarding cell fate after irradiation [259, 260]. Studies overexpressing p21 after irradiation have coincided with increased apoptosis; implying p21 activity expands beyond CDK inhibition [189-191]. It is possible that dysregulation of p21 expression influences the cell to undergo apoptosis instead of cell cycle arrest. In summary, the absence of PRAP1 increases the expression level of p21 in the epithelium, coinciding with increased apoptosis.

While our experiments show a negative correlation between PRAP1 and p21 expression after irradiation, the mechanism by which PRAP1 influences p21 expression remains unknown. Many plausible possibilities exist, including direct or indirect regulation of p21 transcription. Because PRAP1 is an intrinsically disordered protein, it is likely that PRAP1 can weakly bind a variety of proteins. Interestingly, p21 is also an intrinsically disordered protein and it is this attribute that allows p21 to weakly bind of variety of proteins, promoting the formation of protein complexes and therefore influencing a variety of cellular responses [174]. If PRAP1 is

also important for the formation of different protein complexes, it is possible that in the absence of PRAP1, proper cellular response to irradiation is less efficient. This could either directly affect the induction of p21 expression or cause suboptimal function of critical signaling proteins, including p21 itself. To further understand the relationship between PRAP1, p21 and apoptosis it will be critical to identify the proteins bound to PRAP1 after irradiation. Because PRAP1 is a naturally abundant protein, co-immunoprecipitations on cell lysate from irradiated mouse intestinal tissue seems technically plausible. After isolating PRAP1, mass spectrometry could be used to identify the proteins bound to PRAP1. Because PRAP1 is intrinsically disordered and therefore "sticky", it is likely the mass spectrometry will reveal a long list of possible interacting proteins. It will also be useful to perform an additional co-immunoprecipitation on cell lysate from un-irradiated intestinal tissue. This will allow comparison of proteins bound to PRAP1 before and after irradiation, allowing a more reliable way of identifying proteins relevant to PRAP1 function after irradiation. Identifying proteins bound to PRAP1 before and after irradiation will be a critical next step to understanding the mechanism behind PRAP1's ability to prevent irradiation-induced apoptosis.

Lastly, because we show that PRAP1 is important for cellular survival following irradiation, future studies should involve the investigation of PRAP1 expression altering the ability of cancer cells to resist chemotherapeutic treatments. Cell fate after DNA damage is largely determined by the transcriptional activity of p53 [253]. Depending on the dose and timing of the damage, p53 activation can lead to the expression of cell cycle arrest proteins and/or pro-apoptotic proteins [254]. Both outcomes are largely dependent on p53 activation and are important for preventing tumor formation and progression. Indeed, mutations in p53 are found in approximately 50% of invasive tumors [261]. These mutations usually inhibit the ability

of p53 to induce transcription of cell cycle regulators and pro-apoptotic proteins [262]. The inability of the cell to undergo cell cycle arrest or apoptosis following DNA damage promotes tumor survival [263]. Because PRAP1 has been found to prevent apoptosis in non-malignant cells following irradiation, it is important to determine the expression level of PRAP1 in tumor cells. Perhaps PRAP1 expression is increased during tumorigenesis and this increased PRAP1 expression could make cancer cells more resistant to chemotherapeutic treatments or irradiation by preventing apoptosis. Whether or not PRAP1 expression is altered in cancer cells, silencing PRAP1 expression or inhibiting PRAP1 activity specifically in cancer cells could pose as a possible avenue to increase the effectiveness of current chemotherapeutic strategies.

**PRAP1 Function in the Uterus**

While Chapter 2 focuses on PRAP1 function in the small intestinal epithelium, supplemental data shows that PRAP1 is also highly expressed in the endometrium, or uterine epithelium. While PRAP1 is always highly expressed in the small intestine, it is only detected in the endometrium during a stage of the hormonal cycle called estrus. Another interesting difference between the small intestine and uterus concerning PRAP1 is the cellular localization. In the small intestine, PRAP1 was only observed intracellularly, despite using fixations that would preserve any kind of luminal secretion. In contrast, during estrus, PRAP1 was clearly secreted into the lumen of the uterus. Indeed, PRAP1 has a signal peptide at the N terminus, a classic characteristic of secreted proteins. Because we did not observe convincing PRAP1 secretion in the small intestine before or after irradiation and because of its role in the cellular response to irradiation, we believe PRAP1 is functioning intracellularly in the intestinal epithelium. It is possible that PRAP1 has an additional function in the lumen of the uterus that remains to be understood. Despite its secretion in the uterus, we cannot ignore the interesting

connection between our findings in the gut and the events that take place in the uterus during estrus. Throughout the hormonal cycle, the endometrium undergoes dramatic changes that coincide with the initiation of high amounts of proliferation and apoptosis. Interestingly, estrus is the stage in the hormonal cycle where the luminal epithelium experiences the least amount of apoptosis, followed by metestrus, when the luminal epithelium then has a dramatic increase in apoptosis [264]. It is possible that the abundant expression of PRAP1 in the endometrium during estrus is important for the low levels of apoptosis observed. To investigate this possibility further, it will be helpful to measure the amounts of apoptosis in the uterine luminal epithelium in carefully staged wildtype and *Prap1*$^{-/-}$ cycling female mice. If PRAP1 is important for the prevention of apoptosis in the uterus, we hypothesize that the *Prap1*$^{-/-}$ females will display increased amounts of apoptosis during estrus. Understanding the function of PRAP1 in the uterus will not only improve our understanding of PRAP1 but could reveal additional functions specific to this tissue.

**Lactobacilli are Beneficial in both the Gut and Reproductive Tract**

It has become increasingly appreciated that the microbiota plays a significant role in host health in multiple mucosal tissues. Although effects of the microbiota are now being identified well beyond their local mucosa, research investigating the relationship between the microbiota and human health started in the gastrointestinal tract. Here, many have shown using mouse models that the presence of the microbiota can influence intestinal epithelial barrier repair, inflammatory status and breakdown of dietary components for enhanced nutrient absorption [74, 161, 162]. While the increased susceptibility of germ-free mice to GI challenge underscores the importance of the gut microbiota, there are certain bacterial species that have been attributed to specific benefits. These bacteria have been termed “probiotics” and one example of a well-

studied probiotic is *Lactobacillus rhamnosus* GG (LGG) [265]. Our lab has shown that oral ingestion of LGG prior to GI challenge such as DSS colitis or irradiation significantly improves outcomes, with increased epithelial repair and barrier restoration [4, 266]. While the identification of probiotics and their benefits on host health are intriguing, much more focus has now been placed on the mechanism by which certain probiotics elicit their beneficial effects. To determine the ways in which oral ingestion of LGG led to protection from GI injury, Jones et al. [4] fed germ-free mice PBS, LGG or a commensal E. coli as a bacterial control. Colonic tissue was harvested from these mice 4 hours later and RNA sequencing was performed. Transcriptomic analysis revealed several genes specifically induced in the colon by LGG and not the E. coli control. Many of the genes induced were dependent on Nrf2 activation, eliciting increased cytoprotection and providing a solid explanation for the mechanism by which LGG elicits beneficial effects in the gastrointestinal tract. In addition to the known cytoprotective genes induced were others with less known function, such as PRAP1. In Chapter 2 we functionally characterize PRAP1 and show that PRAP1 expression protects the gastrointestinal epithelium from irradiation-induced apoptosis. Although induced by LGG in colon, PRAP1 does not have an antioxidant response element (ARE) within its promotor and therefore it is unlikely that PRAP1 is an additional gene transcribed downstream of LGG induced-Nrf2 activation. Instead, others have shown that PRAP1 contains a binding site for p53, indicating that PRAP1 induction could be downstream of p53 activation in the colon [167]. Indeed, LGG has been shown to induce other genes downstream of p53 activation [267, 268]. It is possible that the induction of PRAP1 expression via p53 activation is just one of many ways in which LGG oral gavage protects the intestinal epithelium from irradiation injury.

While significant strides have been made regarding the role of the gut microbiota on human health, characterizing the role of the vaginal microbiota in human health and pregnancy has been more difficult. While it is well accepted that a healthy human vaginal microbiota is dominated by *Lactobacillus* species, it is unclear why this dominance occurs and the requirements for its maintenance [221, 232]. While *Lactobacillus* species are generally thought to be beneficial in both the gut and the vagina, the bacterial community structure between these two tissues is significantly different. It is currently understood that a highly diverse gut microbiota is considered healthy while the opposite is considered for the vagina. High diversity of the vaginal microbiota with loss of *Lactobacillus* dominance is a major component of bacterial vaginosis, a common condition among women that causes uncomfortable symptoms and increases the risk of pregnancy complications [211]. While the vaginal microbiota has endless potential roles in reproductive health, our understanding of its maintenance and interaction with the host remains poorly understood, with a main limitation being the lack of a reliable animal model.

**Limitations of using Animal Models to Study the Human Vaginal Microbiota**

Sampling and sequencing the bacteria found in the human vagina has given a clear picture of bacteria that are present in both healthy and disease states. The most common microbial syndrome seen in women of child-bearing age is bacterial vaginosis (BV), affecting approximately 1/3 of women in the United States [269, 270]. While only 15.7% of women report having vaginal symptoms, BV predisposes women to STD infections, pelvic inflammatory disease and pre-term birth during pregnancy [210, 269]. 16S sequencing has revealed five different community state types (CST) among reproductive-age women and one of these CSTs (CST IV) lack *Lactobacillus* dominance and instead have increased diversity and increased

abundance of *Gardnerella* and *Prevotella* bacteria [206]. While we have a clear understanding of the bacterial communities seen in healthy and BV conditions, we do not understand why some women have persistent recurrence of BV and the mechanism by which BV increases pregnancy complications [221]. To investigate the mechanisms by which certain bacterial communities affect reproductive health, utilization of an animal model would eliminate significant complications and limitations present in human studies. Unfortunately, development of a reliable animal model to study the human vaginal microbiota has been extremely difficult. The main reason for this difficulty is that when considering all placental mammals investigated, humans have a unique vaginal microbiota [230, 231]. We are the only species having a vaginal microbiota dominated by *Lactobacillus*. Even the vaginal microbiota found in baboons is significantly more diverse [229]. The unique natural bacterial community structure found in humans makes development of an animal model challenging. The natural vaginal microbiota structure of animal models differs significantly from the human vaginal microbiota and therefore experiments in animal models involving the microbiota and reproductive function are not highly translational.

Mice are a common animal model with the possibility of genetic modification and can be maintained in a gnotobiotic setting, allowing more control of their microbiota. While there has not been much research on the natural vaginal microbiota of mice housed in a research facility, one study by Vrbanac et al. [271] showed that the murine vaginal microbiota of C57/BL6 mice from Jackson separated into five community state types (mCSTs), with the most common being dominated by *Staphylococcus*. While about 50% of the samples belonged to mCST I (dominated by *Staphylococcus*), the other 50% of samples belonged to the other four mCSTs that were dominated by either *Enterococcus*, *Staphylococcus* and *Enterococcus*, *Lactobacillus*, or no

particular bacterial genus. While there was a community state type dominated by *Lactobacillus*, this community state type and others seemed unstable, with individual mice displaying multiple CSTs throughout the sampling period. This shift in the vaginal microbiota did not correlate with different stages of the hormonal cycle [271]. This high amount of variability in the murine vaginal microbiota poses considerable challenges when attempting to model the human vaginal microbiota. In order to improve the mouse model, others have isolated bacterial strains from women, expanded this bacteria in culture and then mono-colonized germ-free mice. They found that they were able to successfully colonize the murine vaginal tract with *Gardnerella vaginalis* and this colonization was decreased when they first inoculated the mice with *Lactobacillus johnsonii* [272]. While this approach successfully introduced relevant bacteria into the vaginal tract of the mouse, it was only one bacterial species and does not accurately recapitulate the human vaginal microbiota.

In Chapter 3 we aimed to further improve this model using germ-free mice housed in micro-isolator cages to generate human microbiota-associated (HMA) mice. Unlike traditional germ-free housing that keeps several cages of germ free mice in a single isolator, the micro-isolator cage allows housing of a single mouse in an isolator [216]. This permits colonization of several mice with unique bacterial samples or in this case, vaginal swabs from patients. Utilizing HMA mice, our goal was to generate mice that had a vaginal microbiota similar to their respective donor and therefore serve as a model to study the human vaginal microbiota in pregnancy outcomes. If successful, this would improve the current models that rely on mono-colonization. After swabbing the germ-free females, we waited two weeks to allow bacterial colonization before setting up a timed pregnancy. Pregnant females were sacrificed the day before delivery and the vaginal tissue was harvested for 16S analysis. Microbiota analysis of

both the patient swab and the murine vagina revealed inadequate colonization of bacteria in the mouse that was representative of the human vaginal microbiota. While patients with a healthy vaginal microbiota were dominated with *Lactobacillus*, their respective mice did not have *Lactobacillus* dominance. Likewise, BV patients had *Gardnerella* and *Prevotella* species present in their swab but those species were not found at similar abundance in the respective murine vaginal microbiota. We conclude that this particular protocol for HMA mouse generation was not successful in producing an adequate model for the study of the human vaginal microbiota. Future endeavors in generating a similar mouse model should consider several technical limitations that arose.

When generating the HMA mice using human vaginal swabs, several technical limitations existed. The most obvious concern early in the protocol was the handling of the patient swab before inoculating the germ-free mouse. The vaginal swab was self-collected by the patient and stored in a sterile tube and immediately transferred to the research lab at Emory. We would then transfer it into the BSL2 mouse facility housing the germ-free females in micro-isolator cages. Although we inoculated the mice as quickly as possible, at least an hour would transpire between patient collection and mouse inoculation. It is unclear how many bacteria were viable by the time the mice were swabbed, since 16S analysis of the swab includes non-viable bacteria. To improve this aspect in the future, patient swabs could be kept on ice and/or the swab could be placed in a cold buffer such as PBS to preserve the bacteria. If maintaining viability of the bacteria on the swab is still an issue, another approach to sample collection and inoculation should be considered. Because we are fairly familiar with the community state types that exist in the human vaginal microbiota, it could be possible to isolate the major bacterial species that make up each community state type to generate a kind of standardized cocktail that could then be

introduced to the mouse. Isolation of several relevant bacterial species and culturing them in the lab would increase the number of CFU introduced to the mouse and it would be easier to ensure their viability. A similar approach has been successfully implemented concerning the generation of mice with a specific gut microbiota. The altered Schaedler flora (ASF) is a standardized cocktail of eight bacterial species that is commonly employed to study gut-microbe interactions in mice [273, 274]. A similar approach could be used to study the vaginal microbiota, with the use of the standardized cocktail of bacteria that represent a healthy human vaginal microbiota. This approach has its own set of limitations as well, such as the ability to easily culture the relevant bacteria in the lab and the likelihood that less abundant but functionally important bacterial species would likely not be included in the cocktail.

Additionally, the hormonal stage of the germ-free female on the day of inoculation could affect the success of the colonization. Our lab and others have shown that bacterial abundance in the vaginal tract tends to be higher during the hormonal stage of estrus and lower in non-cycling females (diestrus) [271]. If the germ-free females are not cycling when inoculated, this could hinder the ability of the bacteria to successfully colonize the vaginal tract. To improve this protocol, the germ-free females could be introduced to male bedding from germ free cages or they could receive an injection of estrogen to induce cycling. Ensuring cycling of the females before inoculation would be much more feasible if the mice were being inoculated with a standardized cocktail of bacteria instead of a patient swab. Patient swabs arrive unexpectedly, and it would be difficult to ensure estrus in the females before inoculation.

One technical issue that was not expected was the success of the 16S sequencing on the murine vaginal tissue the day before delivery. While the vagina of a conventional mouse may have orders of magnitude less bacteria in the vagina than in the GI tract, it is still fairly possible

to isolate enough microbial DNA from the tissue to produce a reliable 16S band after PCR amplification. During pilot studies in which we colonized mice with patient swabs and waited two weeks, we were able to collect enough microbial DNA to successfully amplify the 16S gene via PCR. But when we repeated this protocol on vaginal tissue from pregnant mice the day before delivery, it was significantly harder to amplify the 16S gene by PCR due to low microbial DNA yield. To determine whether this was an issue specific to the HMA mice and possibly indicative of inadequate colonization, we collected a conventional female the day before delivery and again had similar issues. We concluded that at this stage of pregnancy in the mice, there is a very low abundance of bacteria in the vagina. Although we were still able to amplify the 16S gene using two successive rounds of PCR, this was not ideal. To improve this protocol, additional research needs to be conducted to determine the bacterial load in the murine vagina and how this changes during different stages of pregnancy. Choosing to sacrifice the mouse during a different stage of pregnancy may yield more microbial DNA that would ultimately be more informative concerning the successful modeling of the human vaginal microbiota. It is also possible that pregnancy itself decreases the bacterial load in the murine vagina and modeling the human vaginal microbiota in mice would be more successful in non-pregnant mice.

In conclusion, our work in Chapter 3 has underscored the need to better understand the murine vaginal microbiota and the ways in which we can manipulate it to accurately model the human vaginal microbiota. Mice have certainly served as useful models for the human gut microbiota. Further investigation concerning the reproductive tract of mice housed in research facilities will better position future endeavors to generate a useful mouse model of the human vaginal microbiota.

## References

[1] Van den Abbeele P, Verstraete W, El Aidy S, Geirnaert A, Van de Wiele T. Prebiotics, faecal transplants and microbial network units to stimulate biodiversity of the human gut microbiome. Microb Biotechnol 2013;6(4):335-40.

[2] Neish AS. The gut microflora and intestinal epithelial cells: a continuing dialogue. Microbes Infect 2002;4(3):309-17.

[3] Caballero S, Pamer EG. Microbiota-mediated inflammation and antimicrobial defense in the intestine. Annu Rev Immunol 2015;33:227-56.

[4] Jones RM, Desai C, Darby TM, Luo L, Wolfarth AA, Scharer CD, Ardita CS, Reedy AR, Keebaugh ES, Neish AS. Lactobacilli Modulate Epithelial Cytoprotection through the Nrf2 Pathway. Cell Rep 2015;12(8):1217-25.

[5] Kaplan GG. The global burden of IBD: from 2015 to 2025. Nat Rev Gastroenterol Hepatol 2015;12(12):720-7.

[6] Ben-Horin S, Kopylov U, Chowers Y. Optimizing anti-TNF treatments in inflammatory bowel disease. Autoimmun Rev 2014;13(1):24-30.

[7] Kopylov U, Ben-Horin S, Seidman E. Therapeutic drug monitoring in inflammatory bowel disease. Ann Gastroenterol 2014;27(4):304-12.

[8] Greenwood-Van Meerveld B, Johnson AC, Grundy D. Gastrointestinal Physiology and Function. Handb Exp Pharmacol 2017;239:1-16.

[9] Zheng L, Kelly CJ, Colgan SP. Physiologic hypoxia and oxygen homeostasis in the healthy intestine. A Review in the Theme: Cellular Responses to Hypoxia. Am J Physiol Cell Physiol 2015;309(6):C350-60.

[10] Gu S, Chen D, Zhang JN, Lv X, Wang K, Duan LP, Nie Y, Wu XL. Bacterial community mapping of the mouse gastrointestinal tract. PLoS One 2013;8(10):e74957.

[11] Zoetendal EG, Raes J, van den Bogert B, Arumugam M, Booijink CC, Troost FJ, Bork P, Wels M, de Vos WM, Kleerebezem M. The human small intestinal microbiota is driven by rapid uptake and conversion of simple carbohydrates. ISME J 2012;6(7):1415-26.

[12] Luo Q, Kumar P, Vickers TJ, Sheikh A, Lewis WG, Rasko DA, Sistrunk J, Fleckenstein JM. Enterotoxigenic Escherichia coli secretes a highly conserved mucin-degrading metalloprotease to effectively engage intestinal epithelial cells. Infect Immun 2014;82(2):509-21.

[13] Mouricout M. Interactions between the enteric pathogen and the host. An assortment of bacterial lectins and a set of glycoconjugate receptors. Adv Exp Med Biol 1997;412:109-23.

[14] Broer S, Fairweather SJ. Amino Acid Transport Across the Mammalian Intestine. Compr Physiol 2018;9(1):343-73.

[15] Chen C, Yin Y, Tu Q, Yang H. Glucose and amino acid in enterocyte: absorption, metabolism and maturation. Front Biosci (Landmark Ed) 2018;23:1721-39.

[16] Haber AL, Biton M, Rogel N, Herbst RH, Shekhar K, Smillie C, Burgin G, Delorey TM, Howitt MR, Katz Y, Tirosh I, Beyaz S, Dionne D, Zhang M, Raychowdhury R, Garrett WS, Rozenblatt-Rosen O, Shi HN, Yilmaz O, Xavier RJ, Regev A. A single-cell survey of the small intestinal epithelium. Nature 2017;551(7680):333-9.

[17] Sato T, van Es JH, Snippert HJ, Stange DE, Vries RG, van den Born M, Barker N, Shroyer NF, van de Wetering M, Clevers H. Paneth cells constitute the niche for Lgr5 stem cells in intestinal crypts. Nature 2011;469(7330):415-8.

[18] Ermund A, Schutte A, Johansson ME, Gustafsson JK, Hansson GC. Studies of mucus in mouse stomach, small intestine, and colon. I. Gastrointestinal mucus layers have different properties depending on location as well as over the Peyer's patches. Am J Physiol Gastrointest Liver Physiol 2013;305(5):G341-7.

[19] Gribble FM, Reimann F. Enteroendocrine Cells: Chemosensors in the Intestinal Epithelium. Annu Rev Physiol 2016;78:277-99.

[20] Gerbe F, van Es JH, Makrini L, Brulin B, Mellitzer G, Robine S, Romagnolo B, Shroyer NF, Bourgaux JF, Pignodel C, Clevers H, Jay P. Distinct ATOH1 and Neurog3 requirements define tuft cells as a new secretory cell type in the intestinal epithelium. J Cell Biol 2011;192(5):767-80.

[21] Nevo S, Kadouri N, Abramson J. Tuft cells: From the mucosa to the thymus. Immunol Lett 2019;210:1-9.

[22] Nevalainen TJ. Ultrastructural characteristics of tuft cells in mouse gallbladder epithelium. Acta Anat (Basel) 1977;98(2):210-20.

[23] Gerbe F, Sidot E, Smyth DJ, Ohmoto M, Matsumoto I, Dardalhon V, Cesses P, Garnier L, Pouzolles M, Brulin B, Bruschi M, Harcus Y, Zimmermann VS, Taylor N, Maizels RM, Jay P. Intestinal epithelial tuft cells initiate type 2 mucosal immunity to helminth parasites. Nature 2016;529(7585):226-30.

[24] Gerbe F, Legraverend C, Jay P. The intestinal epithelium tuft cells: specification and function. Cell Mol Life Sci 2012;69(17):2907-17.

[25] Turner JR. Intestinal mucosal barrier function in health and disease. Nat Rev Immunol 2009;9(11):799-809.

[26] Farquhar MG, Palade GE. Junctional complexes in various epithelia. J Cell Biol 1963;17:375-412.

[27] Odenwald MA, Turner JR. The intestinal epithelial barrier: a therapeutic target? Nat Rev Gastroenterol Hepatol 2017;14(1):9-21.

[28] Hartsock A, Nelson WJ. Adherens and tight junctions: structure, function and connections to the actin cytoskeleton. Biochim Biophys Acta 2008;1778(3):660-9.

[29] Van Itallie CM, Anderson JM. Claudins and epithelial paracellular transport. Annu Rev Physiol 2006;68:403-29.

[30] Furuse M, Furuse K, Sasaki H, Tsukita S. Conversion of zonulae occludentes from tight to leaky strand type by introducing claudin-2 into Madin-Darby canine kidney I cells. J Cell Biol 2001;153(2):263-72.

[31] Wada M, Tamura A, Takahashi N, Tsukita S. Loss of claudins 2 and 15 from mice causes defects in paracellular Na+ flow and nutrient transport in gut and leads to death from malnutrition. Gastroenterology 2013;144(2):369-80.

[32] Capaldo CT, Powell DN, Kalman D. Layered defense: how mucus and tight junctions seal the intestinal barrier. J Mol Med (Berl) 2017;95(9):927-34.

[33] Fihn BM, Sjoqvist A, Jodal M. Permeability of the rat small intestinal epithelium along the villus-crypt axis: effects of glucose transport. Gastroenterology 2000;119(4):1029-36.

[34] Watson AJ, Chu S, Sieck L, Gerasimenko O, Bullen T, Campbell F, McKenna M, Rose T, Montrose MH. Epithelial barrier function in vivo is sustained despite gaps in epithelial layers. Gastroenterology 2005;129(3):902-12.

[35] Gum JR, Jr., Hicks JW, Toribara NW, Siddiki B, Kim YS. Molecular cloning of human intestinal mucin (MUC2) cDNA. Identification of the amino terminus and overall sequence similarity to prepro-von Willebrand factor. J Biol Chem 1994;269(4):2440-6.

[36] Ambort D, Johansson ME, Gustafsson JK, Nilsson HE, Ermund A, Johansson BR, Koeck PJ, Hebert H, Hansson GC. Calcium and pH-dependent packing and release of the gel-forming MUC2 mucin. Proc Natl Acad Sci U S A 2012;109(15):5645-50.

[37] Ridley C, Kouvatsos N, Raynal BD, Howard M, Collins RF, Desseyn JL, Jowitt TA, Baldock C, Davis CW, Hardingham TE, Thornton DJ. Assembly of the respiratory mucin MUC5B: a new model for a gel-forming mucin. J Biol Chem 2014;289(23):16409-20.

[38] Gustafsson JK, Ermund A, Ambort D, Johansson ME, Nilsson HE, Thorell K, Hebert H, Sjovall H, Hansson GC. Bicarbonate and functional CFTR channel are required for proper mucin secretion and link cystic fibrosis with its mucus phenotype. J Exp Med 2012;209(7):1263-72.

[39] Heazlewood CK, Cook MC, Eri R, Price GR, Tauro SB, Taupin D, Thornton DJ, Png CW, Crockford TL, Cornall RJ, Adams R, Kato M, Nelms KA, Hong NA, Florin TH, Goodnow CC, McGuckin MA. Aberrant mucin assembly in mice causes endoplasmic reticulum stress and spontaneous inflammation resembling ulcerative colitis. PLoS Med 2008;5(3):e54.

[40] Johansson ME. Fast renewal of the distal colonic mucus layers by the surface goblet cells as measured by in vivo labeling of mucin glycoproteins. PLoS One 2012;7(7):e41009.

[41] Vaishnava S, Yamamoto M, Severson KM, Ruhn KA, Yu X, Koren O, Ley R, Wakeland EK, Hooper LV. The antibacterial lectin RegIIIgamma promotes the spatial segregation of microbiota and host in the intestine. Science 2011;334(6053):255-8.

[42] Janeway CA, Jr. The immune system evolved to discriminate infectious nonself from noninfectious self. Immunol Today 1992;13(1):11-6.

[43] Hayashi F, Smith KD, Ozinsky A, Hawn TR, Yi EC, Goodlett DR, Eng JK, Akira S, Underhill DM, Aderem A. The innate immune response to bacterial flagellin is mediated by Toll-like receptor 5. Nature 2001;410(6832):1099-103.

[44] Neal MD, Leaphart C, Levy R, Prince J, Billiar TR, Watkins S, Li J, Cetin S, Ford H, Schreiber A, Hackam DJ. Enterocyte TLR4 mediates phagocytosis and translocation of bacteria across the intestinal barrier. J Immunol 2006;176(5):3070-9.

[45] Medzhitov R, Preston-Hurlburt P, Kopp E, Stadlen A, Chen C, Ghosh S, Janeway CA, Jr. MyD88 is an adaptor protein in the hToll/IL-1 receptor family signaling pathways. Mol Cell 1998;2(2):253-8.

[46] Obermeier F, Dunger N, Strauch UG, Grunwald N, Herfarth H, Scholmerich J, Falk W. Contrasting activity of cytosin-guanosin dinucleotide oligonucleotides in mice with experimental colitis. Clin Exp Immunol 2003;134(2):217-24.

[47] Schnare M, Barton GM, Holt AC, Takeda K, Akira S, Medzhitov R. Toll-like receptors control activation of adaptive immune responses. Nat Immunol 2001;2(10):947-50.

[48] Uematsu S, Fujimoto K, Jang MH, Yang BG, Jung YJ, Nishiyama M, Sato S, Tsujimura T, Yamamoto M, Yokota Y, Kiyono H, Miyasaka M, Ishii KJ, Akira S. Regulation of humoral and cellular gut immunity by lamina propria dendritic cells expressing Toll-like receptor 5. Nat Immunol 2008;9(7):769-76.

[49] Rakoff-Nahoum S, Paglino J, Eslami-Varzaneh F, Edberg S, Medzhitov R. Recognition of commensal microflora by toll-like receptors is required for intestinal homeostasis. Cell 2004;118(2):229-41.

[50] Lee J, Mo JH, Katakura K, Alkalay I, Rucker AN, Liu YT, Lee HK, Shen C, Cojocaru G, Shenouda S, Kagnoff M, Eckmann L, Ben-Neriah Y, Raz E. Maintenance of colonic homeostasis by distinctive apical TLR9 signalling in intestinal epithelial cells. Nat Cell Biol 2006;8(12):1327-36.

[51] Inohara N, Koseki T, Lin J, del Peso L, Lucas PC, Chen FF, Ogura Y, Nunez G. An induced proximity model for NF-kappa B activation in the Nod1/RICK and RIP signaling pathways. J Biol Chem 2000;275(36):27823-31.

[52] Park JH, Kim YG, McDonald C, Kanneganti TD, Hasegawa M, Body-Malapel M, Inohara N, Nunez G. RICK/RIP2 mediates innate immune responses induced through Nod1 and Nod2 but not TLRs. J Immunol 2007;178(4):2380-6.

[53] Sorbara MT, Ellison LK, Ramjeet M, Travassos LH, Jones NL, Girardin SE, Philpott DJ. The protein ATG16L1 suppresses inflammatory cytokines induced by the intracellular sensors Nod1 and Nod2 in an autophagy-independent manner. Immunity 2013;39(5):858-73.

[54] Chamaillard M, Hashimoto M, Horie Y, Masumoto J, Qiu S, Saab L, Ogura Y, Kawasaki A, Fukase K, Kusumoto S, Valvano MA, Foster SJ, Mak TW, Nunez G, Inohara N. An essential role for NOD1 in host recognition of bacterial peptidoglycan containing diaminopimelic acid. Nat Immunol 2003;4(7):702-7.

[55] Girardin SE, Boneca IG, Carneiro LA, Antignac A, Jehanno M, Viala J, Tedin K, Taha MK, Labigne A, Zahringer U, Coyle AJ, DiStefano PS, Bertin J, Sansonetti PJ, Philpott DJ. Nod1 detects a unique muropeptide from gram-negative bacterial peptidoglycan. Science 2003;300(5625):1584-7.

[56] McDonald C, Inohara N, Nunez G. Peptidoglycan signaling in innate immunity and inflammatory disease. J Biol Chem 2005;280(21):20177-80.

[57] Barnich N, Aguirre JE, Reinecker HC, Xavier R, Podolsky DK. Membrane recruitment of NOD2 in intestinal epithelial cells is essential for nuclear factor-{kappa}B activation in muramyl dipeptide recognition. J Cell Biol 2005;170(1):21-6.

[58] Ogura Y, Inohara N, Benito A, Chen FF, Yamaoka S, Nunez G. Nod2, a Nod1/Apaf-1 family member that is restricted to monocytes and activates NF-kappaB. J Biol Chem 2001;276(7):4812-8.

[59] Hugot JP, Chamaillard M, Zouali H, Lesage S, Cezard JP, Belaiche J, Almer S, Tysk C, O'Morain CA, Gassull M, Binder V, Finkel Y, Cortot A, Modigliani R, Laurent-Puig P, Gower-Rousseau C, Macry J, Colombel JF, Sahbatou M, Thomas G. Association of NOD2 leucine-rich repeat variants with susceptibility to Crohn's disease. Nature 2001;411(6837):599-603.

[60] Ogura Y, Bonen DK, Inohara N, Nicolae DL, Chen FF, Ramos R, Britton H, Moran T, Karaliuskas R, Duerr RH, Achkar JP, Brant SR, Bayless TM, Kirschner BS, Hanauer SB, Nunez G, Cho JH. A frameshift mutation in NOD2 associated with susceptibility to Crohn's disease. Nature 2001;411(6837):603-6.

[61] Macho Fernandez E, Valenti V, Rockel C, Hermann C, Pot B, Boneca IG, Grangette C. Anti-inflammatory capacity of selected lactobacilli in experimental colitis is driven by NOD2-mediated recognition of a specific peptidoglycan-derived muropeptide. Gut 2011;60(8):1050-9.

[62] Watanabe T, Asano N, Murray PJ, Ozato K, Tailor P, Fuss IJ, Kitani A, Strober W. Muramyl dipeptide activation of nucleotide-binding oligomerization domain 2 protects mice from experimental colitis. J Clin Invest 2008;118(2):545-59.

[63] Couturier-Maillard A, Secher T, Rehman A, Normand S, De Arcangelis A, Haesler R, Huot L, Grandjean T, Bressenot A, Delanoye-Crespin A, Gaillot O, Schreiber S, Lemoine Y, Ryffel B, Hot D, Nunez G, Chen G, Rosenstiel P, Chamaillard M. NOD2-mediated dysbiosis predisposes mice to transmissible colitis and colorectal cancer. J Clin Invest 2013;123(2):700-11.

[64] Migeotte I, Communi D, Parmentier M. Formyl peptide receptors: a promiscuous subfamily of G protein-coupled receptors controlling immune responses. Cytokine Growth Factor Rev 2006;17(6):501-19.

[65] Jesaitis AJ, Naemura JR, Sklar LA, Cochrane CG, Painter RG. Rapid modulation of N-formyl chemotactic peptide receptors on the surface of human granulocytes: formation of high-affinity ligand-receptor complexes in transient association with cytoskeleton. J Cell Biol 1984;98(4):1378-87.

[66] Sklar LA, Hyslop PA, Oades ZG, Omann GM, Jesaitis AJ, Painter RG, Cochrane CG. Signal transduction and ligand-receptor dynamics in the human neutrophil. Transient responses and occupancy-response relations at the formyl peptide receptor. J Biol Chem 1985;260(21):11461-7.

[67] Wentworth CC, Jones RM, Kwon YM, Nusrat A, Neish AS. Commensal-epithelial signaling mediated via formyl peptide receptors. Am J Pathol 2010;177(6):2782-90.

[68] Lambeth JD. NOX enzymes and the biology of reactive oxygen. Nat Rev Immunol 2004;4(3):181-9.

[69] Ha EM, Oh CT, Bae YS, Lee WJ. A direct role for dual oxidase in Drosophila gut immunity. Science 2005;310(5749):847-50.

[70] Ha EM, Oh CT, Ryu JH, Bae YS, Kang SW, Jang IH, Brey PT, Lee WJ. An antioxidant system required for host protection against gut infection in Drosophila. Dev Cell 2005;8(1):125-32.

[71] Barford D. The role of cysteine residues as redox-sensitive regulatory switches. Curr Opin Struct Biol 2004;14(6):679-86.

[72] Kamata H, Honda S, Maeda S, Chang L, Hirata H, Karin M. Reactive oxygen species promote TNFalpha-induced death and sustained JNK activation by inhibiting MAP kinase phosphatases. Cell 2005;120(5):649-61.

[73] Rhee SG, Kang SW, Jeong W, Chang TS, Yang KS, Woo HA. Intracellular messenger function of hydrogen peroxide and its regulation by peroxiredoxins. Curr Opin Cell Biol 2005;17(2):183-9.

[74] Alam A, Leoni G, Wentworth CC, Kwal JM, Wu H, Ardita CS, Swanson PA, Lambeth JD, Jones RM, Nusrat A, Neish AS. Redox signaling regulates commensal-mediated mucosal homeostasis and restitution and requires formyl peptide receptor 1. Mucosal Immunol 2014;7(3):645-55.

[75] Neish AS. Redox signaling mediated by the gut microbiota. Free Radic Res 2013;47(11):950-7.

[76] Neish AS, Jones RM. Redox signaling mediates symbiosis between the gut microbiota and the intestine. Gut Microbes 2014;5(2):250-3.

[77] de Lau W, Kujala P, Schneeberger K, Middendorp S, Li VS, Barker N, Martens A, Hofhuis F, DeKoter RP, Peters PJ, Nieuwenhuis E, Clevers H. Peyer's patch M cells derived from Lgr5(+) stem cells require SpiB and are induced by RankL in cultured "miniguts". Mol Cell Biol 2012;32(18):3639-47.

[78] Mabbott NA, Donaldson DS, Ohno H, Williams IR, Mahajan A. Microfold (M) cells: important immunosurveillance posts in the intestinal epithelium. Mucosal Immunol 2013;6(4):666-77.

[79] Hase K, Kawano K, Nochi T, Pontes GS, Fukuda S, Ebisawa M, Kadokura K, Tobe T, Fujimura Y, Kawano S, Yabashi A, Waguri S, Nakato G, Kimura S, Murakami T, Iimura M, Hamura K, Fukuoka S, Lowe AW, Itoh K, Kiyono H, Ohno H. Uptake through glycoprotein 2 of FimH(+) bacteria by M cells initiates mucosal immune response. Nature 2009;462(7270):226-30.

[80] Hase K, Ohshima S, Kawano K, Hashimoto N, Matsumoto K, Saito H, Ohno H. Distinct gene expression profiles characterize cellular phenotypes of follicle-associated epithelium and M cells. DNA Res 2005;12(2):127-37.

[81] Nakato G, Hase K, Suzuki M, Kimura M, Ato M, Hanazato M, Tobiume M, Horiuchi M, Atarashi R, Nishida N, Watarai M, Imaoka K, Ohno H. Cutting Edge: Brucella abortus exploits a cellular prion protein on intestinal M cells as an invasive receptor. J Immunol 2012;189(4):1540-4.

[82] Terahara K, Yoshida M, Igarashi O, Nochi T, Pontes GS, Hase K, Ohno H, Kurokawa S, Mejima M, Takayama N, Yuki Y, Lowe AW, Kiyono H. Comprehensive gene expression profiling of

Peyer's patch M cells, villous M-like cells, and intestinal epithelial cells. J Immunol 2008;180(12):7840-6.

[83] Bradford BM, Sester DP, Hume DA, Mabbott NA. Defining the anatomical localisation of subsets of the murine mononuclear phagocyte system using integrin alpha X (Itgax, CD11c) and colony stimulating factor 1 receptor (Csf1r, CD115) expression fails to discriminate dendritic cells from macrophages. Immunobiology 2011;216(11):1228-37.

[84] Mabbott NA, Kenneth Baillie J, Hume DA, Freeman TC. Meta-analysis of lineage-specific gene expression signatures in mouse leukocyte populations. Immunobiology 2010;215(9-10):724-36.

[85] Hase K, Murakami T, Takatsu H, Shimaoka T, Iimura M, Hamura K, Kawano K, Ohshima S, Chihara R, Itoh K, Yonehara S, Ohno H. The membrane-bound chemokine CXCL16 expressed on follicle-associated epithelium and M cells mediates lympho-epithelial interaction in GALT. J Immunol 2006;176(1):43-51.

[86] Iwasaki A, Kelsall BL. Localization of distinct Peyer's patch dendritic cell subsets and their recruitment by chemokines macrophage inflammatory protein (MIP)-3alpha, MIP-3beta, and secondary lymphoid organ chemokine. J Exp Med 2000;191(8):1381-94.

[87] Zhao X, Sato A, Dela Cruz CS, Linehan M, Luegering A, Kucharzik T, Shirakawa AK, Marquez G, Farber JM, Williams I, Iwasaki A. CCL9 is secreted by the follicle-associated epithelium and recruits dome region Peyer's patch CD11b+ dendritic cells. J Immunol 2003;171(6):2797-803.

[88] Lycke N, Erlandsson L, Ekman L, Schon K, Leanderson T. Lack of J chain inhibits the transport of gut IgA and abrogates the development of intestinal antitoxic protection. J Immunol 1999;163(2):913-9.

[89] Salzman NH, Hung K, Haribhai D, Chu H, Karlsson-Sjoberg J, Amir E, Teggatz P, Barman M, Hayward M, Eastwood D, Stoel M, Zhou Y, Sodergren E, Weinstock GM, Bevins CL, Williams CB, Bos NA. Enteric defensins are essential regulators of intestinal microbial ecology. Nat Immunol 2010;11(1):76-83.

[90] Hooper LV, Stappenbeck TS, Hong CV, Gordon JI. Angiogenins: a new class of microbicidal proteins involved in innate immunity. Nat Immunol 2003;4(3):269-73.

[91] Jager S, Stange EF, Wehkamp J. Inflammatory bowel disease: an impaired barrier disease. Langenbecks Arch Surg 2013;398(1):1-12.

[92] Mukherjee S, Hooper LV. Antimicrobial defense of the intestine. Immunity 2015;42(1):28-39.

[93] Stowell SR, Arthur CM, Dias-Baruffi M, Rodrigues LC, Gourdine JP, Heimburg-Molinaro J, Ju T, Molinaro RJ, Rivera-Marrero C, Xia B, Smith DF, Cummings RD. Innate immune lectins kill bacteria expressing blood group antigen. Nat Med 2010;16(3):295-301.

[94] De Smet K, Contreras R. Human antimicrobial peptides: defensins, cathelicidins and histatins. Biotechnol Lett 2005;27(18):1337-47.

[95] Bals R, Wilson JM. Cathelicidins--a family of multifunctional antimicrobial peptides. Cell Mol Life Sci 2003;60(4):711-20.

[96] Ganz T. Antimicrobial polypeptides. J Leukoc Biol 2004;75(1):34-8.

[97] Harwig SS, Tan L, Qu XD, Cho Y, Eisenhauer PB, Lehrer RI. Bactericidal properties of murine intestinal phospholipase A2. J Clin Invest 1995;95(2):603-10.

[98] Zanetti M. The role of cathelicidins in the innate host defenses of mammals. Curr Issues Mol Biol 2005;7(2):179-96.

[99] Chu H, Pazgier M, Jung G, Nuccio SP, Castillo PA, de Jong MF, Winter MG, Winter SE, Wehkamp J, Shen B, Salzman NH, Underwood MA, Tsolis RM, Young GM, Lu W, Lehrer RI, Baumler AJ, Bevins CL. Human alpha-defensin 6 promotes mucosal innate immunity through self-assembled peptide nanonets. Science 2012;337(6093):477-81.

[100] Shimada T, Park BG, Wolf AJ, Brikos C, Goodridge HS, Becker CA, Reyes CN, Miao EA, Aderem A, Gotz F, Liu GY, Underhill DM. Staphylococcus aureus evades lysozyme-based peptidoglycan digestion that links phagocytosis, inflammasome activation, and IL-1beta secretion. Cell Host Microbe 2010;7(1):38-49.

[101] Bajaj-Elliott M, Fedeli P, Smith GV, Domizio P, Maher L, Ali RS, Quinn AG, Farthing MJ. Modulation of host antimicrobial peptide (beta-defensins 1 and 2) expression during gastritis. Gut 2002;51(3):356-61.

[102] Boughan PK, Argent RH, Body-Malapel M, Park JH, Ewings KE, Bowie AG, Ong SJ, Cook SJ, Sorensen OE, Manzo BA, Inohara N, Klein NJ, Nunez G, Atherton JC, Bajaj-Elliott M. Nucleotide-binding oligomerization domain-1 and epidermal growth factor receptor: critical regulators of beta-defensins during Helicobacter pylori infection. J Biol Chem 2006;281(17):11637-48.

[103] George JT, Boughan PK, Karageorgiou H, Bajaj-Elliott M. Host anti-microbial response to Helicobacter pylori infection. Mol Immunol 2003;40(7):451-6.

[104] Hase K, Eckmann L, Leopard JD, Varki N, Kagnoff MF. Cell differentiation is a key determinant of cathelicidin LL-37/human cationic antimicrobial protein 18 expression by human colon epithelium. Infect Immun 2002;70(2):953-63.

[105] O'Neil DA, Porter EM, Elewaut D, Anderson GM, Eckmann L, Ganz T, Kagnoff MF. Expression and regulation of the human beta-defensins hBD-1 and hBD-2 in intestinal epithelium. J Immunol 1999;163(12):6718-24.

[106] Schroeder BO, Wu Z, Nuding S, Groscurth S, Marcinowski M, Beisner J, Buchner J, Schaller M, Stange EF, Wehkamp J. Reduction of disulphide bonds unmasks potent antimicrobial activity of human beta-defensin 1. Nature 2011;469(7330):419-23.

[107] Jandhyala SM, Talukdar R, Subramanyam C, Vuyyuru H, Sasikala M, Nageshwar Reddy D. Role of the normal gut microbiota. World J Gastroenterol 2015;21(29):8787-803.

[108] Mendez-Samperio P, Miranda E, Trejo A. Expression and secretion of cathelicidin LL-37 in human epithelial cells after infection by Mycobacterium bovis Bacillus Calmette-Guerin. Clin Vaccine Immunol 2008;15(9):1450-5.

[109] Liu L, Roberts AA, Ganz T. By IL-1 signaling, monocyte-derived cells dramatically enhance the epidermal antimicrobial response to lipopolysaccharide. J Immunol 2003;170(1):575-80.

[110] Verway M, Bouttier M, Wang TT, Carrier M, Calderon M, An BS, Devemy E, McIntosh F, Divangahi M, Behr MA, White JH. Vitamin D induces interleukin-1beta expression: paracrine macrophage epithelial signaling controls M. tuberculosis infection. PLoS Pathog 2013;9(6):e1003407.

[111] Haisma EM, Rietveld MH, de Breij A, van Dissel JT, El Ghalbzouri A, Nibbering PH. Inflammatory and antimicrobial responses to methicillin-resistant Staphylococcus aureus in an in vitro wound infection model. PLoS One 2013;8(12):e82800.

[112] Percoco G, Merle C, Jaouen T, Ramdani Y, Benard M, Hillion M, Mijouin L, Lati E, Feuilloley M, Lefeuvre L, Driouich A, Follet-Gueye ML. Antimicrobial peptides and pro-inflammatory cytokines are differentially regulated across epidermal layers following bacterial stimuli. Exp Dermatol 2013;22(12):800-6.

[113] Sorensen OE, Thapa DR, Rosenthal A, Liu L, Roberts AA, Ganz T. Differential regulation of beta-defensin expression in human skin by microbial stimuli. J Immunol 2005;174(8):4870-9.

[114] Guo L, Chen W, Zhu H, Chen Y, Wan X, Yang N, Xu S, Yu C, Chen L. Helicobacter pylori induces increased expression of the vitamin d receptor in immune responses. Helicobacter 2014;19(1):37-47.

[115] Peyrin-Biroulet L, Beisner J, Wang G, Nuding S, Oommen ST, Kelly D, Parmentier-Decrucq E, Dessein R, Merour E, Chavatte P, Grandjean T, Bressenot A, Desreumaux P, Colombel JF, Desvergne B, Stange EF, Wehkamp J, Chamaillard M. Peroxisome proliferator-activated receptor gamma activation is required for maintenance of innate antimicrobial immunity in the colon. Proc Natl Acad Sci U S A 2010;107(19):8772-7.

[116] Wilson CL, Ouellette AJ, Satchell DP, Ayabe T, Lopez-Boado YS, Stratman JL, Hultgren SJ, Matrisian LM, Parks WC. Regulation of intestinal alpha-defensin activation by the metalloproteinase matrilysin in innate host defense. Science 1999;286(5437):113-7.

[117] Bjerknes M, Cheng H. Intestinal epithelial stem cells and progenitors. Methods Enzymol 2006;419:337-83.

[118] Marshman E, Booth C, Potten CS. The intestinal epithelial stem cell. Bioessays 2002;24(1):91-8.

[119] Barker N, Clevers H. Leucine-rich repeat-containing G-protein-coupled receptors as markers of adult stem cells. Gastroenterology 2010;138(5):1681-96.

[120] van der Flier LG, Clevers H. Stem cells, self-renewal, and differentiation in the intestinal epithelium. Annu Rev Physiol 2009;71:241-60.

[121] Clevers HC, Bevins CL. Paneth cells: maestros of the small intestinal crypts. Annu Rev Physiol 2013;75:289-311.

[122] Garabedian EM, Roberts LJ, McNevin MS, Gordon JI. Examining the role of Paneth cells in the small intestine by lineage ablation in transgenic mice. J Biol Chem 1997;272(38):23729-40.

[123] Barker N, van Es JH, Kuipers J, Kujala P, van den Born M, Cozijnsen M, Haegebarth A, Korving J, Begthel H, Peters PJ, Clevers H. Identification of stem cells in small intestine and colon by marker gene Lgr5. Nature 2007;449(7165):1003-7.

[124] Sato T, Vries RG, Snippert HJ, van de Wetering M, Barker N, Stange DE, van Es JH, Abo A, Kujala P, Peters PJ, Clevers H. Single Lgr5 stem cells build crypt-villus structures in vitro without a mesenchymal niche. Nature 2009;459(7244):262-5.

[125] Yan KS, Chia LA, Li X, Ootani A, Su J, Lee JY, Su N, Luo Y, Heilshorn SC, Amieva MR, Sangiorgi E, Capecchi MR, Kuo CJ. The intestinal stem cell markers Bmi1 and Lgr5 identify two functionally distinct populations. Proc Natl Acad Sci U S A 2012;109(2):466-71.

[126] Sangiorgi E, Capecchi MR. Bmi1 is expressed in vivo in intestinal stem cells. Nat Genet 2008;40(7):915-20.

[127] Ishizuya-Oka A, Hasebe T. Sonic hedgehog and bone morphogenetic protein-4 signaling pathway involved in epithelial cell renewal along the radial axis of the intestine. Digestion 2008;77 Suppl 1:42-7.

[128] Semont A, Mouiseddine M, Francois A, Demarquay C, Mathieu N, Chapel A, Sache A, Thierry D, Laloi P, Gourmelon P. Mesenchymal stem cells improve small intestinal integrity through regulation of endogenous epithelial cell homeostasis. Cell Death Differ 2010;17(6):952-61.

[129] Ogaki S, Shiraki N, Kume K, Kume S. Wnt and Notch signals guide embryonic stem cell differentiation into the intestinal lineages. Stem Cells 2013;31(6):1086-96.

[130] Pinto D, Clevers H. Wnt, stem cells and cancer in the intestine. Biol Cell 2005;97(3):185-96.

[131] Korinek V, Barker N, Moerer P, van Donselaar E, Huls G, Peters PJ, Clevers H. Depletion of epithelial stem-cell compartments in the small intestine of mice lacking Tcf-4. Nat Genet 1998;19(4):379-83.

[132] Hardwick JC, Kodach LL, Offerhaus GJ, van den Brink GR. Bone morphogenetic protein signalling in colorectal cancer. Nat Rev Cancer 2008;8(10):806-12.

[133] Ireland H, Houghton C, Howard L, Winton DJ. Cellular inheritance of a Cre-activated reporter gene to determine Paneth cell longevity in the murine small intestine. Dev Dyn 2005;233(4):1332-6.

[134] Cash HL, Whitham CV, Behrendt CL, Hooper LV. Symbiotic bacteria direct expression of an intestinal bactericidal lectin. Science 2006;313(5790):1126-30.

[135] Putsep K, Axelsson LG, Boman A, Midtvedt T, Normark S, Boman HG, Andersson M. Germ-free and colonized mice generate the same products from enteric prodefensins. J Biol Chem 2000;275(51):40478-82.

[136] Bevins CL, Salzman NH. Paneth cells, antimicrobial peptides and maintenance of intestinal homeostasis. Nat Rev Microbiol 2011;9(5):356-68.

[137] Ayabe T, Satchell DP, Wilson CL, Parks WC, Selsted ME, Ouellette AJ. Secretion of microbicidal alpha-defensins by intestinal Paneth cells in response to bacteria. Nat Immunol 2000;1(2):113-8.

[138] Pedron T, Mulet C, Dauga C, Frangeul L, Chervaux C, Grompone G, Sansonetti PJ. A crypt-specific core microbiota resides in the mouse colon. MBio 2012;3(3).

[139] Savage DC, Blumershine RV. Surface-surface associations in microbial communities populating epithelial habitats in the murine gastrointestinal ecosystem: scanning electron microscopy. Infect Immun 1974;10(1):240-50.

[140] Shroyer NF, Wallis D, Venken KJ, Bellen HJ, Zoghbi HY. Gfi1 functions downstream of Math1 to control intestinal secretory cell subtype allocation and differentiation. Genes Dev 2005;19(20):2412-7.

[141] Sartor RB. Microbial influences in inflammatory bowel diseases. Gastroenterology 2008;134(2):577-94.

[142] Manichanh C, Rigottier-Gois L, Bonnaud E, Gloux K, Pelletier E, Frangeul L, Nalin R, Jarrin C, Chardon P, Marteau P, Roca J, Dore J. Reduced diversity of faecal microbiota in Crohn's disease revealed by a metagenomic approach. Gut 2006;55(2):205-11.

[143] Ott SJ, Musfeldt M, Wenderoth DF, Hampe J, Brant O, Folsch UR, Timmis KN, Schreiber S. Reduction in diversity of the colonic mucosa associated bacterial microflora in patients with active inflammatory bowel disease. Gut 2004;53(5):685-93.

[144] Walker AW, Sanderson JD, Churcher C, Parkes GC, Hudspith BN, Rayment N, Brostoff J, Parkhill J, Dougan G, Petrovska L. High-throughput clone library analysis of the mucosa-associated microbiota reveals dysbiosis and differences between inflamed and non-inflamed regions of the intestine in inflammatory bowel disease. BMC Microbiol 2011;11:7.

[145] Palm NW, de Zoete MR, Cullen TW, Barry NA, Stefanowski J, Hao L, Degnan PH, Hu J, Peter I, Zhang W, Ruggiero E, Cho JH, Goodman AL, Flavell RA. Immunoglobulin A coating identifies colitogenic bacteria in inflammatory bowel disease. Cell 2014;158(5):1000-10.

[146] Swidsinski A, Ladhoff A, Pernthaler A, Swidsinski S, Loening-Baucke V, Ortner M, Weber J, Hoffmann U, Schreiber S, Dietel M, Lochs H. Mucosal flora in inflammatory bowel disease. Gastroenterology 2002;122(1):44-54.

[147] Peterson CT, Sharma V, Elmen L, Peterson SN. Immune homeostasis, dysbiosis and therapeutic modulation of the gut microbiota. Clin Exp Immunol 2015;179(3):363-77.

[148] Nieuwenhuis EE, Matsumoto T, Lindenbergh D, Willemsen R, Kaser A, Simons-Oosterhuis Y, Brugman S, Yamaguchi K, Ishikawa H, Aiba Y, Koga Y, Samsom JN, Oshima K, Kikuchi M,

Escher JC, Hattori M, Onderdonk AB, Blumberg RS. Cd1d-dependent regulation of bacterial colonization in the intestine of mice. J Clin Invest 2009;119(5):1241-50.

[149] Macpherson A, Khoo UY, Forgacs I, Philpott-Howard J, Bjarnason I. Mucosal antibodies in inflammatory bowel disease are directed against intestinal bacteria. Gut 1996;38(3):365-75.

[150] Pirzer U, Schonhaar A, Fleischer B, Hermann E, Meyer zum Buschenfelde KH. Reactivity of infiltrating T lymphocytes with microbial antigens in Crohn's disease. Lancet 1991;338(8777):1238-9.

[151] Lozupone CA, Stombaugh JI, Gordon JI, Jansson JK, Knight R. Diversity, stability and resilience of the human gut microbiota. Nature 2012;489(7415):220-30.

[152] Hollander D, Vadheim CM, Brettholz E, Petersen GM, Delahunty T, Rotter JI. Increased intestinal permeability in patients with Crohn's disease and their relatives. A possible etiologic factor. Ann Intern Med 1986;105(6):883-5.

[153] Buhner S, Buning C, Genschel J, Kling K, Herrmann D, Dignass A, Kuechler I, Krueger S, Schmidt HH, Lochs H. Genetic basis for increased intestinal permeability in families with Crohn's disease: role of CARD15 3020insC mutation? Gut 2006;55(3):342-7.

[154] Wallace JL. Prostaglandins, NSAIDs, and gastric mucosal protection: why doesn't the stomach digest itself? Physiol Rev 2008;88(4):1547-65.

[155] Aw TY. Intestinal glutathione: determinant of mucosal peroxide transport, metabolism, and oxidative susceptibility. Toxicol Appl Pharmacol 2005;204(3):320-8.

[156] Beyfuss K, Hood DA. A systematic review of p53 regulation of oxidative stress in skeletal muscle. Redox Rep 2018;23(1):100-17.

[157] Edelblum KL, Yan F, Yamaoka T, Polk DB. Regulation of apoptosis during homeostasis and disease in the intestinal epithelium. Inflamm Bowel Dis 2006;12(5):413-24.

[158] Soderholm JD, Perdue MH. Stress and gastrointestinal tract. II. Stress and intestinal barrier function. Am J Physiol Gastrointest Liver Physiol 2001;280(1):G7-G13.

[159] Bischoff SC, Barbara G, Buurman W, Ockhuizen T, Schulzke JD, Serino M, Tilg H, Watson A, Wells JM. Intestinal permeability--a new target for disease prevention and therapy. BMC Gastroenterol 2014;14:189.

[160] Peterson LW, Artis D. Intestinal epithelial cells: regulators of barrier function and immune homeostasis. Nat Rev Immunol 2014;14(3):141-53.

[161] Abella V, Scotece M, Conde J, Pino J, Gonzalez-Gay MA, Gomez-Reino JJ, Mera A, Lago F, Gomez R, Gualillo O. Leptin in the interplay of inflammation, metabolism and immune system disorders. Nat Rev Rheumatol 2017;13(2):100-9.

[162] Hernandez-Chirlaque C, Aranda CJ, Ocon B, Capitan-Canadas F, Ortega-Gonzalez M, Carrero JJ, Suarez MD, Zarzuelo A, Sanchez de Medina F, Martinez-Augustin O. Germ-free and Antibiotic-treated Mice are Highly Susceptible to Epithelial Injury in DSS Colitis. J Crohns Colitis 2016;10(11):1324-35.

[163] Ciorba MA, Riehl TE, Rao MS, Moon C, Ee X, Nava GM, Walker MR, Marinshaw JM, Stappenbeck TS, Stenson WF. Lactobacillus probiotic protects intestinal epithelium from radiation injury in a TLR-2/cyclo-oxygenase-2-dependent manner. Gut 2012;61(6):829-38.

[164] Altschul SF, Gish W, Miller W, Myers EW, Lipman DJ. Basic local alignment search tool. J Mol Biol 1990;215(3):403-10.

[165] Zhang J, Rajkumar N, Hooi SC. Characterization and expression of the mouse pregnant specific uterus protein gene and its rat homologue in the intestine and uterus. Biochim Biophys Acta 2000;1492(2-3):526-30.

[166] Kasik J, Rice E. A novel complementary deoxyribonucleic acid is abundantly and specifically expressed in the uterus during pregnancy. Am J Obstet Gynecol 1997;176(2):452-6.

[167] Huang BH, Zhuo JL, Leung CH, Lu GD, Liu JJ, Yap CT, Hooi SC. PRAP1 is a novel executor of p53-dependent mechanisms in cell survival after DNA damage. Cell Death Dis 2012;3:e442.

[168] Xiong GF, Zhang YS, Han BC, Chen W, Yang Y, Peng JP. Estradiol-regulated proline-rich acid protein 1 is repressed by class I histone deacetylase and functions in peri-implantation mouse uterus. Mol Cell Endocrinol 2011;331(1):23-33.

[169] Xue B, Dunbrack RL, Williams RW, Dunker AK, Uversky VN. PONDR-FIT: a meta-predictor of intrinsically disordered amino acids. Biochim Biophys Acta 2010;1804(4):996-1010.

[170] Greenfield NJ. Using circular dichroism spectra to estimate protein secondary structure. Nat Protoc 2006;1(6):2876-90.

[171] Herrero J, Muffato M, Beal K, Fitzgerald S, Gordon L, Pignatelli M, Vilella AJ, Searle SM, Amode R, Brent S, Spooner W, Kulesha E, Yates A, Flicek P. Ensembl comparative genomics resources. Database (Oxford) 2016;2016.

[172] Williams JP, Brown SL, Georges GE, Hauer-Jensen M, Hill RP, Huser AK, Kirsch DG, Macvittie TJ, Mason KA, Medhora MM, Moulder JE, Okunieff P, Otterson MF, Robbins ME, Smathers JB, McBride WH. Animal models for medical countermeasures to radiation exposure. Radiat Res 2010;173(4):557-78.

[173] Wright PE, Dyson HJ. Intrinsically disordered proteins in cellular signalling and regulation. Nat Rev Mol Cell Biol 2015;16(1):18-29.

[174] Yoon MK, Mitrea DM, Ou L, Kriwacki RW. Cell cycle regulation by the intrinsically disordered proteins p21 and p27. Biochem Soc Trans 2012;40(5):981-8.

[175] Weber SC, Brangwynne CP. Getting RNA and protein in phase. Cell 2012;149(6):1188-91.

[176] Zhang J, Wong H, Ramanan S, Cheong D, Leong A, Hooi SC. The proline-rich acidic protein is epigenetically regulated and inhibits growth of cancer cell lines. Cancer Res 2003;63(20):6658-65.

[177] Rosshart SP, Vassallo BG, Angeletti D, Hutchinson DS, Morgan AP, Takeda K, Hickman HD, McCulloch JA, Badger JH, Ajami NJ, Trinchieri G, Pardo-Manuel de Villena F, Yewdell JW, Rehermann B. Wild Mouse Gut Microbiota Promotes Host Fitness and Improves Disease Resistance. Cell 2017;171(5):1015-28 e13.

[178] Wang L, Fouts DE, Starkel P, Hartmann P, Chen P, Llorente C, DePew J, Moncera K, Ho SB, Brenner DA, Hooper LV, Schnabl B. Intestinal REG3 Lectins Protect against Alcoholic Steatohepatitis by Reducing Mucosa-Associated Microbiota and Preventing Bacterial Translocation. Cell Host Microbe 2016;19(2):227-39.

[179] Mashimo H, Wu DC, Podolsky DK, Fishman MC. Impaired defense of intestinal mucosa in mice lacking intestinal trefoil factor. Science 1996;274(5285):262-5.

[180] Madesh M, Benard O, Balasubramanian KA. Apoptotic process in the monkey small intestinal epithelium: 2. Possible role of oxidative stress. Free Radic Biol Med 1999;26(3-4):431-8.

[181] Sodhi CP, Fulton WB, Good M, Vurma M, Das T, Lai CS, Jia H, Yamaguchi Y, Lu P, Prindle T, Ozolek JA, Hackam DJ. Fat composition in infant formula contributes to the severity of necrotising enterocolitis. Br J Nutr 2018;120(6):665-80.

[182] Li X, Wei X, Sun Y, Du J, Li X, Xun Z, Li YC. High-fat diet promotes experimental colitis by inducing oxidative stress in the colon. Am J Physiol Gastrointest Liver Physiol 2019;317(4):G453-G62.

[183] Ma'ayeh SY, Knorr L, Skold K, Garnham A, Ansell BRE, Jex AR, Svard SG. Responses of the Differentiated Intestinal Epithelial Cell Line Caco-2 to Infection With the Giardia intestinalis GS Isolate. Front Cell Infect Microbiol 2018;8:244.

[184] Camilleri M. Leaky gut: mechanisms, measurement and clinical implications in humans. Gut 2019;68(8):1516-26.

[185] Westwood FR. The female rat reproductive cycle: a practical histological guide to staging. Toxicol Pathol 2008;36(3):375-84.

[186] Dixon D, Alison R, Bach U, Colman K, Foley GL, Harleman JH, Haworth R, Herbert R, Heuser A, Long G, Mirsky M, Regan K, Van Esch E, Westwood FR, Vidal J, Yoshida M. Nonproliferative and proliferative lesions of the rat and mouse female reproductive system. J Toxicol Pathol 2014;27(3-4 Suppl):1S-107S.

[187] Vriesendorp HM, Vigneulle RM, Kitto G, Pelky T, Taylor P, Smith J. Survival after total body irradiation: effects of irradiation of exteriorized small intestine. Radiother Oncol 1992;23(3):160-9.

[188] Follis AV, Galea CA, Kriwacki RW. Intrinsic protein flexibility in regulation of cell proliferation: advantages for signaling and opportunities for novel therapeutics. Adv Exp Med Biol 2012;725:27-49.

[189] Chen A, Huang X, Xue Z, Cao D, Huang K, Chen J, Pan Y, Gao Y. The Role of p21 in Apoptosis, Proliferation, Cell Cycle Arrest, and Antioxidant Activity in UVB-Irradiated Human HaCaT Keratinocytes. Med Sci Monit Basic Res 2015;21:86-95.

[190] Sheikh MS, Rochefort H, Garcia M. Overexpression of p21WAF1/CIP1 induces growth arrest, giant cell formation and apoptosis in human breast carcinoma cell lines. Oncogene 1995;11(9):1899-905.

[191] Choi YH, Yoo YH. Taxol-induced growth arrest and apoptosis is associated with the upregulation of the Cdk inhibitor, p21WAF1/CIP1, in human breast cancer cells. Oncol Rep 2012;28(6):2163-9.

[192] Matthews JD, Owens JA, Naudin CR, Saeedi BJ, Alam A, Reedy AR, Hinrichs BH, Sumagin R, Neish AS, Jones RM. Neutrophil-Derived Reactive Oxygen Orchestrates Epithelial Cell Signaling Events during Intestinal Repair. Am J Pathol 2019;189(11):2221-32.

[193] Caligioni CS. Assessing reproductive status/stages in mice. Curr Protoc Neurosci 2009;Appendix 4:Appendix 4I.

[194] Alam A, Leoni G, Quiros M, Wu H, Desai C, Nishio H, Jones RM, Nusrat A, Neish AS. The microenvironment of injured murine gut elicits a local pro-restitutive microbiota. Nat Microbiol 2016;1:15021.

[195] Grabinger T, Delgado E, Brunner T. Analysis of Cell Death Induction in Intestinal Organoids In Vitro. Methods Mol Biol 2016;1419:83-93.

[196] O'Rourke KP, Dow LE, Lowe SW. Immunofluorescent Staining of Mouse Intestinal Stem Cells. Bio Protoc 2016;6(4).

[197] Cucchiara S, Latiano A, Palmieri O, Canani RB, D'Inca R, Guariso G, Vieni G, De Venuto D, Riegler G, De'Angelis GL, Guagnozzi D, Bascietto C, Miele E, Valvano MR, Bossa F, Annese V, Italian Society of Pediatric G, Nutrition. Polymorphisms of tumor necrosis factor-alpha but not MDR1 influence response to medical therapy in pediatric-onset inflammatory bowel disease. J Pediatr Gastroenterol Nutr 2007;44(2):171-9.

[198] Mendling W. Vaginal Microbiota. Adv Exp Med Biol 2016;902:83-93.

[199] Kaminska D, Gajecka M. Is the role of human female reproductive tract microbiota underestimated? Benef Microbes 2017:1-18.

[200] Franasiak JM, Scott RT. Endometrial microbiome. Curr Opin Obstet Gynecol 2017;29(3):146-52.

[201] Aagaard K, Ma J, Antony KM, Ganu R, Petrosino J, Versalovic J. The placenta harbors a unique microbiome. Sci Transl Med 2014;6(237):237ra65.

[202] Reid G. Cervicovaginal Microbiomes-Threats and Possibilities. Trends Endocrinol Metab 2016;27(7):446-54.

[203] Charbonneau MR, Blanton LV, DiGiulio DB, Relman DA, Lebrilla CB, Mills DA, Gordon JI. A microbial perspective of human developmental biology. Nature 2016;535(7610):48-55.

[204] Sykiotis GP, Bohmann D. Keap1/Nrf2 signaling regulates oxidative stress tolerance and lifespan in Drosophila. Dev Cell 2008;14(1):76-85.

[205] Gajer P, Brotman RM, Bai G, Sakamoto J, Schutte UM, Zhong X, Koenig SS, Fu L, Ma ZS, Zhou X, Abdo Z, Forney LJ, Ravel J. Temporal dynamics of the human vaginal microbiota. Sci Transl Med 2012;4(132):132ra52.

[206] Ravel J, Gajer P, Abdo Z, Schneider GM, Koenig SS, McCulle SL, Karlebach S, Gorle R, Russell J, Tacket CO, Brotman RM, Davis CC, Ault K, Peralta L, Forney LJ. Vaginal microbiome of reproductive-age women. Proc Natl Acad Sci U S A 2011;108 Suppl 1:4680-7.

[207] Kessel SS, Kleinman JC, Koontz AM, Hogue CJ, Berendes HW. Racial differences in pregnancy outcomes. Clin Perinatol 1988;15(4):745-54.

[208] Goldenberg RL, Iams JD, Mercer BM, Meis PJ, Moawad AH, Copper RL, Das A, Thom E, Johnson F, McNellis D, Miodovnik M, Van Dorsten JP, Caritis SN, Thurnau GR, Bottoms SF. The preterm prediction study: the value of new vs standard risk factors in predicting early and all spontaneous preterm births. NICHD MFMU Network. Am J Public Health 1998;88(2):233-8.

[209] Leitich H, Bodner-Adler B, Brunbauer M, Kaider A, Egarter C, Husslein P. Bacterial vaginosis as a risk factor for preterm delivery: a meta-analysis. Am J Obstet Gynecol 2003;189(1):139-47.

[210] Koumans EH, Sternberg M, Bruce C, McQuillan G, Kendrick J, Sutton M, Markowitz LE. The prevalence of bacterial vaginosis in the United States, 2001-2004; associations with symptoms, sexual behaviors, and reproductive health. Sex Transm Dis 2007;34(11):864-9.

[211] Nasioudis D, Linhares IM, Ledger WJ, Witkin SS. Bacterial vaginosis: a critical analysis of current knowledge. BJOG 2017;124(1):61-9.

[212] Swidsinski A, Verstraelen H, Loening-Baucke V, Swidsinski S, Mendling W, Halwani Z. Presence of a polymicrobial endometrial biofilm in patients with bacterial vaginosis. PLoS One 2013;8(1):e53997.

[213] Moreno I, Codoner FM, Vilella F, Valbuena D, Martinez-Blanch JF, Jimenez-Almazan J, Alonso R, Alama P, Remohi J, Pellicer A, Ramon D, Simon C. Evidence that the endometrial microbiota has an effect on implantation success or failure. Am J Obstet Gynecol 2016;215(6):684-703.

[214] Ley RE, Backhed F, Turnbaugh P, Lozupone CA, Knight RD, Gordon JI. Obesity alters gut microbial ecology. P Natl Acad Sci USA 2005;102(31):11070-5.

[215] Marcobal A, Kashyap PC, Nelson TA, Aronov PA, Donia MS, Spormann A, Fischbach MA, Sonnenburg JL. A metabolomic view of how the human gut microbiota impacts the host metabolome using humanized and gnotobiotic mice. Isme Journal 2013;7(10):1933-43.

[216] Paik J, Pershutkina O, Meeker S, Yi JJ, Dowling S, Hsu C, Hajjar AM, Maggio-Price L, Beck DA. Potential for using a hermetically-sealed, positive-pressured isocage system for studies involving germ-free mice outside a flexible-film isolator. Gut Microbes 2015;6(4):255-65.

[217] Nunn KL, Forney LJ. Unraveling the Dynamics of the Human Vaginal Microbiome. Yale J Biol Med 2016;89(3):331-7.

[218] Marcobal A, Kashyap PC, Nelson TA, Aronov PA, Donia MS, Spormann A, Fischbach MA, Sonnenburg JL. A metabolomic view of how the human gut microbiota impacts the host metabolome using humanized and gnotobiotic mice. ISME J 2013;7(10):1933-43.

[219] Ridaura VK, Faith JJ, Rey FE, Cheng J, Duncan AE, Kau AL, Griffin NW, Lombard V, Henrissat B, Bain JR, Muehlbauer MJ, Ilkayeva O, Semenkovich CF, Funai K, Hayashi DK, Lyle BJ, Martini MC, Ursell LK, Clemente JC, Van Treuren W, Walters WA, Knight R, Newgard CB, Heath AC, Gordon JI. Gut microbiota from twins discordant for obesity modulate metabolism in mice. Science 2013;341(6150):1241214.

[220] Chassaing B, Koren O, Goodrich JK, Poole AC, Srinivasan S, Ley RE, Gewirtz AT. Dietary emulsifiers impact the mouse gut microbiota promoting colitis and metabolic syndrome. Nature 2015;519(7541):92-6.

[221] Bradshaw CS, Sobel JD. Current Treatment of Bacterial Vaginosis-Limitations and Need for Innovation. J Infect Dis 2016;214 Suppl 1:S14-20.

[222] Suto J. Genetic analysis of litter size in mice. J Vet Med Sci 2015;77(3):353-8.

[223] Pavlidis I, Spiller OB, Sammut Demarco G, MacPherson H, Howie SEM, Norman JE, Stock SJ. Cervical epithelial damage promotes Ureaplasma parvum ascending infection, intrauterine inflammation and preterm birth induction in mice. Nat Commun 2020;11(1):199.

[224] Racicot K, Cardenas I, Wunsche V, Aldo P, Guller S, Means RE, Romero R, Mor G. Viral infection of the pregnant cervix predisposes to ascending bacterial infection. J Immunol 2013;191(2):934-41.

[225] DiGiulio DB, Romero R, Kusanovic JP, Gomez R, Kim CJ, Seok KS, Gotsch F, Mazaki-Tovi S, Vaisbuch E, Sanders K, Bik EM, Chaiworapongsa T, Oyarzun E, Relman DA. Prevalence and diversity of microbes in the amniotic fluid, the fetal inflammatory response, and pregnancy outcome in women with preterm pre-labor rupture of membranes. Am J Reprod Immunol 2010;64(1):38-57.

[226] Han YW, Redline RW, Li M, Yin L, Hill GB, McCormick TS. Fusobacterium nucleatum induces premature and term stillbirths in pregnant mice: implication of oral bacteria in preterm birth. Infect Immun 2004;72(4):2272-9.

[227] Gonzalez G. Determining the Stage of the Estrous Cycle in Female Mice by Vaginal Smear. Cold Spring Harb Protoc 2016;2016(8).

[228] Finn CA. Menstruation: a nonadaptive consequence of uterine evolution. Q Rev Biol 1998;73(2):163-73.

[229] Miller EA, Livermore JA, Alberts SC, Tung J, Archie EA. Ovarian cycling and reproductive state shape the vaginal microbiota in wild baboons. Microbiome 2017;5(1):8.

[230] Swartz JD, Lachman M, Westveer K, O'Neill T, Geary T, Kott RW, Berardinelli JG, Hatfield PG, Thomson JM, Roberts A, Yeoman CJ. Characterization of the Vaginal Microbiota of Ewes and Cows Reveals a Unique Microbiota with Low Levels of Lactobacilli and Near-Neutral pH. Front Vet Sci 2014;1:19.

[231] Yildirim S, Yeoman CJ, Janga SC, Thomas SM, Ho M, Leigh SR, Primate Microbiome C, White BA, Wilson BA, Stumpf RM. Primate vaginal microbiomes exhibit species specificity without universal Lactobacillus dominance. ISME J 2014;8(12):2431-44.

[232] Miller EA, Beasley DE, Dunn RR, Archie EA. Lactobacilli Dominance and Vaginal pH: Why Is the Human Vaginal Microbiome Unique? Front Microbiol 2016;7:1936.

[233] Galinsky R, Polglase GR, Hooper SB, Black MJ, Moss TJ. The consequences of chorioamnionitis: preterm birth and effects on development. J Pregnancy 2013;2013:412831.

[234] Oliver RS, Lamont RF. Infection and antibiotics in the aetiology, prediction and prevention of preterm birth. J Obstet Gynaecol 2013;33(8):768-75.

[235] Goldenberg RL, Culhane JF, Iams JD, Romero R. Epidemiology and causes of preterm birth. Lancet 2008;371(9606):75-84.

[236] Romero R, Dey SK, Fisher SJ. Preterm labor: one syndrome, many causes. Science 2014;345(6198):760-5.

[237] Andrews WW, Hauth JC, Goldenberg RL. Infection and preterm birth. Am J Perinatol 2000;17(7):357-65.

[238] Tita AT, Andrews WW. Diagnosis and management of clinical chorioamnionitis. Clin Perinatol 2010;37(2):339-54.

[239] Agrawal V, Hirsch E. Intrauterine infection and preterm labor. Semin Fetal Neonatal Med 2012;17(1):12-9.

[240] Lahra MM, Jeffery HE. A fetal response to chorioamnionitis is associated with early survival after preterm birth. Am J Obstet Gynecol 2004;190(1):147-51.

[241] Corwin EJ, Hogue CJ, Pearce B, Hill CC, Read TD, Mulle J, Dunlop AL. Protocol for the Emory University African American Vaginal, Oral, and Gut Microbiome in Pregnancy Cohort Study. BMC Pregnancy Childbirth 2017;17(1):161.

[242] Nugent RP, Krohn MA, Hillier SL. Reliability of diagnosing bacterial vaginosis is improved by a standardized method of gram stain interpretation. J Clin Microbiol 1991;29(2):297-301.

[243] Forney LJ, Gajer P, Williams CJ, Schneider GM, Koenig SS, McCulle SL, Karlebach S, Brotman RM, Davis CC, Ault K, Ravel J. Comparison of self-collected and physician-collected vaginal swabs for microbiome analysis. J Clin Microbiol 2010;48(5):1741-8.

[244] VanInsberghe D, Elsherbini JA, Varian B, Poutahidis T, Erdman S, Polz MF. Diarrhoeal events can trigger long-term Clostridium difficile colonization with recurrent blooms. Nat Microbiol 2020;5(4):642-50.

[245] Callahan BJ, McMurdie PJ, Rosen MJ, Han AW, Johnson AJ, Holmes SP. DADA2: High-resolution sample inference from Illumina amplicon data. Nat Methods 2016;13(7):581-3.

[246] Goldstein M, Kastan MB. The DNA damage response: implications for tumor responses to radiation and chemotherapy. Annu Rev Med 2015;66:129-43.

[247] Potten CS, Booth C. The role of radiation-induced and spontaneous apoptosis in the homeostasis of the gastrointestinal epithelium: a brief review. Comp Biochem Physiol B Biochem Mol Biol 1997;118(3):473-8.

[248] MacNaughton WK. Review article: new insights into the pathogenesis of radiation-induced intestinal dysfunction. Aliment Pharmacol Ther 2000;14(5):523-8.

[249] Quastler H. The nature of intestinal radiation death. Radiat Res 1956;4(4):303-20.

[250] Mason KA, Withers HR, McBride WH, Davis CA, Smathers JB. Comparison of the gastrointestinal syndrome after total-body or total-abdominal irradiation. Radiat Res 1989;117(3):480-8.

[251] Kirsch DG, Santiago PM, di Tomaso E, Sullivan JM, Hou WS, Dayton T, Jeffords LB, Sodha P, Mercer KL, Cohen R, Takeuchi O, Korsmeyer SJ, Bronson RT, Kim CF, Haigis KM, Jain RK, Jacks T. p53 controls radiation-induced gastrointestinal syndrome in mice independent of apoptosis. Science 2010;327(5965):593-6.

[252] Lane DP. Cancer. p53, guardian of the genome. Nature 1992;358(6381):15-6.

[253] Merritt AJ, Potten CS, Kemp CJ, Hickman JA, Balmain A, Lane DP, Hall PA. The role of p53 in spontaneous and radiation-induced apoptosis in the gastrointestinal tract of normal and p53-deficient mice. Cancer Res 1994;54(3):614-7.

[254] Chen J. The Cell-Cycle Arrest and Apoptotic Functions of p53 in Tumor Initiation and Progression. Cold Spring Harb Perspect Med 2016;6(3):a026104.

[255] Riley T, Sontag E, Chen P, Levine A. Transcriptional control of human p53-regulated genes. Nat Rev Mol Cell Biol 2008;9(5):402-12.

[256] Merritt AJ, Allen TD, Potten CS, Hickman JA. Apoptosis in small intestinal epithelial from p53-null mice: evidence for a delayed, p53-independent G2/M-associated cell death after gamma-irradiation. Oncogene 1997;14(23):2759-66.

[257] Harper JW, Adami GR, Wei N, Keyomarsi K, Elledge SJ. The p21 Cdk-interacting protein Cip1 is a potent inhibitor of G1 cyclin-dependent kinases. Cell 1993;75(4):805-16.

[258] Karimian A, Ahmadi Y, Yousefi B. Multiple functions of p21 in cell cycle, apoptosis and transcriptional regulation after DNA damage. DNA Repair (Amst) 2016;42:63-71.

[259] Georgakilas AG, Martin OA, Bonner WM. p21: A Two-Faced Genome Guardian. Trends Mol Med 2017;23(4):310-9.

[260] Parveen A, Akash MS, Rehman K, Kyunn WW. Dual Role of p21 in the Progression of Cancer and Its Treatment. Crit Rev Eukaryot Gene Expr 2016;26(1):49-62.

[261] Duffy MJ, Synnott NC, Crown J. Mutant p53 as a target for cancer treatment. Eur J Cancer 2017;83:258-65.

[262] Schlereth K, Beinoraviciute-Kellner R, Zeitlinger MK, Bretz AC, Sauer M, Charles JP, Vogiatzi F, Leich E, Samans B, Eilers M, Kisker C, Rosenwald A, Stiewe T. DNA binding cooperativity of p53 modulates the decision between cell-cycle arrest and apoptosis. Mol Cell 2010;38(3):356-68.

[263] Bieging KT, Mello SS, Attardi LD. Unravelling mechanisms of p53-mediated tumour suppression. Nat Rev Cancer 2014;14(5):359-70.

[264] Wood GA, Fata JE, Watson KL, Khokha R. Circulating hormones and estrous stage predict cellular and stromal remodeling in murine uterus. Reproduction 2007;133(5):1035-44.

[265] Pace F, Pace M, Quartarone G. Probiotics in digestive diseases: focus on Lactobacillus GG. Minerva Gastroenterol Dietol 2015;61(4):273-92.

[266] Lin PW, Nasr TR, Berardinelli AJ, Kumar A, Neish AS. The probiotic Lactobacillus GG may augment intestinal host defense by regulating apoptosis and promoting cytoprotective responses in the developing murine gut. Pediatr Res 2008;64(5):511-6.

[267] Gamallat Y, Meyiah A, Kuugbee ED, Hago AM, Chiwala G, Awadasseid A, Bamba D, Zhang X, Shang X, Luo F, Xin Y. Lactobacillus rhamnosus induced epithelial cell apoptosis, ameliorates inflammation and prevents colon cancer development in an animal model. Biomed Pharmacother 2016;83:536-41.

[268] Wu S, Yuan L, Zhang Y, Liu F, Li G, Wen K, Kocher J, Yang X, Sun J. Probiotic Lactobacillus rhamnosus GG mono-association suppresses human rotavirus-induced autophagy in the gnotobiotic piglet intestine. Gut Pathog 2013;5(1):22.

[269] Onderdonk AB, Delaney ML, Fichorova RN. The Human Microbiome during Bacterial Vaginosis. Clin Microbiol Rev 2016;29(2):223-38.

[270] Reiter S, Kellogg Spadt S. Bacterial vaginosis: a primer for clinicians. Postgrad Med 2019;131(1):8-18.

[271] Vrbanac A, Riestra AM, Coady A, Knight R, Nizet V, Patras KA. The murine vaginal microbiota and its perturbation by the human pathogen group B Streptococcus. BMC Microbiol 2018;18(1):197.

[272] Teixeira GS, Carvalho FP, Arantes RME, Nunes AC, Moreira JLS, Mendonca M, Almeida RB, Farias LM, Carvalho MAR, Nicoli JR. Characteristics of Lactobacillus and Gardnerella vaginalis from women with or without bacterial vaginosis and their relationships in gnotobiotic mice. J Med Microbiol 2012;61(Pt 8):1074-81.

[273] Lyte JM, Proctor A, Phillips GJ, Lyte M, Wannemuehler M. Altered Schaedler flora mice: A defined microbiota animal model to study the microbiota-gut-brain axis. Behav Brain Res 2019;356:221-6.

[274] Wymore Brand M, Wannemuehler MJ, Phillips GJ, Proctor A, Overstreet AM, Jergens AE, Orcutt RP, Fox JG. The Altered Schaedler Flora: Continued Applications of a Defined Murine Microbial Community. ILAR J 2015;56(2):169-78.